Models and interactive tools in support of environmental decisions:

Enhancing 3D spatial analysis through efficient integration of data, models and technology

Azarakhsh Rafiee

Contents

Chapter 1: Introduction

1.1. Geospatial information for environmental problems

Human intervention in our environment often has undesirable consequences, including major environmental problems such as global warming, threatening our environment, the life of humans and other species. Clearly, we need to make proper decisions when encountering environmental problems and find solutions for the mitigation of their effects. However, taking decisions regarding environmental issues is difficult due to the multi criteria nature of environmental problems, the involvement of stakeholders from different domains, and the uncertainty and complexity of environmental problems. The first step to address is to have reliable and updated information on the current situation. The activity of processing this information is an essential constituent of a planning procedure (Scholten and Stillwell, 1990). A major type of information in this context is geospatial information, as it provides crucial knowledge on the formation and inter-relation of different environmental phenomena, and environmental solutions often depend on the spatial context.

[Geospatial] information can be acquired from different sources, such as local people, traditional surveying methods and modern technologies, having different reliability, cost and update frequency characteristics. The data, acquired from different sources, can be stored, processed and managed in a Geographic Information System (GIS) (Longley et al., 2001). In addition to geospatial data, GIS can be enriched with different models and algorithms for the efficient and automated processing and analyzing of information from raw data.

The feasibility and efficiency (in terms of costs and computing power) of data acquisition, processing and information extraction is related to the study scale; the larger the extent (and therefore higher coverage), the less detailed the captured data and the derived information. Currently, technological advancements have led to extracting more detailed information on larger areas both due to developments in data capturing devices (e.g. advanced airborne LIDAR) as well as computer processing and optimizations in (semi) automated information extraction algorithms. Integration of these advancements in a unified platform can lead to more detailed information presentation and analysis on a larger scale, which can provide a better picture on the information and processes of the current situation. This can boost the first step of a decision process, since a proper understanding of the current situation supports its evaluation in terms of its state and functionalities, which play a crucial role in proposing the subsequent alterations.

The second step is to design the alterations meant for the mitigation of the environmental problem. In this step, an interactive platform for scenario analysis can play an important role in the designing of different alternatives. In addition, like the previous step, reliable and updated information and process models are crucial for the impact analysis of the different scenarios and the final decision. The interactivity of the platform and the optimized performance of the underlying models also help in the integrated performance of a recursive decision making

framework, wherein the different components of the decision process should be visited several times.

1.2. A framework and requirements for a multi-disciplinary decision making process

Information on the current situation, as the initial step of a decision process, as well as the subsequent alteration designs, requires the access, maintenance, processing and presenting of the acquired geospatial datasets, calling for the delineation of a pertinent [geospatial] framework. In the Netherlands, different attempts were made during the last decades for the proper design of geospatial frameworks in the environmental domain. In 1989, an Environmental GIS (MILGIS) project was initiated in the National Institute of Public Health and Environmental Protection (RIVM) for the description and prediction of the quality of the environment. MILGIS contained four levels that were integrated with geographical data/results shared between them (van Beurden and Scholten, 1990). The highest level of MILGIS was mainly focused on data gathering from different institutes, data structuring and preparation for usage by different users, leading to the design of the central database. The second level contained GIS for laboratories (LABGIS) where the laboratory data of primary processes were used, selected or produced based on the particular research. The third level was analytical GIS wherein GIS software for spatial analysis (e.g. overlays, interpolation and zoning) were used in addition to models. The fourth level was the graphical level which focused on the presentation of the output, maps and graphs of the previous three levels. GIS data structure and storage were used in RIVM for serving input data to models. As the computer models often operated separately from other software, an interface between GIS and the models was required. For this purpose, Spans GIS software was used wherein models could run on its command processes and the GIS database (as inputs of the models) could be accessed through it.

Misseyer (1999) constructed a multi-dimensional framework for supporting governmental authorities to implement a proper environmental monitoring structure. This framework consists of five dimension, namely: *environmental legislation*, *environmental policy*, *information infrastructure and management*, *information needs and requirements* and *information and communication technology*. This defined model aimed at more efficient (and even maybe more effective) analysis, processing and presenting of environmental issues. Van Herwijnen (1999) developed a framework consisting of different multi-objective decision methods in combination with spatial analyses approaches to produce enhanced techniques in spatial environmental problems. Fabbri (2002) developed a framework for structuring a decision situation by coastal managers and decision makers. The integration of different methods and tools, in this study, aimed to support decision making in environmental management. These studies all emphasized the importance of appropriate frameworks for the proper integration of geospatial data (from different resources) with environmental models in the provision of a proper insight of the current situation and the support of decision making regarding environmental issues.

Following the attempts to define geospatial frameworks for decision making regarding environmental issues, a framework of methods and techniques for an efficient and integrated design-impact for environmental decision making is investigated in this study. Geodesign, as

the planning and design method which pairs design and its resulting impacts by geographic context (Flaxman, 2010), was researched for its efficiency as the framework of this study. Though rooted in the beginning of the 20th century (Manning, 1913), recent technological advancements support the implementation of this framework for direct design-impact feedbacks (Dias et al., 2013).

Geodesign, as the development and employment of design-related processes for alterations in geography, is a collection of methods and concepts derived from the geospatial domain as well as design-related disciplines (Steinitz, 2012). This iterative design and planning approach, when combined with geospatial technology, provides the scope for a simultaneous design-evaluation process, which can lead to a more robust design (Lee et al., 2014). The geodesign framework proposed by Steinitz (1990) includes six questions regarding the current situation as well as alterations in the study area, which should be reviewed iteratively and discussed by the stakeholders from different involved domains, during the planning process. This structure makes geodesign an appropriate framework for applying in multi-disciplinary environmental decision making processes.

Data incorporation and the visualization platform are the two main components of a geodesign framework. Current technological advancements have led to the availability of detailed (in terms of spatial as well as temporal resolutions) geospatial data. However, the employment of these datasets in decision processes confronts major limitations, mainly due to costs, volume and formatting issues. Emerging national and worldwide open data initiatives, e.g. UK Ordnance Survey open data (OS OpenData, 2019), and Dutch open data from the Ministry of Infrastructure and Environment (Open data van de Overheid, 2019), has broadened the opportunities for a wider application of the geospatial datasets produced. Despite these initiatives, there are substantial constraints on applying open geospatial datasets to their full extent: volume extensiveness and formatting incompatibilities with the platform used are among the main obstacles to the use of open geospatial data (Martin et al., 2013; Liu et al., 2015). In addition, the integration of data from different domains can face challenges due to inconsistencies in disciplines, scales and information models. An instance here is the integration of the Building Information Model (BIM) in the GIS environment. While BIM contains detailed semantic and geometric information on the construction level, it is often not geolocated and detached from its environment. The defined information model of BIM is focused on the building level, in line with the architecture domain. However, the focus of the GIS domain lies in the geospatial relations between [existing] objects on larger scales, with lower detail and more simplified geometry (Isikdag and Zlatanova, 2009; Mignard and Nicolle, 2014).

The visualization platform is another major component of a geodesign framework. Visualization is the main link between the quantitative substance of data and human intuition (Donalek et al., 2014). The design of a visualization environment, in terms of information content, presentation style and interactivity, can have great influence on the user perception of the environment. The information content is composed of the extent, dimension, level of detail and [domain] diversity. In addition to data availability and accessibility, these elements are limited to the computer processing and rendering capacities. Geospatial visualization platforms should mainly focus on one element and sacrifice other elements due to performance issues.

This limits the provision of a comprehensive situational picture to stakeholders which can affect the subsequent steps of the decision process. Therefore, an optimized visualization platform with boosted capacity on information content can play an important role in a decision process (Jude, 2008). Here, dimension, specifically, can have significant impact on user perception. Studies mention that users perceive 3D geospatial information better than simplified 2D, due to easier association between the information and our 3D environment (Alkodmany, 2002; Dias et al., 2003). However, in the GIS domain, 2D platforms are still mainstream and 3D visualization platforms face challenges on large extents due to both performance issues as well as the scarcity of 3D geospatial information. This, in turn, is related to the burden of processing massive 3D geospatial data as well as the implementation complexity of 3D object extraction algorithms on large extents. The interactivity of a visualization platform is the other key feature for boosted perception. Different studies have shown the influence of platform-user interaction on a better perception as well as more active involvement of stakeholders in a decision process (Santhanam and Wiedenbeck, 1993; Al-Kodmany, 1999). The interactivity of a visualization platform is related to platform responsiveness as well as its [user interface] design. Agile responsiveness of a visualization platform is restricted to performance capacity. Therefore optimization on platform responsiveness can enhance its interactivity.

Subsequent to the perception and the evaluation of the current situation, involved stakeholders should pose and discuss alteration scenarios for enhancements within the defined target framework. In this stage, a common platform where all stakeholders can collaborate together on designing adaptation scenarios benefits the decision making process (Eikelboom and Janssen, 2017). The effectiveness of such a platform is reliant on several factors, among which [user interface] design, interactivity, responsiveness and ease of use play the most important roles (Shiffer, 1992; Simonovic and Bender, 1996). Furthermore, the proper incorporation and design of [geospatial] data from different domains is an influential factor for an effectual scenario design procedure in a multidisciplinary planning process, as it provides multi-aspect insight on the current situation and a foundation upon which alteration scenarios should be designed. Similar to the visualization of the current situation, in the case of the design platform the provision of 3D geospatial model can also boost the user perception. While studies have shown the importance of the mentioned factors, performance problems due to intensive data processing and rendering requirements present an important obstacle in the transition to an interactive 3D geospatial design platform.

A proposed alteration scenario cannot be evaluated regardless of its mutual impact with its environment. This requires the development of new models or the employment of existing environmental models. On a micro-scale, these models require detailed information both for their development and their implementation. While for smaller extents, the processing of the detailed [geospatial] information is still manageable, it becomes more problematic as the study area expands. This is due to machine performance as well as data availability constraints. Therefore, in both cases of model development and implementation, studies should mainly observe the trade-off between detail level and study extent. However, this restriction can impose considerable inaccuracies when assessing the impact of a posed scenario which might cause a negative influence on the final decision. Therefore, approaches and routines for optimizing the

accessibility and processing of detailed [input] data on a large extent, for model development as well as model implementation, can be of great value.

In addition to the ability to develop and/or implement environmental models on a more detailed level and in a larger extent, their implementation speed also considerably influences the decision process, as boosting the responsiveness of scenario impact analysis can support seamless scenario configurations and impact assessments. This results in an intertwined discussion process which in turn can enhance the efficiency of a decision process (Jude, 2008; Dias et al., 2013). The implementation speed of environmental models is, however, dependent on the model complexity as well as the study extent. In other words, the speed is restricted to the machine performance in the processing of input geospatial data as well as the model computations. Employing optimization techniques to boost the implementation speed of environmental models in large extent will therefore support higher responsiveness of scenario impact analysis, the overall interactivity of the scenario design platform and the conjunction of the scenario configuration/evaluation discussions.

To summarize this section, Table 1 demonstrates the elements of a spatial decision support system requiring more research for its improvement. These improvements can be carried out on a single element as well as on integrating a collection of inter-related elements.

Table 1. Limitations of current Spatial Decision Support Systems.

Limitations	**Environmental decision making process components**	**Current Situation**	**Alterations**
Accessibility	Data	✓	✓
Interoperability		✓	✓
Scale		✓	✓
Dimension (3D)	Data, Visualization	✓	✓
Interactivity	Visualization, Design platform	✓	✓
Information content		✓	✓
Experimental model development on a city scale	Process models	✓	
Responsiveness	Design platform		✓
Implementation speed of simulation models	Impact models		✓
Speed/Scale proportion			✓

1.3. Efficient Data-Model-Technology integration towards an optimized spatial decision support system

In line with the mentioned research gaps and limitations in the development of an effectual spatial decision support system, which can improve the decision making process, this thesis introduces the development of different components for supporting environmental decisions. These components comprise data processing and information extraction, interactive presentation, the development of process models (for current processes as well as for impact analysis of new scenarios) and an interactive platform for flexible scenario design and intertwined discussion processes. This thesis focuses especially on the effective integration of these components for optimizing the performance of spatial decision support systems. Different technologies, datasets and environmental models have been employed for the development of these components. Two major environmental problems, namely *energy* and *liveability*, have been chosen as the use cases for the development of the components of effective spatial decision support systems. The developed components belong to one or both domains. The scheme of this thesis, including the developed/applied components are illustrated in Figure 1.

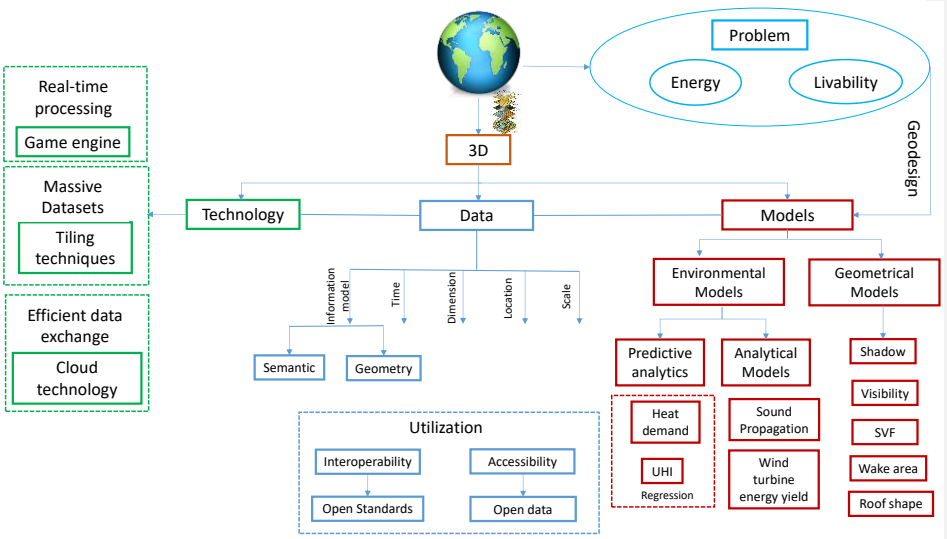

Figure 1. Thesis schema; the development of components for optimized performance of SDSS in different domains, through the efficient integration of Data-Models-Technology components.

Our environment is encountering many problems. To be able to take proper decisions regarding these problems, our environment and its interrelated processes should be described properly in each step of the decision process. The proper combination of *data*, *models* and *technology* can support us in describing and presenting our environment and its processes. Energy and liveability related environmental problems, being two major issues of concern for our era, have been chosen as the use cases of this thesis. A geodesign outline is applied for the design of the

decision support components regarding these environmental problems. Each component can belong to one or more steps of geodesign framework.

Data, which is mainly comprised of geospatial data in this thesis, has different properties. In this thesis, the focus lies on scale, location, dimension and information model attributes. These parameters have different impacts on the analyses we aim to perform. The extent to which we can handle the [geospatial] data is a function of scale, dimension, time and the efficiency of the information model (which can contain geometry as well as geometry/semantic). A major focus of this thesis is the efficient employment of technology to increase the extent of the analyses while maintained high detail. The [geospatial] data dimension is 3D and the scale is at micro scale on all the analyses of this study. In addition to data characteristics, the potential utilization of data plays an important role on the scale and extent of different analyses. Data utilization is comprised of its accessibility and interoperability. Another major objective of this study is to apply nationwide open data and open standards to boost the accessibility and interoperability of geospatial data, respectively, for the different analyses involved. The former broadens the variety of data and extent of data from different domains, which can enrich the analyses and the latter avoids formatting problems between different datasets, which is a major impediment in many studies. Different open standard web services have been employed and embedded in the designed modules of this study for the accessibility of nationwide open data from different domains and their interoperability with each other. The *data* component plays an important role in the representation model as well as the process and impact models (as the input of the underlying models) of a geodesign framework.

Models are applied to depict the different processes within our environment. They can be used to describe current processes, using current environmental configurations, as well as the posed alteration scenario impacts. In this thesis, two categories of models, namely environmental models and geometrical models have been employed for the description of current/changed environmental settings, for the different studies involved. Environmental models, in turn, comprise two groups of predictive analytics and analytical models in this thesis. Predictive analytics, here, comprised mainly multi-linear regression models for the exploration of the different influential geospatial parameters on Urban Heat Island (UHI) and household heat demands in two studies. Analytical models include sound propagation models as well as a wind turbine energy yield model for the simulation of wind turbine sound impacts on the neighbouring buildings and energy yield estimations, respectively, as the two main geospatially related parameters. Geometrical models are comprised of 3D shadow, visibility, sky view factor, roof shape and wake area models. 3D shadow and visibility models are applied for the impact analysis of wind turbine shading and visibility impacts on the surrounding buildings. Furthermore these models have also been used for the shading impact of trees on the roof of a residential BIM model as well as the green/grey view coverage of its windows. The wake area model is used for each wind turbine to avoid energy yield reduction due to the proximity of wind turbines. Sky view factor is applied to estimate the urban configuration impact on UHI and household heat demand. Roof shape model is applied to estimate its impact on household heat demand.

Technology plays an important role in the efficient application and integration of *data* and *models* for the development of a decision support platform. In this thesis, different technologies have been used to optimize the performance of different components of the designed decision support systems for the environmental problems to be addressed. The core technologies applied are game engine, tiling techniques and cloud technology. Game engine is used for real-time data processing and model implementation of the wind turbine decision support system. Through applying different rendering and physics engine functionalities of the Unity game engine, different processes within the decision support system, such as 3D scene rendering and spatial operations could be optimized. This led to the real-time performance of 3D analytical and geometrical models. While game engines can have optimized performance for high details on a small scene, their performance decreases for larger areas. For this reason, geospatial tiling techniques were applied in this study to increase the extent of the study area to the whole country. Furthermore, embedding cloud technology for efficient data exchange has broadened the possibilities beyond limited (commercially) available data. Incorporating open data and open standards, in combination with the embedded tiling techniques, has increased the study extent as well as the variety of geospatial data, integrated from different domains. The integration of game engine optimized performance with GIS tiling techniques and open standards has led to the real-time performance of the underlying process/impact models as well as optimized 3D rendering for representation and change models of a geodesign framework. This performance enhancement can play a crucial role for the integrity of a decision process.

1.4. Thesis outline: Research objectives and applied methodologies

This thesis is composed of seven chapters that cover the main goal of this thesis, namely, efficient [geospatial] Data-Model-Technology integration for the development of different components of optimized decision support systems in energy and liveability domains. The following research objectives are defined to fulfil the main goal of this study. They comprise the development/implementation of:

- Methodologies for efficient accessibility to massive 2D/3D open geospatial data from different resources and different domains on a large extent

- Methodologies for efficient integration and interoperability between the geospatial datasets from different domains and disciplines

- Approaches for boosting visualization from both information content as well as interactivity and scene rendering perspectives

- Experimental environmental model development on an extended (city) scale and the third dimension

- Techniques for the development of interactive and responsive 3D design platforms with augmented information content and rendering capabilities

- Methods for boosting the speed and scale of implemented simulation models

Each study of this thesis follows certain objectives, which are sub-classes of the overall research objectives. Data-Model-Technology integration is used to achieve these research objectives. Each of the Data, Model and Technology groups contains sub-categorical elements, as depicted in the thesis schema (Figure 1). Each study employs a set of these elements to fulfil its objectives.

Following the research objectives, subsequent research questions have been posed which are answered in this thesis:

1. How can [massive] 2D/3D open geospatial data, from different domains, be efficiently served in portraying current spatial configuration in representation and change models?
2. How can the interactivity, extent and responsiveness of a 3D spatial design platform be enhanced through the employment and integration of technology from different domains?
3. What is the benefit of 3D geospatial information on the development of process models?

More specifically on process models, based on the defined use cases of this study, the following research questions have been posed:

4. What is the influence of tree volume on nocturnal Urban Heat Island (UHI)?
5. How do spatial context parameters affect household heat consumption?
6. How can geospatial information be efficiently extracted from data to be used as inputs of predictive analytics on the whole city extent and high level of detail?
7. How can BIM-GIS integration support the efficiency of construction-environment impact analyses?

A more detailed overview on the research performed within the depicted thesis framework follows:

1.4.1. Local impact of tree volume on nocturnal urban heat island: A case study in Amsterdam

One of the environmental problems of the current era is Urban Heat Island. Urban Heat Island (UHI) is the temperature increase in urban areas compared to rural areas due to human activities. UHI can cause health problems to citizens, moreover, it increases the energy demand related to air-conditioning. The growth in urbanization leads to higher construction in urban areas, which in turn, leads to higher urban heat island. As the urban configuration has a high influence on the heat released, proper urban design is of great importance for UHI mitigation. The first step for a proper design is information on the parameters influencing UHI. Studies show the effects of different parameters, among which urban compactness and vegetation cover have considerable impacts on UHI (See Chapter 2 for more details). In this study, Chapter 2 focuses on the quantification of the local impact of tree volumes on nocturnal urban heat island intensity. This research area is in the liveability domain. An empirical model, through a multi-linear regression model, was developed to explain the contribution of local tree volume to UHI.

The urbanization degree, as a regional factor, and the sky view factor, as a local factor, were also taken into account. While the impact of vegetation cover on UHI has been investigated in different studies, it is mainly restricted to 2D vegetation surface estimation and/or on a limited extent. In our study, we have employed 3D tree models of the whole of Amsterdam for the estimation of their impact on its nocturnal UHI. Scale was taken into account by testing different radii to explore the radius wherein the aggregated tree volume has the highest impact on UHI. An additional contribution of this research is the demonstration of a scalable methodology for the automated extraction of geospatial information, to be employed in the analysis, at a city scale using geospatial data and GIS techniques, which can be employed in similar studies. This research covers the following research objectives:

- The improvement in process models: Exploring the impact of tree volume (rather than vegetation surface) on urban heat island
- Information extraction from massive point cloud data: Calculating sky view factor and tree volumes for the whole city, using airborne LiDAR technology and efficient 3D data processing

1.4.2. Developing a wind turbine planning platform: Integration of "sound propagation model–GIS-game engine" triplet

CO2 increase and global warming resulting from the excessive use of fossil fuel is another environmental problem of our current era. This has prompted the growth of renewable energy as an alternative clean energy source. Wind energy is an important source of renewable energy which is being employed in many countries. The Netherlands has a long history in using wind energy due to its climatic conditions, and is aiming to expand it in accordance with European renewable energy targets. In spite of the benefits of wind energy as a clean source, wind turbine development projects are hindered by citizens' opposition due to wind turbine externalities. Therefore, planning the proper location of wind turbines for the minimum environmental externalities and maximum energy yield are of great importance. In addition, citizens' involvement, from the beginning phase of the project, in the decision making process for wind turbine allocations can increase their trust and support.

The first step for the efficient involvement of citizens is a properly designed information system to provide a common picture to citizens and other involved stakeholders. In this study, we developed an interactive 3D wind turbine planning platform aimed at the effective involvement of stakeholders from different backgrounds. The platform focuses on wind turbine visual and sound externalities. The designed/implemented framework for this integrated environmental information system [for the support of wind turbine planning processes] is described in detail in this study. This system integrates game engine, GIS and analytical sound propagation models. This integration supported the optimized performance of the different components of the system and led to real-time wind turbine sound calculation in any location of the whole country. The interactive 3D virtual environment, provided through Unity game engine, can support an immersive experience for the users. Massive 3D models were derived through LIDAR point cloud and generated on-the-fly for both visualization in the virtual 3D

environment as well as employment in the sound propagation models. The GIS component of the system supported the serving of massive geospatial data through tiling techniques as well as accessibility and interoperability to different datasets from different sources through the employment of cloud-based architecture and the incorporation of open geospatial standard protocols. The integration of state-of-the-art sound propagation models (through Unity game engine C# scripting API) supports the provision of more accurate information on the sound impact of a wind turbine on the surrounding buildings. This can attract stakeholders from different domains such as noise experts and legislation authorities, along with citizens. Different sound propagation modules were optimized through the employment of different game engine and GIS functionalities. This led to the real-time performance of sound propagation modules which normally take a long time in a conventional sound/GIS software. The real-time performance of wind turbine sound propagation models supports an intertwined discussion process where no interruptions for the (re)calculations are required.

This system can be used for the presentation of data and processes on a current situation (such as 3D building and terrain model) through an interactive 3D visualization platform. The incorporation of open standard protocols as well as tiling techniques in this system enables the flexible incorporation of other open geospatial data and [process] model results through the web. Being able to effectively present the current situation is an important aspect for proper evaluation of the situation, serving as a bridge for subsequent alteration designs. In the next step, this system can be applied as an interactive design platform for posing different alteration scenarios by interactively placing different 3D wind turbine models from different suppliers in the game engine scene. This step is followed by an immediate impact analysis of each design scenario, including aesthetic and wind turbine sound impacts on the surrounding buildings, which will be evaluated by the stakeholders. This study covers the following research objectives of this thesis:

- Development of an interactive 3D design platform
- Connection to analytical (wind turbine sound) models
- Incorporation of open geospatial standards and employment of open geospatial data for visualization as well as input for the sound models as impact analysis models
- Scalability to the whole country and even beyond
- Real-time performance of sound models

1.4.3. Interactive 3D geodesign tool for multidisciplinary wind turbine planning

Wind turbine site planning is a multidisciplinary task involving many stakeholders from different domains. The final location of a wind turbine should be discussed among the stakeholders involved who will have different, and sometimes conflicting, interests and priorities. This makes the siting of a wind turbine a multi-criteria decision making process. An information system which is capable of integrating knowledge on the different aspects of a wind turbine can play an important role in providing a more comprehensive picture to the stakeholders involved of the different domains and backgrounds. Such information system

should act as the interface between the different components of a participatory plan process from providing information on the current situation and the subsequent evaluation to the design of the new situation, the evaluation of its impacts and the convergence to a final decision. This makes geodesign a proper framework for the design of a wind turbine multidisciplinary tool. In Chapter 4, we have developed an interactive 3D information system for planning wind turbine locations in any location in the Netherlands. The architecture developed for wind turbine planning through the game engine-GIS-sound model integration of the previous chapter, can be an appropriate basis for further development of the tool to include other aspects in wind turbine planning.

This system supports iterative design loops and has been designed based on the geodesign framework proposed by Steinitz (1990) aiming to support an interactive multidisciplinary plan process. Each of the geodesign models, namely *representation models, process models, evaluation models, change models, impact models* and *decision models* has been implemented in Falcon and together they form a multi-criteria decision support system for wind turbine siting in the Netherlands. Different game engine, GIS functionalities and analytical models have been employed in the design and efficient implementation of these geodesign models.

The criteria applied in this system are: wind turbine sound, shadow, visibility from buildings, energy yield, wake effects and regulations. Game engine-GIS-analytical model integration, as introduced in the previous chapter, supported the real-time performance of the different analytical models applied (e.g. sound, energy) in this system in any location in the country. This has been achieved through optimizing the performance of these models by employing different game engine as well as GIS functionalities in the model implementations. The interactivity and the real-time feedbacks as well as the applicability of the system for any location in the country, support the seamless exploration of various scenarios and their real-time environmental impacts in different locations which can help an intertwined discussion process. The multi-aspectual feature of this system supports the provision of a more comprehensive depiction of the environmental impacts of wind turbines in their site planning which can broaden its applications and lead to the involvement and collaboration of stakeholders from different backgrounds. This study covers the following research objectives:

- Development of a multidisciplinary interactive 3D design platform
- Connection to analytical and geometrical (wind turbine sound, shadow, visibility and wake area) models as impact analysis models
- Incorporation of open geospatial standards and employment of open geospatial data for visualization as well as input for the sound models
- Scalability to the whole country and even beyond
- Real-time performance of wind turbine sound, shadow, visibility and wake area models

1.4.4. Analyzing the impact of spatial context on the heat consumption of individual households

Heating demand, especially in countries with colder climates, when combined with the use of fossil fuels increases global warming and environmental problems. The heating of houses accounts for a considerable share of total energy consumption. Therefore, a reduction in the heating demand of residential buildings leads to significant energy demand mitigation. The first step for such a mitigation is to have information on the factors affecting the heat demand of the residential sector. When these factors and their behaviour are known, proper policies can be taken in order to achieve the heat demand reduction target.

Four major groups of factors have an impact on household heat demand: occupants' behaviour, (interior) building design, the system's efficiency and the spatial context. While the first three factors depend mostly on individual choices that are difficult to influence through urban planning, the last factor (spatial context) can be influenced by planners. Yet the impact of spatial context on household heat demand has had limited attention. This may be due to the lack of geospatial data and massive computer processing requirements. The aim of this study is to explore the combined impact of building shape and its surroundings on household heat consumption, both at individual household level and postal code level. Highly detailed geospatial data has been used to capture the characteristics of all individual buildings in Amsterdam and their spatial context. The 2D/3D spatial context of all the buildings is characterized using the spatial data processing routines that characterized buildings' shapes and their surroundings. The applied routines employed massive geospatial data and mathematical algorithms for the automated extraction of building shape characteristics, height, area, roof shape, exposed perimeter, as well as their spatial context variables, sky view factor, urbanization degree and tree volume. These variables, together with other building characteristics (year of construction) and the measured gas consumption per household have been applied in a multi-linear regression analysis to explore the relation between the heat consumption of individual buildings and their spatial context. In addition to the individual level, a separate regression analysis was performed at postal code level to study the impact of urban configuration variables on heat consumption at a different scale. At this scale, we are able to include demographic variables in the regression model, which enables us to investigate the relative contribution of these variables compared to that of spatial context variables on heat consumption. This study covers the following research objectives of this thesis:

- Improving process models (through exploring the impact of the geospatial context (2D and 3D) on household heat demand).
- Increasing the detail level of process models to individual household level
- Expanding the research area to the whole city rather than specific parts
- Applying detailed 2D/3D open geospatial data as the explanatory variables

1.4.5. From BIM to geo-analysis: view coverage and shadow analysis by BIM/GIS integration

Environmental analyses in urban areas, play an important role in different decision making processes. This includes analyses regarding current processes as well as those of new designs. An important aspect in such analyses is a consideration of the multiple processes which play a role in an urban area. This expresses the necessity of data integration from different domains and sources. These data might be from different disciplines, levels of detail and information models, which makes integration challenging. A well-known instance of such an integration challenge is BIM-GIS integration. BIM (Building Information Model), an important information source for different urban area analyses (such as urban planning), contains detailed geometrical and semantic information of a construction. This rich information source is often, however, not integrated with large-scale geospatial data due to the different level of detail in the BIM information model compared to geospatial datasets in a GIS system, caused by different scales. GIS, on the other hand, contains a physical and functional representation of the environment. The integration of BIM and GIS enriches both BIM and GIS environments and provides the opportunity for different automated detailed analyses on a large extent and will broaden analysis possibilities on the mutual impact of a building (including detailed semantic/geometric information) and its environment. [From a BIM perspective] This integration can be beneficial in different phases of BIM, from initial planning to maintenance, due to the impact of the environment on the construction and the corresponding decisions and actions which should be taken. [From a GIS perspective] This integration provides the opportunity for detailed analyses on the impact of BIM (building and infrastructure) on the environment.

While BIM can be modelled through different proprietary formats, the employment of open standards can reduce its interoperability obstacles and support its broader applications in different domains. Industry Foundation Classes (IFC) is the most common open standard for BIM data exchange. It is an object-based data model for the exchange of detailed geometric and semantic information on a construction. In this study, we have developed and implemented a routine for the automated integration of an IFC BIM model in a 3D GIS environment. We have applied BIM-GIS integration in two studies, namely, view coverage and shadow analysis. In the view coverage analysis, detailed information on windows have been extracted automatically from a BIM model, which was integrated in the 3D GIS environment. Based on the location and geometry of each window, the view quality for each window has been determined through an indicator, defined from existing 3D geospatial elements (3D building and 3D tree models). In the second study, roof segments derived from the BIM model were used with the generated 3D shadow models of surrounding buildings and trees (using 3D buildings and tree models) to estimate the rooftop portions lying in the shadow (for a specific time and date). The routines developed lead to the automation of the whole process from BIM-GIS integration to the different analyses, which is beneficial for fast and accurate analyses on a large scale. This study covers the following research objectives:

- Integration of data from different domains
- Applying open standards for the incorporation of geospatial data

- Connection to process/impact models for view coverage and shadow analysis
- Applying 3D geospatial data for these analyses

The position of the chapters within the framework of this thesis is depicted in Figure 2.

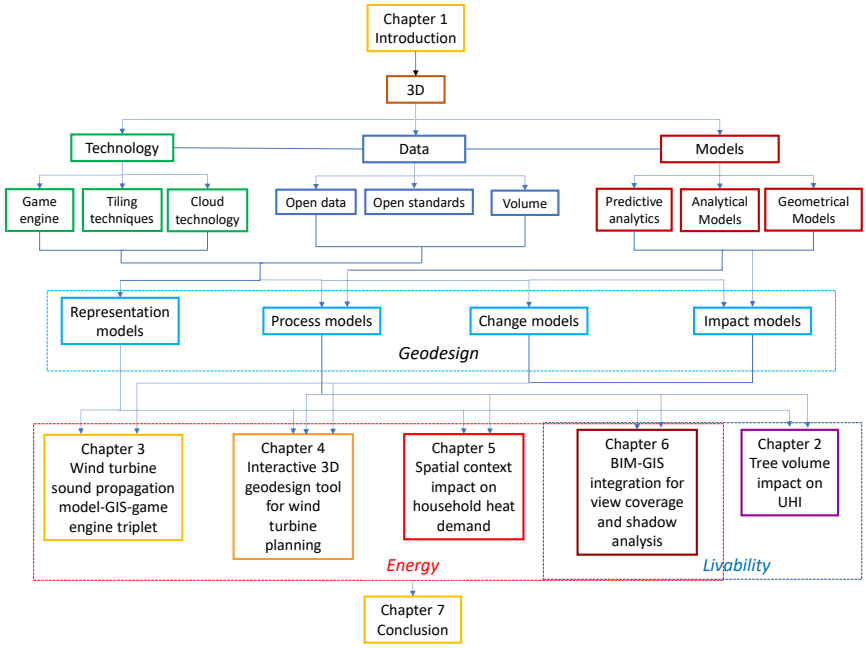

Figure 2. Thesis outline: the position of research papers in the thesis framework.

Chapter 2: Local impact of tree volume on nocturnal urban heat island: A case study in Amsterdam[1]

Abstract

The aim of this research is to quantify the local impacts of tree volumes on the nocturnal urban heat island intensity (UHI). Volume of each individual tree is estimated through a 3D tree model dataset derived from LIDAR data and modelled with geospatial technology. Air temperature is measured on 103 different locations of the city on a relatively warm summer night. We tested an empirical model, using multi-linear regression analysis, to explain the contribution of tree volume to UHI while also taking into account urbanization degree and sky view factor at each location. We also explored the scale effect by testing variant radii for the aggregated tree volume to uncover the highest impact on UHI. The results of this study indicate that, in our case study area, tree volume has the highest impact on UHI within 40 meters and that a one degree temperature reduction is predicted for an increase of 60,000 m^3 tree canopy volume in this 40 meter buffer. In addition, we present how geospatial technology is used in automating data extraction procedures to enable scalability (data availability for large extents) for efficient analysis of the UHI relation with urban elements.

2. 1. Introduction

A negative impact of urbanization is the urban heat island phenomenon which is the increase in temperature of a metropolitan area (in relation to the rural outside) due to human activities (Oke, 1995). Two instances of extreme urban heat island hazards are the heat-related deaths of 485 people during the Chicago heat-wave in 1995 (Whitman et al., 1997) and the 130% increased mortality rate in Paris and suburbs during the Western Europe heat-wave in 2003 (Grynszpan, 2003). In addition to the public health effects, urban heat island increases the demand for air-conditioning-related energy consumption (Akbari, 2005). When considering the contemporary rapid urbanization growth (McMichael, 2000), serious attempts should be dedicated to mitigate the heat island formation in urban areas. This study contributes to exploring the role of trees on UHI mitigation. This is performed by inspecting tree volume influence on UHI variations across the city of Amsterdam, the Netherlands.

[1] This chapter is published in Urban Forestry & Urban Greening journal as: Rafiee, A., Dias, E., & Koomen, E. (2016). Local impact of tree volume on nocturnal urban heat island: A case study in Amsterdam. Urban forestry & urban greening, 16, 50-61.

Formatted: Font: 16 pt, Font color: Auto, English (United States)

Formatted: Font: Calibri, 11 pt, Not Bold, English (United States)

Formatted: Justified

Formatted: English (United States)

Formatted: Font: Not Bold

Formatted: Font: Not Bold, Font color: Auto

Formatted: Font: Not Bold

Formatted: Font: Not Bold, Font color: Auto

Formatted: Font: Not Bold

Formatted: Font: Not Bold, Font color: Auto

Formatted: Font: Not Bold

2.1.1. Relevant Studies

Urbanization and construction growth in cities have a direct influence on the urban heat island formation and its increase. Urbanization causes surface and atmospheric changes that lead to warmer temperatures, especially at night (Voogt and Oke, 2003). Chen et al. (2006) concluded that the urbanization in Pearl River Delta was the major contributor to the regional temperature rise in this region from 1990 to 2000. Next to the regional impact of urbanization, certain parameters have more local influence on UHI, such as different street designs and built environment configuration can lead to different UHI values across neighbourhoods (Shashua-Bar and Hoffman, 2003; Swaid and Hoffman, 1990; Bourbia and Boucheriba, 2010; Nakamura and Oke, 1988; Giridharan et al., 2005). A key urban design parameter is Sky View Factor (SVF), which is the extent of visible sky from a location. SVF relates to the ability of that location to cool down, where low SVF causes a slow rate of heat emission at night (Oke, 1982). Previous studies have demonstrated that the locations which are more open to the sky, e.g. near the top of the canyon, lose heat approximately four times faster than the points near to the floor (Oke, 1988), making SVF a very useful indicator to express the magnitude of urban heat island (Yamashita et al., 1986).

Another important parameter affecting urban heat island intensity is vegetation. Vegetation influences temperature through shading as well as evapotranspiration (Solecki et al., 2005). Previous research concluded that vegetation mitigates UHI and improves urban microclimate through reducing summer temperatures (Dimoudi and Nikolopoulou, 2003). This temperature reduction effect is not only present within the green area itself, but also beyond it. Wong and Yu (2005) observed a maximum of around 4 degree difference between the planted and the central business district in Singapore at summer midnight. Yu and Hien (2006) carried out a research on the thermal benefits of city parks in Singapore. They came to the conclusion that temperature reduction caused by vegetation was not bounded to parks, but also to the neighbouring regions based on their distances to the park. Their other observed phenomenon was the fluctuation stabilization of temperatures by vegetation (more than buildings). Benefits of urban parks on UHI mitigation in different regions have been acknowledged and quantified in various studies (Chang and Li, 2014; Jauregui, 1991; Hamada and Ohta, 2010). Vegetation impact on UHI is not limited to urban forestry and city parks. Pocket parks and local street vegetation might play an important role on UHI, depending on the environmental settings and urban configuration. While in the compact mid-rise urban area of Rotterdam, vegetation can have a dominant influence on local UHI (Heusinkveld et al., 2014), in a compact high-rise region such as Hong Kong, vegetation exclusively might not lead to considerable outdoor temperature reduction. In such an urban environment, impact of parameters like sky view factor and altitude should be fully considered, when introducing vegetation, for noticeable results (Giridharan et al., 2008). While the studies regarding vegetation impact on UHI mainly use vegetation surface in their investigations, information on vegetation volume can produce additional insights as the shading and evapotranspiration cooling characteristics are more correlated with the vegetation 3D geometry rather than its surface. However, according to Armson et al. (2012), the three dimensional characteristics of trees have not sufficiently being investigated in UHI studies. In this research we have used the 3D information of individual

Formatted: Space After: 10 pt
Formatted: English (United States)
Formatted: Font: Not Bold, English (United States)
Formatted: Font: Times New Roman, 12 pt
Formatted: Normal, Justified
Formatted: Font: Times New Roman
Formatted: Font: Times New Roman, Font color: Auto
Formatted: Font: Times New Roman

urban trees, extracted from high resolution LIDAR dataset, to estimate the spatial extent and volumetric impact of trees on nocturnal UHI in the city of Amsterdam. We believe that estimating the impact of local street trees on UHI can inform urban planners, designers and urban health practitioners on the endorsement of the urban green planning for more liveable cities.

2.1.2. Research objectives

This research attempts to investigate the effect of trees, in particular tree crown volume, in its capacity to mitigate UHI in the city of Amsterdam. While it is acknowledged that the presence of trees may reduce temperature, this study demonstrates a methodology that studies how many trees and of which size is necessary to plant in order to achieve significant effects. An additional contribution of this research is the demonstration of a scalable methodology to determine the impact of tree volume. The added value of geospatial information and GIS techniques in our analysis is presented through automation in information extraction from large datasets. This methodology enables the use of nation-wide datasets for trees in different extents without the need for tree field data measurements.

2.2. Methodology

2.2.1. Study area

Our study area is Amsterdam, the capital and the largest city of the Netherlands, with a total population of around 800000 inhabitants and an area slightly larger than 200 km^2. This city contains diverse land uses including built-up areas, parks, forests, agricultural lands, water bodies and industrial regions which leads to diversity in population distribution in the city (Figure 1).

Formatted: Font: Not Bold
Formatted: Normal
Formatted: Space After: 10 pt
Formatted: Font: Times New Roman, 12 pt
Formatted: Normal, Justified
Formatted: Font: Not Bold
Formatted: Normal
Formatted: Font: 14 pt, English (United States)
Formatted: Heading 2, No bullets or numbering
Formatted: Justified

Figure 1. Map of Amsterdam (municipality borders in blue) depicting the built-up and green spaces in the city.[2]

The vast built-up and the densely populated areas of Amsterdam lead to urban heat island formation in the city. Measurements of the recent heat wave in 2006 revealed the maximum 7-9 degrees nocturnal air temperature difference between Amsterdam and its surrounding suburb. This categorizes Amsterdam as a city with strong urban heat island intensity compared to other European cities (Van der Hoeven and Wandl, 2015).

2.2.2. UHI analysis

Formatted: Heading 2, No bullets or numbering

Formatted: Justified

In this study ordinary least squares regression analysis has been used to determine the contribution of different factors to the UHI variation. Tree volume is expected to have an impact on air temperature from shadowing effects (protecting surrounding structures from direct irradiation therefore absorbing less heat) and from evapotranspiration. Nevertheless, the variation of trees' impact on UHI within different distances is unclear. In order to define the maximum impact of tree volume on UHI from a local perspective, we have studied different buffers with variant radii around each temperature observation. We defined the tree volume for our model by taking into account the total tree volume within different buffer zones and performed an independent regression analysis for each buffer radius. The buffer zones range from 10 meter to 100 meter (using 10 meter increasing steps) and additional buffer radii of 120, 150, 200, 250 and 300 meters. Note that this research aims to assess the impacts of the total tree volumes in different buffer zones around the UHI measurements to explore their influence variation on different extents.

[2] Map background source: TOP10NL, the Dutch cadastral topographic map (http://www.kadaster.nl/web/artikel/producten/TOP10NL.htm); Amsterdam municipality border source: Centraal Bureau voor de Statistiek (http://www.cbs.nl/nl-NL/menu/themas/dossiers/nederland-regionaal/publicaties/geografische-data/archief/2012/2012-wijk-en-buurtkaart-2011-art.htm); visualized using ArcGIS software.

Formatted: English (United States)

As urbanization intensity (the amount of urban) is acknowledged to be the leading factor for urban heat island formation, we take it into account, using a self-defined indicator, in steering the main variations of UHI. Taking this "urbanization degree" (as a regional variable) into account assists in uncovering the influence of local variables in explaining UHI spatial variation. Beside tree volume, sky view factor is another local parameter which is assumed to have influence on UHI. By bringing this local parameter into the regression model, its potential influence on UHI is taken into account and improve the estimations of tree volume impact. Similarly to tree volume, SVF impact on UHI may also vary when using the mean SVF of increasing ranges to a temperature observation location. To account for the influence of the neighbouring locations on the air temperature, this study uses the mean SVF values of the region around the temperature observations. Accordingly, buffers with different radii for the estimation of SVF mean values are defined. In each buffer, a separate regression analysis is performed for the evaluation of SVF impact on UHI in various distances.

Although Amsterdam contains large water bodies and this has been identified to have influence on temperature (Oláh, 2012; Steeneveld et al., 2014), we do not use water in our explanatory model as our UHI observation time (around sunset) corresponds to the moment when water switches from a heat sink to a heat source (Theeuwes et al., 2013). In précis, we have used multi-linear regression method to estimate the impacts of urbanization degree, SVF and tree volume on the variation of UHI (the difference between the measured temperature and the temperature of the rural station). This value presents the temperature difference between inner city and rural suburbs caused by urban heat island.

As the focus of this research is to uncover the impact of tree volume on urban heat island intensity, standardized beta coefficient and significance of the aggregated tree volume for different buffer sizes were calculated to determine the most appropriate buffer that represents the distance within which trees most significantly affect local temperature.

Based on the mentioned variables, we propose the regression model;

$$UHI = \beta_{UD} \times UD + \beta_{TV} \times TV_{Total} + \beta_{SVF} \times SVF_{Mean} + Constant \quad (1)$$

where UHI is the difference between the measured temperature and the temperature at reference rural station, UD is urbanization degree, TV is the total tree volume in the selected buffer (m^3), and SVF is the mean SVF in the selected buffer. Estimation of explanatory variables are explained in more details in the following sections.

2.2.3. *Urbanization degree*

In this study we have classified urban/nonurban elements using the land-use map of the study area to estimate urbanization degree. The aggregated area of non-urban elements (e.g. grasslands and parks) in the proximity of an observation location has been used to separate suburbs from the inner city. We applied the same definition of rural area as Wong and Yu (2005) by taking into account the green spaces and used the same method of determining the degree of urbanization in a circular neighbourhood as in Koomen and Diogo (2015). Urbanization degree is constructed by subtracting the area of the non-urban elements from total

Formatted: Font: Times New Roman, 12 pt
Formatted: Normal, Justified, Space After: 0 pt
Formatted: Font: Times New Roman, 12 pt
Formatted: Justified, Space After: 10 pt
Formatted: English (United States)
Formatted: Justified, Space After: 10 pt, Tab stops: Not at 2,18 cm
Formatted: Heading 2, No bullets or numbering
Formatted: Justified, Space After: 10 pt

buffer area around the observations divided by the buffer area. The proximity distance is a trade-off between a large enough buffer to distinguish the regional-scale urbanized area from local build-up of the city and a small enough radius to separate the urban from suburbs. The radius of the Amsterdam city centre is about 3 km and the lowest area of non-urban elements exist within this region. Therefore to capture the most urbanized region, the buffer distance of 3km is the most suitable for Amsterdam. When the buffer centre moves from the inner city to the suburbs, the portion of non-urban elements increases, which means a decrease in urbanization degree. The processing steps for the estimation of urbanization degree are depicted in Figure 2.

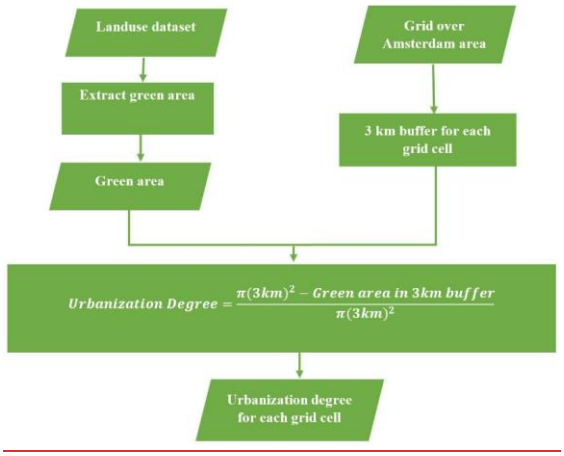

Figure 2. Urbanization degree estimation

2.2.4. SVF estimation

Sky View Factor (SVF) is defined for each given point as the degree to which sky is visible for that point and is not restricted by surrounding objects. It represents the degree of urbanization locally, opposed to the mentioned urbanization degree which is in regional scale. According to Watson and Johnson (1987), SVF is the ratio of solar radiation received by a planar surface to the solar radiation obtained from the whole hemispheric radiating environment. SVF for each point can be calculated using height model of its surrounding.

We used the Johnson and Watson (1984) definition of SVF for the non-symmetrical canyon with finite length:

$$\psi_s = 1 - (1/2\pi\{(\gamma_2 - \gamma_1) + \cos\beta[tan^{-1}(\cos\beta\ \tan\gamma_1) - tan^{-1}(\cos\beta\ \tan\gamma_2)]\}) \quad (2)$$

Formatted: Normal, No bullets or numbering

Formatted: Font: Times New Roman, Not Bold

Formatted: Font: Times New Roman, Not Bold

Formatted: Font: Times New Roman

Formatted: Heading 2, Space After: 0 pt, No bullets or numbering

Formatted: Justified

Formatted: English (United States)

Where ψ_s is SVF, γ_1 *and* γ_2 are the azimuth angles of the wall ends, β is the elevation angle of the wall top from the line passing through the surface element and parallel to the wall. SVF ranges from 0 to 1 which zero means absolute obscured sky and 1 means total visible sky (open area). The higher the SVF for a point, the easier is the heat release at night. A low SVF leads to slower heat release by urban objects (e.g, buildings) at night and therefore higher nocturnal heat island. Based on the Dutch LIDAR[3] data, we generated a detailed height raster grid to calculate SVF map of Amsterdam. This dataset (AHN2[4]) contains point clouds with the average point density of 6 to 10 points per square meter and a maximum of 5 centimetre systematic and stochastic error (Van der Zon, 2011).

As discussed in section 2.2, the mean value of SVF inside different buffer zones around the observation points are estimated and applied in separate regression analysis. Figure 3 illustrates the workflow for SVF estimation within a specific buffer radius around observation locations.

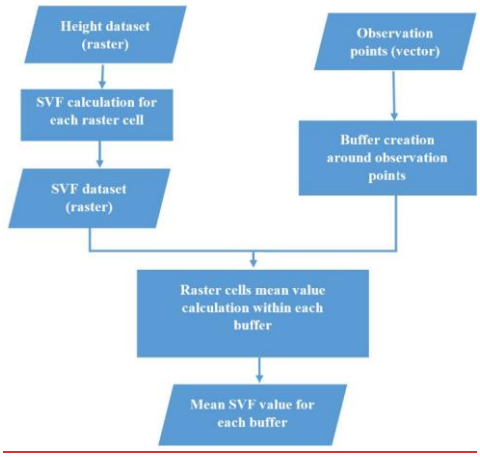

Figure 3. SVF mean value estimation inside a specific buffer zone around temperature observation locations

2.2.5. *Tree Volume*

We calculated the tree volume using an existing 3D tree model dataset[5] of the study area. This dataset represents individual trees based on the Silvistar tree model (Koop, 1989) using the same LIDAR data (AHN2) to determine the parameters.
The Silvistar 3D asymmetric single tree model is described through eight points, namely tree base, first fork location, tree crown top ad base positions and the coordinates of the four periphery points. The locations of the tree base as well as the four peripheral points should

[3] Light Detection And Ranging
[4] AHN2 was collected and made available by the Dutch Water Boards and Rijkswaterstaat, part of the Ministry of Infrastructure and the Environment (http://www.ahn.nl/).
[5] This dataset has been developed by (anonymous due to double-blind review) from Alterra, the Netherlands (http://www.boomregister.nl/)

Formatted: Justified
Formatted: Normal, No bullets or numbering
Formatted: Font: Times New Roman, Not Bold
Formatted: Font: Times New Roman, Not Bold
Formatted: Font: Times New Roman
Formatted: Heading 2, Space After: 0 pt, No bullets or numbering
Formatted: Justified
Formatted: English (United States)
Formatted: English (United States)
Formatted: English (United States)
Formatted: English (United States)

originate from observations while the locations of the tree fork and tree crown top and base are calculated from the tree base eccentricity in the crown projection. Therefore Silvistar 3D single tree model requires the minimum measured points which is explained in Figure 4.

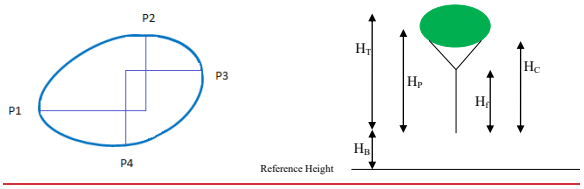

a b

Figure 4. Silvistar tree model parameters (source: Koop, 1989).

Formatted: Justified

The 3D tree model consists of horizontal quarter ellipses and vertical crown curves. Vertical crowns are calculated through quadratic equation of an ellipse with a varying exponent; while the horizontal crown sections are defined through other sets of quarter ellipses at each height level (Koop, 1989). The vertical curves through the tree crown top and base as well as the peripheral points are generated through equation 3 which is cognate to the quadratic equation of the ellipse but with varying E exponent:

$$x^E/a^E + y^E/b^E = 1 \quad (3)$$

where a and b are the axis halves of the vertical crown curve and x and y are the coordinates of the interpolated points on the crown transverse section.

Formatted: Justified

The variance in exponent E makes the vertical curves more convex or concave. At each height level, the horizontal ellipse connects the intersection points between the plane and the vertical curves.

The coordinates of the four input periphery points, tree base and the required tree heights of Silvistar model are extracted from airborne LIDAR dataset. The periphery points are the extreme ends of point clusters of each individual tree which are detected automatically from LIDAR dataset. The resulting 3D tree model consists of 32 faces out of 26 node. Figure 5 demonstrates an example of this 3D tree model.

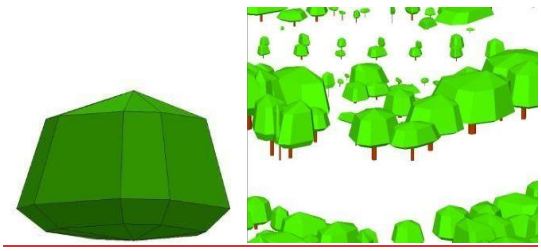

Formatted: Space After: 0 pt

a b

Figure 5. Dutch 3D tree model.
a) single 3D tree model. The models consists of 32 faces and 26 nodes.
b) 3D tree crown models and 3D stem models. Note that the model captures the diversity in size and shape of trees, essential for the volume estimation. The minimum height and width of trees are around 2 meters.

2.3. Results

Formatted: Font: 14 pt, English (United States)

Formatted: Justified

To calculate the influence of trees on Amsterdam's nocturnal heat island, air temperature measurements were performed while riding a bicycle equipped with a thermometer and GPS logger on 18 June 2013 in Amsterdam, starting just after sunset. The devices (GPS logger and thermometer) were shielded from direct wind in an open box mounted on the bicycle (as our measurements occurred just after sunset, it was not necessary to protect the device from solar radiation). The accuracy of these devices are comparable to the similar ones applied in other UHI studies (e.g. koomen and Diogo, 2015; Heusinkveld et al., 2010). The applied temperature measurement devices are easily accessible and relatively simple to use. Deployment of the devices on a bicycle provides the possibility of fast exploration of the city (covering a larger area than if walking and including car-inaccessible locations). The thermometer is sensitive to wind and direct solar radiation, therefore it should be shielded (in the case of diurnal temperature measurements). Table 1 presents the specifications of the devices used for temperature measurements.

Formatted: English (United States)

Table 1. Specifications of the devices used for temperature measurements

Specification	GPS position logger	Temperature logger
Manufacturer	Canmore	Lascar
Model name	GT-730	EL-USB-1-Pro
Logger resolution	0.000001 decimal degree (WGS84)	0.1°C

Formatted: Justified

The sky on this day was clear, there was calm wind (average wind speed was around 2.5 m/s) and temperature was relatively high (the average temperature during the day was around 23 degrees). Temperature observations were performed from 22:30, just after sunset when the highest nocturnal temperature is expected (Oke, 1982; Van Hove et al., 2015) and most important, this time coincides with the start of the resident's sleeping time at which the thermal comfort is a requirement for an appropriate sleep (Ihara et al., 2011).

To calculate UHI, each measured temperature is related to the time-linked temperature reported at Schiphol airport official weather station. This station is situated outside the urban perimeter of Amsterdam (10 km from the city centre) and is embedded in a rural setting. Using this rural reference, we estimate UHI using simple algebra:

$$UHI = Temp - Temp_{ref} \quad (4)$$

where $Temp$ is the measured temperature of a location, $Temp_{ref}$ is the temperature at the reference rural station and UHI is the difference between these two values which indicates the UHI of the location. Figure 6 presents the measurement locations and UHI values overlaid on the aerial photo of Amsterdam.

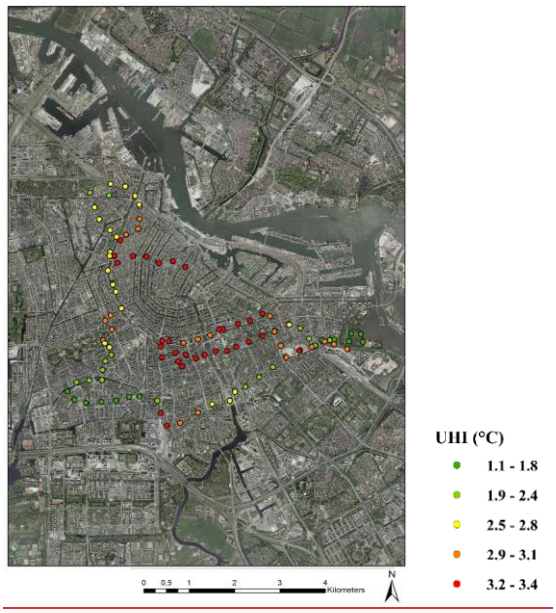

Figure 6. Temperature observations overlaid on the aerial photo of Amsterdam[6].

3D tree models and sky view factor were developed using detailed height data of the Netherlands (AHN2). Figure 7 presents AHN2 dataset and the resulting 3D tree models and building models.

[6] Aerial photo source: PDOK (http://www.PDOK.nl/); visualized using ArcGIS software.

Formatted: Justified

Formatted: Justified

Formatted: English (United States)

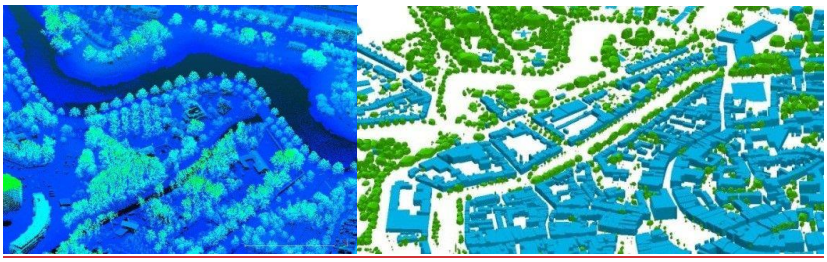

a b

Figure 7. a) LIDAR height data, colorized based on height and b) resulting 3D tree models from Silvistar model next to 3D building models;

Using the 3D tree dataset, we calculated the volume of each individual tree in Amsterdam as one of the independent variables of the regression model. Based on the tree volumes, we classified the trees of our study area into 3 categories using Jenks Natural Break classification. This classification method minimizes the variance within each class and maximizes the variance between classes (Jenks, 1967). The categories include, small, medium and large trees (see Table 2).

Table 2. Characteristics of the tree classes; small, medium and large tree classification based on the tree volume of the study area (using natural break intervals).

Tree Category	**Volume interval (m^3)**	**Average width (m)**	**Average length (m)**	**Average height * (m)**	**Percentage in the study area**
Small	<=1300	6	10	6	85%
Medium	>1300 AND <=4916	14	18	10	13%
Large	>4916	20	30	15	2%

*height indicates the difference between tree top height and tree fork height.

Sky view factor is another local factor, along with tree volume, which has influence on urban heat island intensity. For each given point, SVF was calculated according to equation 2 using height data. As mentioned before, this variable indicates the amount of open sky for any given

Formatted: Centered, Space After: 0 pt

Formatted: Space After: 0 pt

Formatted: Justified

Formatted: Justified

location and reflects the night heat release speed (which was accumulated during the day). Figure 8 presents the SVF map of the study area.

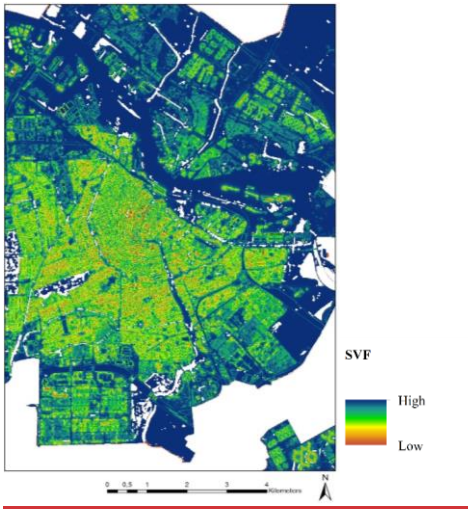

Figure 8. Sky view factor map of Amsterdam.

Opposed to the micro impact of tree volume and SVF, urbanization degree is assumed to have regional effect on UHI. To estimate the local effect of tree volume on UHI, we have included urbanization degree in the regression model to account for its leading impact on urban heat island intensity. Urbanization degree is defined in this research as the urban ratio in 3 km proximity calculated from reclassifying the authoritative land use map of the Netherlands, at the scale 1:10.000[7]. Figure 9 presents the generated urbanization degree of the study area as well as the whole Amsterdam. Red zones demonstrate intense urbanized areas whereas green presents the dominance of non-urban regions.

Formatted: Justified

[7] This dataset has been published by Centraal Bureau voor de Statistiek (CBS) from the Netherlands (http://www.cbs.nl/nl-NL/menu/home/default.htm) in 2010.

Formatted: English (United States)

Formatted: English (United States)

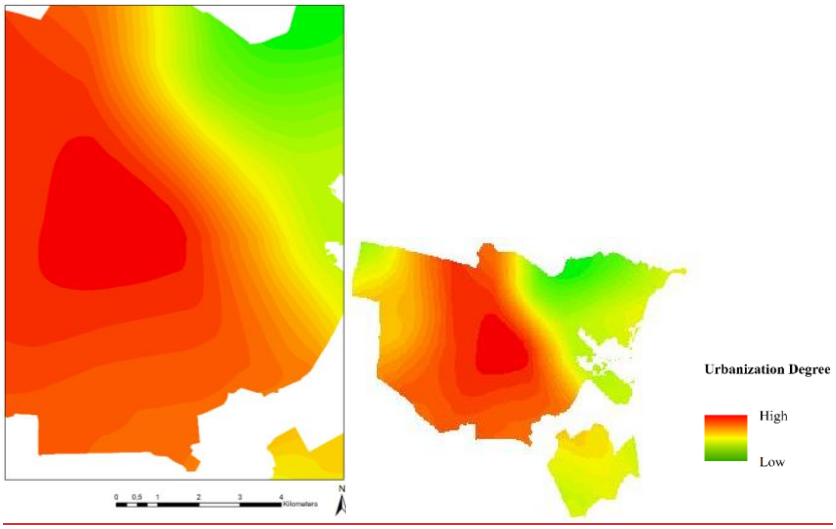

a b

Figure 9. Resulting map from urbanization degree estimation a) study area and b) whole Amsterdam

Table 3 presents the descriptive statistics of the independent variables used in this research.

Table 3. Descriptive statistics of the independent variables

Variable	N	Minimum	Maximum	Mean	Std. Dev
Urbanization Degree (0-1)	103	0.86	0.94	0.91	0.013
Tree Volume (m^3)	103	0.00	1489780.00	129838.82	196643.79
SVF (0-1)	103	0.58	1.00	0.82	0.077

The tree volume impact was studied by exploring different buffers around the UHI measurement points in order to identify the size of the area in which green volume most significantly affects the urban temperature.
For each buffer zone, a separate linear regression analysis is performed in which urbanization degree and SVF remain the same and tree volume differs based on the total tree volumes existing within that zone.

Formatted: Space After: 0 pt
Formatted: Font: Not Bold
Formatted: Justified
Formatted: Justified

The resulting beta coefficients and statistical significances of tree volume from each regression analysis, as well as the R^2 of the model, are presented in Table 4.

Table 4. Regression analysis results for variable tree volume buffer. (N=103, UHI range: 1-3.4°C, Urbanization Degree range: 0.86- 0.94, SVF_{Mean}: range 0.64-0.99.

Formatted: Font: 11 pt, English (United States)

R^2	Variable	Standardized Beta	Beta	Significance	Tree Volume range
0.411	Urban Degree	0.531	23.626	0.000	Tree Vol_{Total}.: 0 – 3529 m^3
	Tree volume (10 meter buffer)	-0.198	0.000	0.012	
	SVF	-0.168	-1.199	0.040	
0.420	Urban Degree	0.512	22.762	0.000	Tree Vol_{Total}.: 0- 18691 m^3
	Tree volume (20 meter buffer)	-0.220	-4.055E-005	0.005	
	SVF	-0.184	-1.308	0.024	
0.442	Urban Degree	0.515	22.901	0.000	Tree Vol_{Total}: 0- 31523 m^3
	Tree volume (30 meter buffer)	-0.264	-2.508E-005	0.001	
	SVF	-0.177	-1.259	0.026	
0.443✤	Urban Degree	0.513	22.79	0.000	Tree Vol_{Total}: 46-51411 m^3
	Tree volume (40 meter buffer)	-0.268	-1.609E-005	0.001	

	SVF	-0.167	-1.189	0.036	
0.438	Urban Degree	0.508	22.606	0.000	Tree Vol_{Total}: 342-77700 m^3
	Tree volume (50 meter buffer)	-0.261	-1.101E-005	0.001	
	SVF	-0.157	-1.121	0.050	
0.442✤	Urban Degree	0.510	22.657	0.000	Tree Vol_{Total}:1139-107096 m^3
	Tree volume (60 meter buffer)	-0.268	-8.646E-006	0.001	
	SVF	-0.150	-1.072	0.060	
0.439	Urban Degree	0.513	22.813	0.000	Tree Vol_{Total}:1608-134026 m^3
	Tree volume (70 meter buffer)	-0.262	-6.723E-006	0.001	
	SVF	-0.149	-1.064	0.063	
0.430	Urban Degree	0.515	22.887	0.000	Tree Vol_{Total}:2718-156417 m^3
	Tree volume (80 meter buffer)	-0.243	-5.140E-006	0.002	
	SVF	-0.154	-1.094	0.058	
0.426	Urban Degree	0.516	22.924	0.000	

	Tree volume (90 meter buffer)	-0.235	-4.188E-006	0.003	Tree Vol_{Total}:2782-180521 m^3
	SVF	-0.159	-1.131	0.050	
0.425	Urban Degree	0.515	22.891	0.000	Tree Vol_{Total}: 2905-208615 m^3
	Tree volume (100 meter buffer)	-0.231	-3.489E-006	0.003	
	SVF	-0.166	-1.186	0.040	
0.416	Urban Degree	0.516	22.940	0.000	Tree Vol_{Total}:4311-269378 m^3
	Tree volume (120 meter buffer)	-0.204	-2.298E-006	0.010	
	SVF	-0.178	-1.271	0.028	
0.407	Urban Degree	0.515	22.888	0.000	Tree Vol_{Total}:7212-3591080m^3
	Tree volume (150 meter buffer)	-0.182	-1.459E-006	0.022	
	SVF	-0.182	-1.297	0.026	
0.420	Urban Degree	0.504	22.422	0.000	Tree Vol_{Total}:36015-699506 m^3
	Tree volume (200 meter buffer)	-0.216	-1.062E-006	0.006	
	SVF	-0.182	-1.299	0.024	

0.413	Urban Degree	0.497	22.115	0.000	Tree Vol_{Total}:57529-1147800 m^3
	Tree volume (250 meter buffer)	-0.199	-6.713E-007	0.013	
	SVF	-0.185	-1.320	0.023	
0.401	Urban Degree	0.503	22.345	0.000	Tree Vol_{Total}:124052-1489780 m^3
	Tree volume (300 meter buffer)	-0.166	-4.201E-007	0.039	
	SVF	-0.185	-1.322	0.024	

Note: SVF is mean SVF within a 30 meter buffer around the temperature observation point. This radius corresponds to the average street canyon width at the observation locations. The effect of varying SVF_{Mean} radii is explored in table 5.

✣ Largest standardized beta coefficient.

Formatted: English (United States)

Formatted: Justified

As expected, urbanization degree, is the most influential factor on urban heat island intensity value. As it can be seen in table 4, the beta coefficient of urbanization degree is the highest compared to tree volume and SVF and does not change considerably with the varying buffer radii. This value stays around 0.512 for different buffer zones and is significant in all buffer radii. Buffer radii between 30 and 70 meters lead to the largest beta coefficient for tree volume and the highest overall R^2. In particular, the buffer radii of 40 and 60 meter produce the highest beta coefficient (standardized beta = -0.268). Consequently, the highest local impact of tree volume on UHI is characterized by the minimum buffer distance of 40 meters. Figure 10 presents the aggregated tree volume in 40 meters buffer distance.

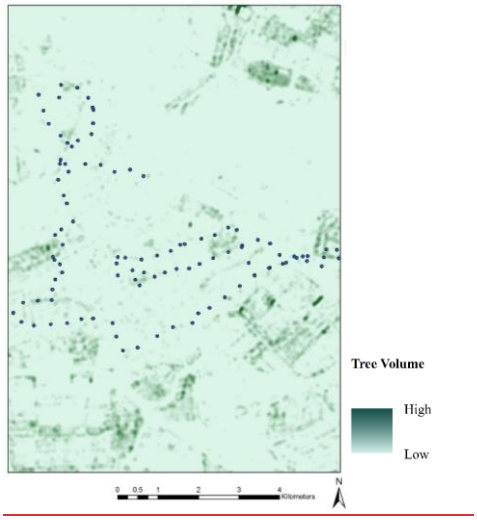

Figure 10. Tree volume map as one of the regression model input. Each cell presents the total tree volume within its 40 meter buffer.

In the 40 meter buffer, the beta coefficient of sky view factor is -0.167 which expresses the weaker impact of this parameter compared to tree volume in this radius. In the next step, the mean value of SVF in different buffer radii is used to investigate the variation of SVF impact and the total R^2 of the regression model using different buffer distances. The buffer radius for tree volume is fixed to 40 meter in these calculations. The results are presented in Table 5.

Table 5. Regression analysis results for variable SVF buffers (N=103, UHI range: 1-3.4°C, Urbanization Degree range: 0.86- 0.94, Tree Vol_{Total} range: 46-51411m^3).

R^2	Variable	Standardized Beta	Beta	Significance	SVF_{Mean} range
0.436	Urban Degree	0.525	23.361	0.000	SVF_{Mean}: 0.61-0.99
	Tree volume	-0.275	-1.654E-005	0.000	
	SVF (15 meter buffer)	-0.140	-0.924	0.076	

Formatted: Font: 11 pt, English (United States)

0.443	Urban Degree	0.513	22.795	0.000	SVF_{Mean}: 0.64-0.99
	Tree volume	-0.268	-1.609E-005	0.001	
	SVF (30 meter buffer)	-0.167	-1.189	0.036	
0.438	Urban Degree	0.519	23.065	0.000	SVF_{Mean}: 0.60-0.99
	Tree volume	-0.266	-1.595E-005	0.001	
	SVF (40 meter buffer)	-0.148	-1.047	0.064	
0.438	Urban Degree	0.520	23.117	0.000	SVF_{Mean} 0.58-0.99
	Tree volume	-0.264	-1.586E-005	0.001	
	SVF (50 meter buffer)	-0.148	-1.030	0.063	
0.442	Urban Degree	0.517	23.004	0.000	SVF_{Mean}: 0.59-0.99
	Tree volume	-0.263	-1.579E-005	0.001	
	SVF (60 meter buffer)	-0.163	-1.165	0.040	

0.451	Urban Degree	0.513	22.798	0.000	SVF_{Mean}: 0.61-0.99
	Tree volume	-0.261	-1.566E-005	0.001	
	SVF (70 meter buffer)	-0.190	-1.415	0.016	
0.462	Urban Degree	0.508	22.585	0.000	SVF_{Mean}: 0.64-0.99
	Tree volume	-0.258	-1.547E-005	0.001	
	SVF (80 meter buffer)	-0.218	-1.734	0.005	
0.466	Urban Degree	0.507	22.536	0.000	SVF_{Mean}: 0.65-0.99
	Tree volume	-0.254	-1.524E-005	0.001	
	SVF (90 meter buffer)	-0.229	-1.910	0.003	
0.467	Urban Degree	0.508	22.572	0.000	SVF_{Mean}: 0.66-0.99
	Tree volume	-0.254	-1.527E-005	0.001	
	SVF (100 meter buffer)	-0.230	-1.986	0.003	

0.472	Urban Degree	0.504	22.393	0.000	SVF_{Mean}: 0.66-0.99
	Tree volume	-0.262	-1.575E-005	0.001	
	SVF (120 meter buffer)	-0.240	-2.144	0.002	

Note: Tree volume is average tree volume within a 40 meter buffer around each temperature observation point.

Figure 11 presents the comparison between tree volume and SVF standardized beta coefficient for different buffer radii.

Formatted: Justified

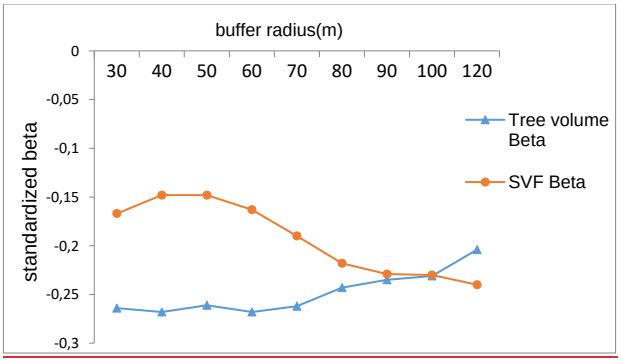

Figure 11. A comparison between tree volume and SVF standardized beta coefficient for different buffer radii.

The influence of sky view factor on urban heat island intensity increases with increasing the buffer radii. In smaller buffer zones, this parameter is not significant while in larger buffer zones it is significant. This behaviour is opposed to the behaviour of tree volume which has higher impact on smaller buffers and lower effects on the larger zones. This indicates that the impact of tree volume is larger at local scales than sky view factor. Choosing 40 meter as the buffer radius in which trees have the most influence on UHI, the regression is expressed as equation 1:

Formatted: Justified

$$UHI = 22.79 \times UD - 1.609 \times 10^{-5} \times TV_{Total} - 1.189 \times SVF_{Mean} + 5.770 \quad (5)$$

Where TV_{Total} is the total tree volume (in m^3) within 40 meter buffer and SVF_{Mean} is the SVF mean value within 30 meter buffer. Concerning the R^2, this model explains 44.3% of the variation of UHI. The remaining variation derives from unaccounted factors. One of these factors could be proximity to water, and since Amsterdam is characterized by interwoven water bodies, its temperature can be significantly influenced by water. However, we assume that around sunset, in a low wind condition, water does not have a direct impact on UHI due to water switching role from heat sink to heat source. While during the day water bodies (e.g. city lakes) act as cooling element and cool down the environment, at night the opposite occurs. During the night, the air temperature is lower than the water temperature and therefore water bodies warm their surroundings. This leads to temperature increase in the proximity of water at night (Theeuwes et al., 2013). This has been acknowledged for the specific case of Amsterdam where water did not present consistent impact on the nocturnal temperature (Koomen and Diogo, 2015).

Figure 12 presents the generated UHI map using the developed regression model (Equation 5).

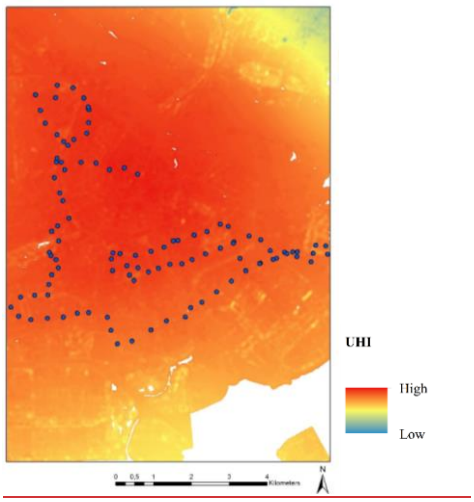

Figure 12. UHI map derived from the regression analysis (equation 4).

These results suggest that if a planner/designer wishes to mitigate one degree of UHI, he would need to account with extra 60000m^3 tree volume in 40 meter buffer zone (according to equation 5). In order to calculate on average how many trees (of which category) are needed to realise this volume, we need to take into consideration the geometrical characteristics of trees in the study area (table 2). The approximate required number trees of each tree class to fulfil 60000m^3 tree volume in 40 meter buffer is 90 small trees or 20 medium trees or 4 large trees (see Table 6).

Table 6. Approximate number of required trees in 40 meter buffer zone of a location for 1 degree UHI reduction based on our model. This number has been estimated through dividing the total

Formatted: Justified

Formatted: English (United States)

Formatted: Space After: 0 pt

Formatted: Justified

required tree volume in 40 meter buffer zone with average volume of an individual tree of each class (defined in Table 2).

Tree class	**Average volume (m^3)**	**Approximate Tree number to achieve 1°C mitigation.**
Small tree	650	90
Medium tree	3108	20
Large tree	13478	4

2.4. Discussion and Conclusion

Formatted: Font: 14 pt, English (United States)
Formatted: Heading 1, Space After: 0 pt
Formatted: Justified, Line spacing: Multiple 1,15 li

This research focused on exploring the impact of local trees on nocturnal urban heat island intensity of Amsterdam. It is acknowledged that trees mitigate UHI due to shading and transpiration. Both processes are related to the three dimensional aspect of trees and should be taken into account in such UHI investigations (Armson et al., 2012). In this study we have applied tree volumes derived from a 3D tree dataset of Amsterdam. To uncover the maximum local impact of trees on UHI, we have defined buffers with varying radii around each air temperature observation and aggregated the volume of trees inside the buffer. For each buffer radius, the impact of the aggregated tree volume on the UHI has been estimated using multi-linear regression analysis. Sky view factor, as another local parameter, and urbanization degree, as a regional parameter, were taken into account for each observation point as additional explanatory variables, next to tree volume, in the regression model.

Applying the regression for each buffer zone, the buffer radius in which tree volume impact is highest, was chosen as the local distance to which tree groups yield the highest influence on the local UHI. Results of this research show that the impact of tree volume is maximum on the smallest buffer radius of 40 meters. The regression model suggests that for the characteristics of the studied day, around 90 smaller trees or 20 medium trees or 4 large trees in 40 meter buffer zone of a location could lead to one degree decrease on its urban heat island intensity.

In addition, we have demonstrated an automated method for accurate data extraction and efficient analysis process using geospatial information. This solves the data scalability challenge and allows for efficient analysis for UHI studies.

The results of this research are derived for temperature observations on a relatively warm summer night of Amsterdam. The spatio-temporal robustness of the results are limited to the specific measurement day and areas surveyed. We expect that during extreme hot days (heat-

wave), when temperature rises above 35 degrees, the results would reveal larger impact of trees on UHI (Perini and Magliocco, 2014). Yet, this should be tested in future research. In addition, we suggest repeating this research for larger portion of Amsterdam as well as other cities with different configurations and characteristics to check the robustness of the developed model. Once more evidence is collected on the tree volume effect on UHI, such knowledge can be implemented in a decision support system to help decision process for urban planning. Further research on the relationship between urban trees and the electricity reduction costs, on large extent, using state of art geospatial data provides more direct outline on the economic benefits of urban trees- when compared with their planting and maintaining costs- since trees throughout a city influence the energy balance which affects the climate of the whole city (Simpson, 2002).

A limitation of this research is that it focussed on the geometric characteristics of trees as a UHI mitigation measurement, while other characteristics, such as evapotranspiration, leaf density and leaf area may play a role but were not included in this model. To address these, further research can also include tree species or field measurements to take into account evapotranspiration in the impact analysis of urban trees on UHI. Tree species, in addition to the crown volume, can be used as a proxy for the evapotranspiration estimations which is an influential factor on UHI (McPherson et al., 1995; Qiu et al., 2013). Alternatively, evapotranspiration can be measured in random locations within the study area through different approaches (Ding et al., 2013; Abtew and Melesse, 2013) and be applied in the analysis together with tree 3D geometrical characteristics for the better estimation of urban tree impact on UHI.

The outcomes of this research help, among others, urban planners and urban designers through providing quantitative results regarding the local impact of tree volume on urban heat island intensity which can be used for instance in cost-benefit analysis. We expect that these results contribute to the ongoing debate of UHI mitigation efforts in city planning by proposing a methodology to quantify local UHI causing factors. Environmental groups, citizens, citizen associations and policy makers can benefit from further research and more results around this debate.

Formatted: English (United States)

Chapter 3: Developing a Wind Turbine Planning Platform: Integration of "Sound Propagation Model–GIS-Game Engine" Triplet[8]

Azarakhsh Rafiee[1,3], Pim Van der Male[2], Eduardo Dias[1,3] and Henk Scholten[1,3]

[1] Department of Spatial Economics/SPINlab, VU University Amsterdam, De Boelelaan 1105, 1081 HV Amsterdam, The Netherlands

[2] Department of Hydraulic Engineering, Delft University of Technology, Mekelweg 2, 2628 CN Delft, The Netherlands

[3] Geodan Research Department, President Kennedylaan 1, 1079MB Amsterdam, The Netherlands

Abstract

In this study, we propose an interactive information system for wind turbine siting scenario formation, considering its visual and sound externalities. This system is an integration of game engine, GIS and analytical sound propagation model in a unified 3D web environment. The game engine-GIS integration provides a 3D virtual environment where users can navigate through the existing geospatial data of the whole country and place different wind turbine types to explore their visual impact on the landscape. The integration of a sound propagation model in the game engine-GIS supports the real-time calculation and feedback regarding wind turbine sound at the surrounding buildings. The platform's GIS component enables massive (on-the-fly) georeferenced data utilization through tiling techniques as well as data accessibility and interoperability via cloud-based architecture and open geospatial standard protocols. The game engine, on the other hand, supports performance optimization for both data display and sound model calculations.

[8] This chapter is published in Environmental Modelling & Software journal as: Rafiee, A., Van der Male, P., Dias, E., & Scholten, H. (2017). Developing a wind turbine planning platform: Integration of "sound propagation model–GIS-game engine" triplet. Environmental Modelling & Software, 95, 326-343.

~~1.~~ 3.1. Introduction

Formatted: Heading 1, No bullets or numbering

Formatted: Font: 12 pt, Not Bold

~~1.1.~~ *3.1.1. Wind energy : benefits and externalities*

Formatted: Font: Not Bold

Formatted: Heading 2, No bullets or numbering

Renewable energy has been widely embedded in European policy targets to reduce fossil energy dependence and, in addition, to limit greenhouse gas emissions (EU Directive, 2009). Among the different renewable energy resources, wind energy is currently very popular in Europe and has been employed for large-scale electricity generation projects (EWEA, 2015). In addition, the low greenhouse gas footprint and the minimum water demand are making wind energy a popular alternative to fossil fuel in Europe (Deal, 2010; Evans et al., 2009). The *EU climate and energy package* has set the target of 20% for the overall EU energy shares from renewable energy resources by 2020 (2020 Climate & Energy Package, 2009), in which the Netherlands target is 14% (EU Directive, 2009). In line with this policy, the Dutch government intends to expand its on-shore wind energy production by 2020 to 6000 MW (SER, 2013).

Despite the potential benefits of wind energy, there is an important debate regarding the wind turbines' externalities, among which noise is perceived as the most critical (Saidur et al., 2011). Studies have explored different impacts of wind turbine noise on human health, among which we find: annoyance, sleep disturbance, psychological distress, headaches, concentration difficulties, tiredness and auditory system problems (Bakker et al., 2012; Pierpont, 2009; Pedersen, 2011). The externalities from wind turbine noise can be severe enough to force people to leave their residences (Arezes et al., 2014) and may lead to a fall in property values in the vicinity of the wind turbine (Saidur et al., 2011). Naturally, the expectation and anticipation of these detriments give rise to resistance among local communities and residents against wind turbine installation in their surroundings.

~~1.2.~~ *3.1.2. Incorporation of an information system into a 3D virtual environment to facilitate discussion*

Formatted: Font: Not Bold

Formatted: Heading 2, Left, Space After: 0 pt, No bullets or numbering

The negative opinion of residents towards wind turbines, due to their noise, can be intensified by the lack of information on the actual consequences of a wind generation project. This amplified negativity may be moderated through access to a validated information system embedded in a collaborative platform that enables discussion and facilitates information-sharing between the local community and the wind energy developers (Groth and Vogt, 2014). Transparent information and the involvement of local communities from the initial phase of the planning process have been reported to restore trust and to influence the social acceptance of projects (Jobert et al., 2007; Hall et al., 2013) and is considered essential for forming long-term solutions that potentially get long-lasting support~~s~~ (Tippett, 2005).

Beyond the information itself, the visualization of the information also influences its understandability and reception (Al-Kodmany, 1999). 3D virtual environments have been used to present information in different planning processes (Stock et al., 2008), including wind turbine planning (Bishop and Stock, 2010; Jallouli and Moreau, 2009). The outcome of these

studies highlighted the advantages of the virtual environment in terms of providing instant feedback, more freedom, a more natural user interface and interactivity as significant positive aspects (Bishop and Stock, 2010). Our contribution, compared to the latter study, is the integration of detailed sound models and their real-time numeric presentation, the incorporation of GIS functionalities into the game engine and therefore the independency from third party software packages and embedding web services and open standard protocols, which together with tiling techniques enables the on-the-fly loading of massive geospatial datasets from different sources and eliminates the interoperability problem between them. These are explained later in the article.

~~1.3.~~ *3.1.3. Game engine-based virtual environment for planning processes*

Formatted: Font: Not Bold

Formatted: Heading 2, Left, Space After: 0 pt, No bullets or numbering

The use of computer games and game engines in environmental applications and planning is increasing due to their advanced performance and interactivity capabilities (Herwig and Paar, 2002). If well designed, games enable the inclusion of target groups without expert proficiencies into a multi-disciplinary environment since they provide familiar settings for unfamiliar subjects. This makes games an effective educational tool that facilitates knowledge and information exchange (Bishop, 2011).

A 3D game engine includes numerous key runtime components that enable efficient game development and performance, such as the rendering engine, physics engine, animation modules, collision detection, scripting, visual effects, threading, memory management and math libraries (Gregory, 2009).

Herwig and Paar (2002) concluded, based on a planning workshop, that the landscape visualization offered by the graphics-assisted games triggers public interest in the planning process. In another study, the application of game engines in participatory design processes was investigated and evaluated through a comparison with conventional participatory tools (O'Coill and Doughty, 2004). ~~The results of d~~Different test~~ed~~ settings ~~reported~~ confirmed the participants' enhanced understanding of design problems through the real-time visualization of information via the computer game, which helped the participatory process to a great extent.

Following these efforts, in this paper we present our study on the development of a 3D GIS-integrated virtual environment based on the Unity game engine (Personal version)[9] for supporting wind turbine planning processes with the emphasis on wind turbine noise estimation. This has been carried out via ~~de~~ the Unity scripting API [10] through the integration of self-developed functionalities as well as applying the existing libraries (mentioned in Software availability Section).

~~1.4.~~ *3.1.4. Actual objects in the virtual environment: GIS integration*

Formatted: Font: Not Bold

Formatted: Heading 2, Left, Space After: 0 pt, No bullets or numbering

Game engines have great potency as a design platform due to their optimized performance, graphic abilities and adaptable (user-friendly) interface, but their detachment from the GIS

[9] https://store.unity.com/products/unity-personal
[10] https://docs.unity3d.com/ScriptReference/index.html

environment limits their ability to be used stand-alone in a planning process, since most existing geospatial information and the analytical impact calculation functionalities are usually only available in GIS environments. The integration of GIS in a game engine, wherein geographic coordinate systems and GIS functionalities are managed, is a crucial step, as identified in previous studies (Bishop and Stock , 2010; Herwig and Paar, 2002). In this research, we have integrated GIS within our gaming environment and called this integration Falcon.

~~1.5.~~ *3.1.5. Environmental information integration through "Sound propagation-GIS-Game engine" incorporation*

Formatted: Font: Not Bold

Formatted: Heading 2, Left, Space After: 0 pt, No bullets or numbering

~~While the presentation of the different geospatial information has an important role on the perception of the wind turbine's visual impacts on the landscape, the integration of numerical information offers an objective view on the turbine's different consequences on the environment.~~ While visual presentation of geospatial information can influence subjective perceptions of visual impacts, including from wind turbines, the results of quantitative modelling provide an objective evaluation of direct environmental consequences. Among these different impacts, wind turbine noise is considered as a major externality (Section 1.1). Our developed system offers the possibility for wind turbine sound estimation on the surrounding buildings, through the incorporation of sound propagation models. The benefits of game engine and GIS integration for the sound model implementation lies in the real-time and interactive performance of its modules for the whole country. The incorporation of sound propagation-GIS-Game engine model triplet supported the development of an integrated environmental information system for wind turbine planning where the interactivity, real-time performance and on-the-fly massive geospatial information visualization are its key features.

~~2.~~ 3.2. Methodology

Formatted: Font: Not Bold

Formatted: Heading 1, Space After: 10 pt, No bullets or numbering

~~2.1.~~ *3.2.1. System architecture*

Formatted: Heading 2, No bullets or numbering

Figure 1 presents the client–server architecture of our developed 3D game engine-based virtual environment as a three-tier configuration. This framework is composed of the visualization/interaction, processing and data tiers, illustrated here as *Unity game engine*, *services* and *database*.

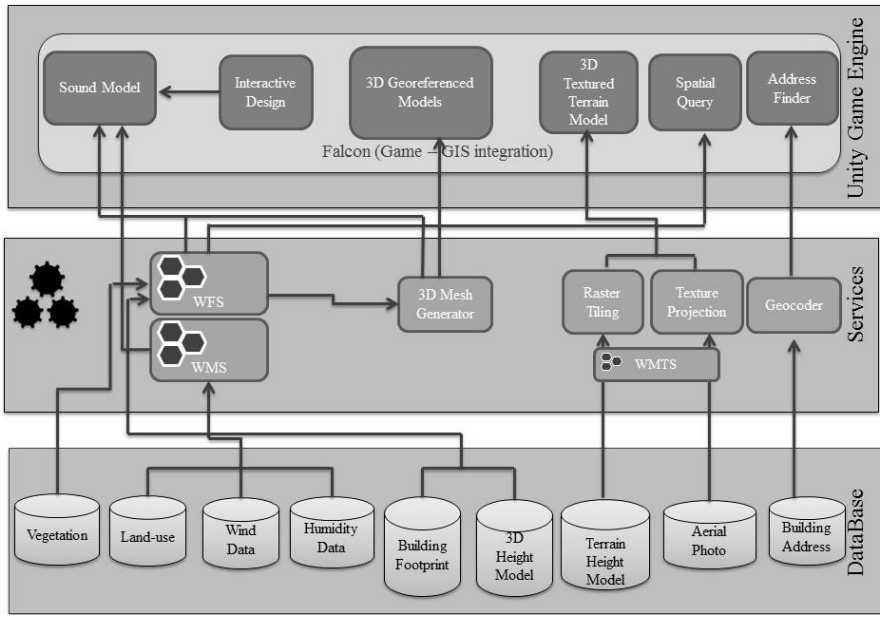

Figure 1. System architecture.

The data tier consists of different distributed databases comprising the input parameters for the sound model, as well as the data for 3D visualization and the background scene. These georeferenced data are stored in the cloud and are transferred through OGC WMS, WFS and WMTS standard web services. Web services are particularly appropriate for an effective visualization purpose, as a key element in decision support systems (Vitolo, et al., 2015).

A 2.5D terrain model of the Netherlands, textured with an aerial photo, is generated using terrain height data and loaded in Falcon. As the terrain model and its aerial photo texture for a large area (in this case, the whole country) are massive, they cannot be served all at once and an efficient technique should be utilized to manage them. Therefore, we have applied raster tiling operations to serve these datasets for the whole country. Raster tiling for the terrain height model and aerial photograph--both with 50 cm spatial resolution--of the whole Netherlands is performed through pre-rendered georeferenced tile generation, for different zoom levels, from the whole raster datasets and served based on the WMTS standard protocol (Masó et al., 2010). Based on the camera position and the zoom level, a request is sent to the server, wherein the predefined tiles are hosted, to get the underlying tiles. Each terrain height tile is RGB color coded and contains 256×~~*~~256 pixels. Each pixel is converted from RGB to height value (in centimeter) through the following transformation:

$$H_t = (256 \times 256 \times R) + (256 \times G) + B \qquad (1)$$

Where H_t is the terrain height in centimeters, and R, G and B ~~is~~ are the red, green and blue values of the color coded tile pixel, respectively.

For each terrain height tile, a game object mesh is generated and the relevant aerial photo tile is queried, based on its georeferenced coordinates. The aerial photo is projected on the terrain height tile through the Unity game object material *shader* class. The result is a tiled 3D terrain height model, textured with an aerial photo, whose height properties can be queried by different components and can be used in different collision detections.

3D building model generation and vector tiling are performed in Falcon for displaying 3D building models of the whole Netherlands. 3D building models are generated by overlaying the open data of (2D) cadastral building footprints[11] on a 3D LIDAR point cloud dataset[12] based on their georeferenced X and Y coordinates. For each building, a statistical height average is estimated from all the intersecting LIDAR point cloud Z values and assigned to the 2D building footprint as its attribute. 2D building footprints with their assigned height attribute are transferred to the cloud through WFS protocol. Falcon's compatibility with the WFS standard makes it possible to retrieve the buildings geometry and the attributes of a specific boundary on the fly from the cloud data repositories using *GetFeature Request*[13]. Upon camera movement in the game scene, its georeferenced coordinates as well as the zoom level of the scene are used for the determination of the boundary for which the buildings geometry and attributes are requested through WFS. This data is sent to the *3D Mesh Generator* module in Falcon, where 3D building models, as game objects, are generated through 2D footprint extrusion based on their height attributes. These models are presented in a Falcon game scene as 3D building models.

The geocoder service is an OpenLS service[14] provided by the Dutch National SDI (PDOK[15]) which specifies the coordinates of an address. Embedding this service into Falcon provides the users with quick navigation to a desired address.

The visualization/interaction tier is a 3D platform based on the Unity game engine. It is developed via the C# API of Unity and can be accessed through a web browser or as a mobile/desktop stand-alone application. Different 2D/3D georeferenced data are retrieved from the web and presented through introducing geospatial coordinate systems and the incorporation of GIS functionalities and data standards in Falcon. Beyond being a geo-visualization tool, the Falcon visualization/interaction tier is also a design platform in which 3D or 2D elements can be added (also removed or altered) to the existing world to compose a new landscape scene, which makes it an interactive input–output platform. In this case study, users can add different 3D wind turbine models of various types (available in the Falcon library), scale and rotate them in different axes, change their position and remove them. The users can then see the visual impact of the wind turbine placement and, beyond that, the influence of its sound on the surrounding buildings is calculated in real time and presented both graphically (by colourizing the buildings based on the received dB) and numerically (through numbers regarding the

[11] http://www.kadaster.nl/web/show/id=102363
[12] http://www.ahn.nl/index.html
[13] This function is defined by OGC WFS and returns features (geometry data and attributes) of a selected region (Vretanos, 2005).
[14] [OpenGIS®] Open Location Service
[15] Publieke Dienstverlening Op de Kaart

distribution of the received dB on buildings) to the user. This is performed through the integration of the sound models into the game engine-based Falcon platform via the Unity C# API. The implemented wind turbine sound models are described in the following section.

The seamless movement of a wind turbine in the game scene enables the user to explore all desired scenarios rather than a pre-defined and discrete set of options. This offers more freedom and provides the scope for more creativity and a sense of user-control in scenario formation and alteration. The fast performance of the platform allows for continuous scenario exploration and analysis by the user without interruption (for calculation), which provides an undistracted and immersive experience.

GIS functionalities are integrated in the game engine platform through self-developed C# code which includes self-written functions as well as existing libraries. The existing libraries our code uses are: GeoAPI, Proj4Net and GeoJSON.Net. All the sound models are implemented and integrated in the system through C# code developed by the authors. The game engine, GIS functionalities and sound models interact with each other through the self-developed scripts in Unity C# API. The services tier contains different processes for the processing and serving the data into the visualization/interaction tier. This is carried out through writing new functionalities in C#, which also make use of existing libraries (namely: Newtonsoft.Json and DotNetZip) for applying standard protocols in Falcon. Geospatial datasets (such as landuse) are served as web services published using Geoserver and ArcGIS, but are not limited to these packages, any software capable of serving the data as a standard web service could be used.

~~2.2.~~ *3.2.2. Wind turbine noise*

~~2.2.1.~~ *3.2.2.1. Noise generation*

Most recent wind turbine noise models couple aero-elastic wind turbine models, for instance based on the blade-element momentum theory or CFD modelling, to aero-acoustic prediction models based on the Ffowcs-Williams–Hawkings equation (Filios et al., 2007; Oerlemans and Schepers, 2009; Tadamasa and Zangeneh, 2011). Grosveld et al. (1995) presented semi-empirical models for the estimation of inflow-turbulence noise, trailing-edge noise and blunt-trailing-edge noise. The state-of-the-art trailing edge noise model was developed at TNO-TPD in the Netherlands and applied by Moriarty et al. (2005). The application of this model requires the description of aerofoil boundary layer aerodynamics, such as the boundary layer thickness, the friction coefficient and the flow velocity at the edge of the boundary layer.

As an alternative, the aerodynamic noise can be estimated on the basis of a rule-of-thumb model. Manwell et al. (2002) suggested an empirical equation to estimate the noise level L_{WA} as a function of the blade tip speed V_{tip} and the diameter D of the rotor:

$$L_{WA} = 50\left(\log_{10} V_{tip}\right) + 10\left(\log_{10} D\right) - 4\,, \qquad (2)$$

Formatted: Heading 2, No bullets or numbering

Formatted: Heading 3, Space Before: 0 pt, No bullets or numbering

Formatted: English (United States)

where L_{WA} is the overall A-weighted sound power level. The L_{WA} according to Equation (2) does not provide the frequency distribution of the sound power level. In addition, Equation (2) expresses the noise source as a point source. Oerlemans et al. (2007) showed that two point sources can be distinguished: one dominant source at the downward moving blade tips and another source at the hub, of which the former mainly results from trailing edge noise and the latter from mechanically generated noise.

With the application of Equation (2), a frequency distribution of the generated sound needs to be assumed, in order to analyse the attenuation of the propagated sound (see Section 3.2.2). To this end, a uniform energy distribution is assumed – with energy content from 500 Hz to 4000 Hz, to which an inverse A-weighting is subsequently applied. This frequency distribution, through which the blade tip speed and the diameter of the particular turbine are expressed, is then used to estimate the propagated sound. To do so, the sound power level is translated into a sound pressure level at unit distance from the sound source first:

$$L_{p_0} = L_W - 10\log_{10}\left(\frac{\rho_{air} c_0 P_{ref}}{4\pi \hat{p}_{ref}^2}\right), \tag{3}$$

in which P_{ref} is the reference power of $10^{-12}\,\mathrm{W}$, c_0 is the speed of the sound through the atmosphere, and ρ_{air} the density of the air.

~~2.2.2.~~ *3.2.2.2. Noise propagation*

~~2.2.2.1.~~ *3.2.2.2.1. Ray tracing model*

Formatted: Heading 3, Space Before: 0 pt, After: 0 pt, No bullets or numbering

Formatted: English (United States)

Formatted: English (United States)

For the prediction of the propagation of the noise from a single sound source, ray tracing models are a frequently applied practical basis (Attenborough et al., 1995; Attenborough et al., 2007; Prospathopoulos and Voutsinas, 2007). These models consider only the propagation of sound in the vertical plane that contains both source and receiver, implying that lateral effects from wind are neglected. Ray tracing models are mainly valid for relatively small wavelengths and are generally applied under assumed homogeneous atmospheric conditions. Given the sound pressure level L_{p_0} at unit distance from a source, the sound pressure L_{p_r} at a receiver location can be obtained from:

$$L_{p_r} = L_{p_0} - \sum A_i\,, \tag{4}$$

where A_i represents the excess attenuation that may result from geometrical spreading A_{geo}, possible ground reflection A_{ref}, atmospheric turbulence A_{turb}, atmospheric absorption A_{air}, absorption through vegetation A_{veg} and diffraction A_{diff}.

~~2.2.2.2.~~ *3.2.2.2.2. Geometrical spreading and reflection*

Formatted: Heading 4, Space Before: 0 pt, After: 0 pt, No bullets or numbering

Formatted: English (United States)

Considering a source at height H and a receiver at B, at a distance L sound waves travel via a direct wave path r_d and a reflected wave path r_r (see Figure 2). As can be seen, a flat boundary is assumed. The point source, which represents a wind turbine, radiates sound with sound pressure level L_{p_0} at unit distance from the source.

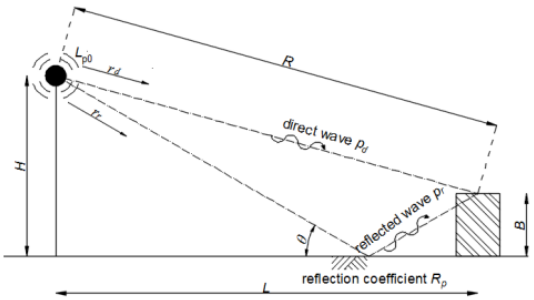

Figure 2. Graphical representation of the direct and reflected wave.

As a result of geometrical spreading, the amplitude of the sound waves decreases. Following the inverse square law, the attenuation from geometrical spreading A_{geo} of a single wave can be found from

$$A_{geo} = 10\log_{10}\left(r_d^2\right), \tag{5}$$

which is defined with respect to the sound level p_0 at unit distance from the source. In the presence of reflected waves, the sound pressure wave p_r at the receiver location can for a given wave number k be expressed in terms of the source wave p_0:

$$\frac{p_r}{p_0} = \frac{e^{ikr_d}}{r_d} + R_p \frac{e^{ikr_r}}{r_r}. \tag{6}$$

This expression, in which $i = \sqrt{-1}$ and which includes the attenuation through geometrical spreading, assumes an acoustically neutral atmosphere, i.e. no refraction, and therefore allows the superposition of the direct and a single reflected wave only (Piercy et al., 1977). R_p ~~R_P~~ is the reflection coefficient of the flat finite impedance boundary. Given the height above the ground of the sound source of a wind turbine, the reflection coefficient R_p can be determined from:

Field Code Changed

$$R_p = \frac{\sin\theta - Z_{air}/Z_{ground}}{\sin\theta + Z_{air}/Z_{ground}}, \tag{7}$$

Where θ is the sound wave incident angle at the ground, $Z_{air} = c_0 \rho_{air}$ is the characteristic impedance of air and Z_{ground} the complex impedance of the ground. Empirical formulae for the real and imaginary part of the ground impedance have been derived by Delany and Bazley (1970) through the investigation of the acoustic properties of fibrous absorbent materials. Validation of these relations on the basis of outdoor measurements can be found in Chessell (1977) and Nicolas et al. (1985), while numerical values for the ~~flow resistivity~~c for a number of ground layer types have been estimated by Embleton et al. (1983) and Attenborough (1992).

The interference of direct and reflected sound waves is disturbed by the presence of atmospheric turbulence. The statistical variation, in terms of the long-term average of the mean square of the sound pressure $\langle \hat{p}^2_{r;turb} \rangle$ relative to $\hat{p}^2_0$ can be estimated from (Daigle et al., 1978; Daigle, 1979):

$$\frac{\langle \hat{p}^2_{r;turb} \rangle}{\hat{p}^2_0} = \frac{2}{r_d r_r} \left\{ \frac{\langle a^2 \rangle}{2} \left(\frac{r_r}{r_d} + |R_p|^2 \frac{r_d}{r_r} \right) + \frac{r_r}{2 r_d} \left(1 - |R_p| \frac{r_d}{r_r} \right)^2 + |R_p| + |R_p| \left(1 + \langle a^2 \rangle \rho_a \right) \cos(\phi_r + \gamma) e^{-\langle \delta^2 \rangle (1 - \rho_\delta)} \right\}, \quad (8)$$

where γ is the phase angle of the complex reflection coefficient, $R_p = |R_p| e^{i\gamma}$. Equation (8) includes the variance of the zero-mean fluctuations of the sound wave amplitude $\langle a^2 \rangle$, where it is assumed that the variance of the direct and reflected waves are equal. The same assumption is applied for $\langle \delta^2 \rangle$, which represents the variance of the wave number fluctuation of the direct and reflected waves. ρ_a and ρ_δ are the covariances of both the amplitude and the phase, for which it is assumed that $\rho_a = \rho_\delta = \rho$, which can be obtained from (Attenborough et al., 2007). Daigle (1979) presented an approach to estimate $\langle a^2 \rangle$ and $\langle \delta^2 \rangle$, employing the fluctuating index of reflexion $\langle \mu^2 \rangle$, which expresses the meteorological conditions, and a specific turbulence length scale L_{turb}. Numerical values for $\langle \mu^2 \rangle$ and L_{tur} were estimated by Johnson et al. (1978) for different weather conditions. The excess attenuation in the presence of turbulence A_{turb}, in addition to the attenuation in non-turbulent circumstances, can be obtained from:

$$A_{turb} = 10 \log_{10} \left(\frac{\hat{p}^2_r}{\hat{p}^2_{r;turb}} \right). \quad (9)$$

The presented model may be simplified for a direct or reflected wave only, for instance if a receiver is located in the shadow zone behind an obstruction. In this situation, diffraction should be accounted for (see Section 3.2.2.4).

~~2.2.2.3.~~ *3.2.2.2.3. ~~A~~Absorption*

The attenuation A_{air} due to atmospheric absorption can be obtained from the integration of the absorption coefficient α over the source–observer length:

Formatted: Heading 4, Space Before: 0 pt, After: 0 pt, No bullets or numbering

Formatted: English (United States)

$$A_{air} = \int_0^R \alpha dr \tag{10}$$

A_{air} results from the integration of the frequency-dependent absorption coefficient α along the wave path over the total length from the source to the receiver. The absorption coefficient α can be estimated from the ambient temperature *T*, relative humidity *h* and atmospheric pressure (Bass et al., 1990). If direct and reflected waves are considered, the atmospheric absorption can be calculated for both.

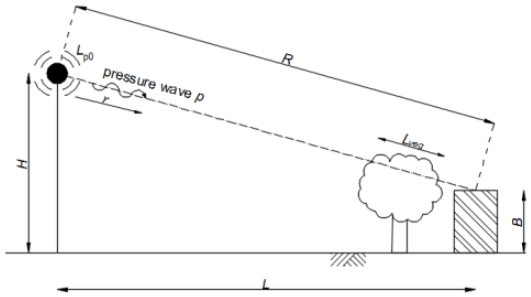

Figure 3. Graphical representation of the absorption through vegetation.

Figure 3 presents a sound wave *p* travelling over a distance *R* from a source towards a building. This sound wave crosses a green belt in front of the building. The crossing distance is L_{veg}. Kurze and Beranek (1971) developed a theoretical model for the attenuation of sound propagation through trees, where the attenuation is only a function of the frequency and the crossing distance:

$$A_{veg} = 0.01 L_{veg} \sqrt[3]{f} \tag{11}$$

~~2.2.2.4.~~ *3.2.2.2.4. ~~D~~Diffraction*

Formatted: Heading 4, Space Before: 0 pt, After: 0 pt, No bullets or numbering

~~Considering buildings to be non-transmittable for sound waves~~ As buildings have very limited transmission of sound waves, the sound level at the back of a building can be assumed to be significantly less than the level in front of the obstruction. Still, as a result of diffraction, sound waves will penetrate into the shadow zone behind the obstruction (see Figure 4). Kurze and Anderson (1971) developed an engineering model to estimate the sound attenuation due to a rigid infinitely long barrier for sound from a point source:

$$A_{diff} = \begin{cases} 20\log_{10}\left(\dfrac{\sqrt{2\pi N}}{\tanh\sqrt{2\pi N}}\right) + 5, & \text{for } N \geq -0.2 \\ 0, & \text{for } N < -0.2 \end{cases} \tag{12}$$

The Fresnel number N is a measure of the distance of the location of the receiver from the line of sight towards the source, relative to the wavelength λ:

$$N = \pm \frac{2}{\lambda}(R_A + R_B - R) \tag{13}$$

N is positive if the receiver is located in the shadow zone behind the barrier, otherwise N is negative.

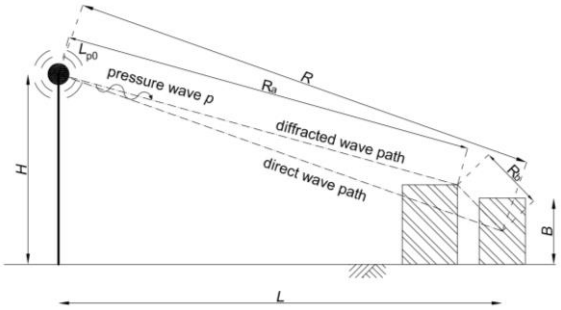

Figure 4. Graphical representation of the direct and diffracted wave.

The attenuation derived with Equation (12) was found to be conservative in comparison with the experimental results presented by Maekawa (1968). Nevertheless, the approach assumes a semi-infinite barrier and does therefore neglect reflections at the ground behind the barrier. Moreover, diffraction from sound waves travelling along the sides of the barrier are not accounted for. To account for this diffraction along the sides, however, the diffraction model given by Equation (13) could be employed too, with R_A and R_B now defining the indirect sideways wave paths.

~~2.2.2.5.~~ 3.2.2.2.5. ~~-~~*Refraction*

The presented noise propagation models did not account for the presence of wind and a temperature gradient, both of which affect the sound pressure level at the receiver location. Wagner et al., (1996) presented an overview of the effects of weather on the propagation of wind turbine noise. Both wind and temperature gradient affect the sound wave pattern, potentially resulting in sound shadow zones.

The location of the edge of a shadow zone can be estimated on the basis of R_{shadow}, according to the following expression:

$$R_{shadow} = c_0\left(1+\frac{V}{c_0}\right)^3\left(-\frac{V}{c_0}\frac{\sqrt{\kappa c_g}}{\sqrt{T}}\frac{dT}{dz}+\frac{dV}{dz}\right)^{-1}. \tag{14}$$

Formatted: Heading 4, Space Before: 0 pt, After: 0 pt, No bullets or numbering

Formatted: English (United States)

This formula contains the wind velocity V and the ambient temperature T, as well as the corresponding gradients with respect to the height z. κ is the adiabatic gas constant, c_g the specific gas constant. The wave propagation velocity through ideal gases can be found from

$$c_0^2 = \kappa c_g T \tag{15}$$

The wind velocity gradient with respect to height can be determined from a reference wind velocity, commonly defined at a height of 10 m – V_{10}:

$$\frac{dV}{dz} = \frac{V_{10}}{z\ln(10/z_0)}, \tag{16}$$

making use of the roughness height z_0. Figure 5 illustrates the shadow zone on the basis of R_{shadow}. Whether a building with a height B is completely located within the shadow zone can be checked on the basis of the following inequality:

$$L \geq \sqrt{R_{shadow}^2 - (R_{shadow} - H)^2} + \sqrt{R_{shadow}^2 - (R_{shadow} - B)^2} \tag{17}$$

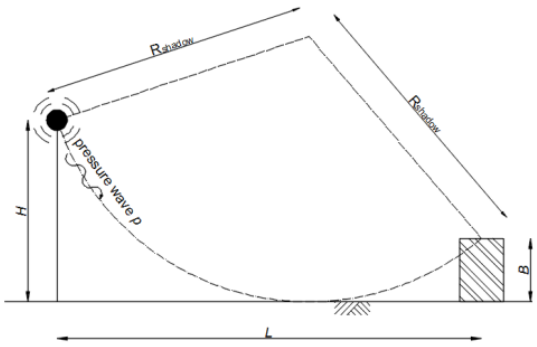

Figure 5. Graphical representation of the shadow zone resulting from the curvature of the sound waves.

~~3.~~3.3. Framework Implementation

The developed framework design is implemented through Unity scripting API.
In addition to 3D building models, users can load raw LIDAR point clouds in Falcon for more detailed interpretation and analysis. Figure 6 presents AHN2 LIDAR point clouds overlaid on 3D building models in Falcon.

Formatted: Heading 1, Outline numbered + Level: 2 + Numbering Style: 1, 2, 3, … + Start at: 2 + Alignment: Left + Aligned at: 0 cm + Indent at: 0,95 cm

Figure 6. AHN2 LIDAR point cloud overlaid on 3D models in Falcon. Different 3D and 2D geospatial data of the whole Netherlands are served to Falcon via web services.

Falcon delivers an extensive library of 3D models of different wind turbine suppliers which are available directly from the interface. For each wind turbine, its geometric and technical specifications, such as hub height, rotor diameter, blade tip speed and rated power are stored in the Falcon database and used both for wind turbine information presentation and also subsequently in the sound models. Figure 7 presents the wind turbine scenario forming in the design environment of Falcon. Users can select a specific wind turbine from the list and add it to the scene. Technical information on the added wind turbine is presented in a separate window.

Figure 7. Wind turbine scenario design in Falcon. Users can select different wind turbine types and bring them into the scene as game objects. By placing a wind turbine in the scene, its geometric and technical characteristics are retrieved from the database and are presented.

Each module of the sound model (e.g. diffraction, ground interference) can be accessed and visualized separately in Falcon. Integration of these sub-modules in the game engine-based Falcon helps the user to gain ~~getting more~~ insight into the wind turbine noise behaviour and offers noise experts an interactive fast-performing platform to carry out various types of analysis on the constituents of wind turbine noise. Table 1 presents the implementation architecture of the sound propagation sub-modules. The applied technique types and domains as well as the deployed datasets are described in this table.

Table 1. The applied techniques and data for each sound sub-module.

Sound Module	**Technique**		**Data**
	type	**domain**	
Geometrical Spreading	3D Distance	Game engine	3D building models
			Wind turbine characteristics
Atmospheric Absorption	GetFeatureInfo Request*	GIS	Temperature
			Humidity
	3D Distance	Game engine	3D building models
Vegetation Absorption	3D Line Casting	Game engine	Land-use
	3D Distance	Game engine	Wind turbine characteristics
	GetFeature Request	GIS	3D building models
Ground Interaction	3D Distance	Game engine	Land-use
			Wind turbine characteristics
	GetFeatureInfo Request GIS		3D building models

			Wind
Obstruction/ Diffraction	3D Distance	Game engine	Wind turbine characteristics
	3D Line casting	Game engine	3D building models
	3D Collision Detection		
Weather Effects/ Refraction	3D Distance	Game engine	Wind
			Temperature
	GetFeatureInfo Request	GIS	3D building models

* This request is defined by the OGC WMS implementation and it retrieves the location and attribute information of a pixel in a specific location of a map (de La Beaujardière, 2002).

Incorporation of the different techniques from the game engine and GIS domains, resulting from the game engine–GIS integration, supports the efficient implementation of the sound sub-modules in an allied environment. While the mutual benefits of game engine and GIS are described in the previous sections, we have performed tests to measure the 3D distance and 3D collision detection performance (in time) with and without game engine-GIS integration. In the first test, 3D distance performance is measured for 2600 buildings in Falcon, with game engine-GIS integration and subsequently, for the same buildings, 3D distance is measured in a pure GIS environment (ArcGIS 10.2.2). The test results indicate that it takes 4 milliseconds for Falcon (game engine-GIS integration) to calculate versus 1.90 seconds in ArcGIS for the 3D distance functionality. In the second test, 3D collision detection performance was tested for the same buildings as the previous test set. These tests indicated that it takes 20 milliseconds for Falcon (game engine-GIS integration) to calculate versus 1 minutes and 47 seconds in ArcGIS for 3D collision detection performance. In both tests, the game engine-GIS integration and the pure GIS environment return the same results and the difference is the performance duration.

The ultimate sound impact of a wind turbine is calculated using the total sound model, composed of all the individual modules. The implementation of each individual sound module is presented as follows.

~~3.1.~~3.3.1. ~~-~~*Noise generation*

Upon adding a wind turbine to the scene, wind turbine characteristics are retrieved from the database and applied in the turbine's overall A-weighted sound pressure level calculation (Equation 3). This value is presented together with other specifications of a selected wind turbine (Figure 7).

~~3.2.~~3.3.2. *Geometrical spreading*

Upon the placement of a wind turbine in the scene, the information on all the buildings within 1km of the turbine is queried. Subsequently, the distance from the turbine to each of these buildings is calculated and the geometrical sound attenuation is computed for the building. The

Formatted: Heading 2, Space Before: 0 pt, After: 0 pt, Outline numbered + Level: 3 + Numbering Style: 1, 2, 3, … + Start at: 1 + Alignment: Left + Aligned at: 0 cm + Indent at: 1,27 cm, Tab stops: Not at 3,97 cm

Formatted: Heading 2, Space Before: 0 pt, After: 0 pt, Outline numbered + Level: 3 + Numbering Style: 1, 2, 3, … + Start at: 1 + Alignment: Left + Aligned at: 0 cm + Indent at: 1,27 cm, Tab stops: Not at 3,97 cm

input parameters for this sub-module are the wind turbine geometrical properties as well as the location and height of the surrounding buildings. The sound attenuation values will change in real time when the user moves the wind turbine in the scene. The attenuation distribution is demonstrated numerically (top right) and graphically through colourized buildings and the ~~[~~similarly~~]~~ colourized chart (top middle). The fast responsiveness of the geometrical attenuation module upon the turbine's movement is illustrated in Film 1.

https://video.vu.nl/media/Developing+a+wind+turbine+planning+platform_Film1/1_6f4x4y7s

Film 1. Quick responsiveness of geometrical attenuation module upon wind turbine movement.

~~3.3.~~3.3.3. ~~-~~*Diffraction*

Formatted: Heading 2, Space Before: 0 pt, After: 0 pt, Outline numbered + Level: 3 + Numbering Style: 1, 2, 3, … + Start at: 1 + Alignment: Left + Aligned at: 0 cm + Indent at: 1,27 cm, Tab stops: Not at 3,97 cm

With the existence of an obstacle between the sound source and the receiver, sound waves diffract around the obstacle to move towards the receiver. This leads to a reduction in the sound level.

For each building, a line of sight is defined from its 3D centre point to the wind turbine hub location. The collision between this line of sight and other buildings is examined by the line casting and collision detection features of the game engine. For detecting a collision between the line of sight and another building, the 3D distances between the receiver–obstacle, the target building–obstacle and the receiver–target are calculated using the collision coordinates information. These 3D distances are applied in the calculation of the Fresnel number (Equation (13)) to estimate the sound attenuation due to the collided building (Equation (12)).

In a GIS system, obstacle detection is commonly performed through the 3D visibility analysis method. This approach is computationally demanding, reducing the performance and limiting its usability for real-time operations. However, the real-time collision detection of the game engine, through its physics engine's physical simulations, greatly increases the efficiency of the real-time diffraction calculation. Film 2 illustrates the real-time calculation/feedback of the obstruction attenuation module. The sound attenuations on the lower buildings whose lines of sight are obstructed by taller buildings are more intense.

https://video.vu.nl/media/Developing+a+wind+turbine+planning+platform_Film2/1_9gmgnque

Film 2. Real-time calculation/feedback of sound attenuation due to obstruction. The game engine's real-time collision detection (performed by its physics engine) supported the instantaneous calculations for this module.

~~3.4.~~3.3.4. *Ground interaction*

Formatted: Heading 2, Space Before: 0 pt, After: 0 pt, Outline numbered + Level: 3 + Numbering Style: 1, 2, 3, … + Start at: 1 + Alignment: Left + Aligned at: 0 cm + Indent at: 1,27 cm, Tab stops: Not at 3,97 cm

The sound level attenuation due to ground reflection on the exposed buildings (buildings without any obstacles to the wind turbine) is calculated based on Equation (8). The input data for this calculation is the land-use map of the Netherlands, the 3D building and wind turbine models and the wind data (derived from the Royal Netherlands Meteorological Institute (KNMI[16]) mean hourly dataset) which is used for the estimation of the reflection fluctuating index. The land-use map of the Netherlands with the scale of 1:10000 is published by the Dutch Central Bureau of Statistics[17]. This dataset is loaded in Falcon through the WMS standard and the raster tiling technique.

For each receiver (i.e. building), the sound wave incidence angle at the ground is calculated using the wind turbine and building coordinates. This angle is used in combination with the impedance characteristics of air and the complex impedance of the ground for the calculation of the ground reflection coefficient (Equation (7)). Real and imaginary parts of the complex impedance of the ground are a function of the flow resistivity of the surface and sound wave frequency. Flow resistivity determines the ease of air movement in and out of the ground and is inversely proportional to porosity (Crocker, 2007). In the case of surfaces of constant porosity, the flow resistivity of the surfaces~~, which determines their absorptive characteristics,~~ can be assigned with a single value (Piercy et al., 1977). ~~-~~Table 2 presents the flow resistivity values used in this research (Piercy et al., 1977; Forrest, 1994).

Table 2. Flow resistivity values for different surface types

Surface	Flow resistivity (cgs rayls)
In forest, pine or hemlock	20-80
Grass, rough pasture	150-300
Roadside dirt, ill-defined, small rocks up to 10 cm diameter	300-800
Sandy silt, hard packed	800-2500
Clean limestone chips, thick layer (12-25mm mesh)	1500-4000
Earth, exposed and rain-packed	4000-8000
Water	10000
Quarry dust, fine, very hard-packed by vehicles	5000-20000
Asphalt, sealed by dust and use	>20000

When a wind turbine is placed on the ground, the land-use type of the location will be queried from the land-use map, through the WMS "*GetFeatureInfo Request*", which will be used to estimate the flow resistivity value. The flow resistivity of the surface, together with the position/height of the wind turbine and the building, are used in the calculation of the reflected sound wave. Figure 8 presents the impact of different land-use types on the receiving noise of

[16] Koninklijk Nederlands Meteorologisch Instituut
[17] Centraal Bureau voor de Statistiek (CBS) (http://www.cbs.nl/nl-NL/menu/home/default.htm)

each exposed building. We assumed the resistivity of arable land in the range of grass, rough pasture, being 250 cgs rayls.

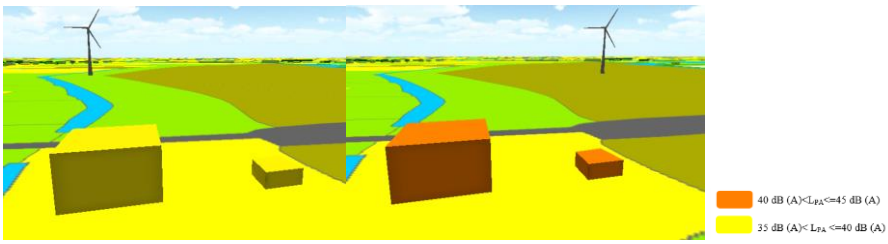

a b

Figure 8. Placement of the wind turbine on different land-use types leads to different noise being received on the same buildings: a) grass field and b) arable land. All other parameters (e.g. wind turbine-building distance) remain the same.

~~3.5.~~3.3.5. *Effect of vegetation*

Formatted: Heading 2, Space Before: 0 pt, After: 0 pt, Outline numbered + Level: 3 + Numbering Style: 1, 2, 3, … + Start at: 1 + Alignment: Left + Aligned at: 0 cm + Indent at: 1,27 cm, Tab stops: Not at 3,97 cm

Dense enough vegetation can lead to sound attenuation if it blocks the view between the sound source and the receiver (Section 3.2.2.3). To distinguish densely vegetated areas from sparse ones, we have extracted the forest regions from the vector land-use map of the Netherlands. The average height of the forested region is estimated using the DSM[18] of the area (derived from the LIDAR point cloud) and assigned to each vector feature. The forest vectors are loaded in Falcon and their geometries and attributes are retrieved through the WFS "*GetFeature*" request. Upon the placement of a wind turbine in the vicinity of a forest, a 3D line-of-sight analysis is performed for each building to detect its visibility status from the wind turbine through the forested area. If the line of sight between a building and the wind turbine is blocked by the forest (considering its height), the sound attenuation on the building due to the forest is calculated using Equation (11). The vegetation length between the wind turbine and each building is estimated through the retrieved forest vector geometries and the building location. For this estimation, two forest polygon vertices, namely the nearest vertex to the wind turbine and the nearest vertex to the building, are queried and applied in the Euclidian distance calculation.

Figure 9 presents the sound attenuation due to vegetation absorption. The AHN2 LIDAR point cloud of the area has been loaded in Falcon to present the 3D morphology of the forested region. The attenuation is different for buildings with different heights and different distances to the wind turbine. To present this geometrical relation, two scenarios have been depicted in Figure 9. In each scenario the wind turbine is sited at a different location and distance relative to the target buildings. As the wind turbine moves further from scenario *a* to *b*, the lines of sight between the wind turbine and more buildings are blocked by the forest and therefore the number of buildings affected by vegetation absorption increases.

[18] Digital Surface Model

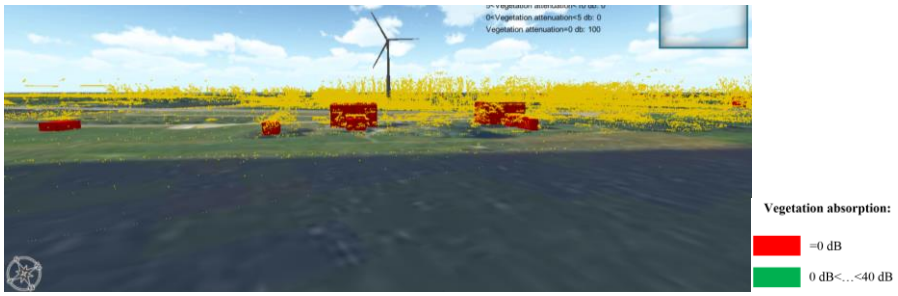

a

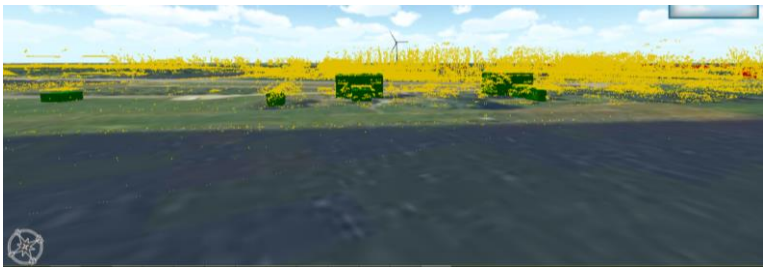

b

Figure 9. Sound attenuation due to vegetation (sound frequency is set to 1000 HZ) depicted in two scenarios. By placing the wind turbine further from the target buildings from scenario *a* to *b* the number of buildings affected by line-of-sight obstruction by the forest increases.

The input data of the vegetation sub-module comprises the wind turbine data, the vector land-use data and the 3D building models. 3D distance and line casting operations are the game engine techniques used in this sub-module.

~~3.6.~~3.3.6. ~~-~~*Effect of atmospheric absorption*

Formatted: Heading 2, Space Before: 0 pt, After: 0 pt, Outline numbered + Level: 3 + Numbering Style: 1, 2, 3, … + Start at: 1 + Alignment: Left + Aligned at: 0 cm + Indent at: 1,27 cm, Tab stops: Not at 3,97 cm

Upon the placement of a wind turbine on a location, the temperature and humidity values of the site (obtained from the KNMI hourly open data) are queried and employed in the atmospheric absorption sub-module.

Alternatively, the user can define the temperature and humidity of each location manually using the sliders provided in the Falcon interface. This offers the possibility of comparative studies (e.g. on different seasons or extreme case scenario assessments), where different temperature and humidity values lead to different atmospheric absorption attenuation and the final wind turbine sound effects. Figure 10 presents the implementation of atmospheric absorption attenuation in the Falcon interface under two different humidity conditions. Figure 10a presents the atmospheric absorption for the current humidity situation of the study area. As mentioned above, the humidity of a location is estimated based on the KNMI hourly data, which is 80.6% for this location. Figure 10b shows the humidity adjustment possibility in Falcon and its influence on the atmospheric absorption results. In this case, the humidity is set as 20%. It can be seen that in the lower humidity condition, the atmospheric absorption is higher. This leads

to a lower sound level being received at the surrounding buildings. The real-time calculation/feedback of the atmospheric absorption module upon the wind turbine's movement and humidity alteration is illustrated in Film 3.

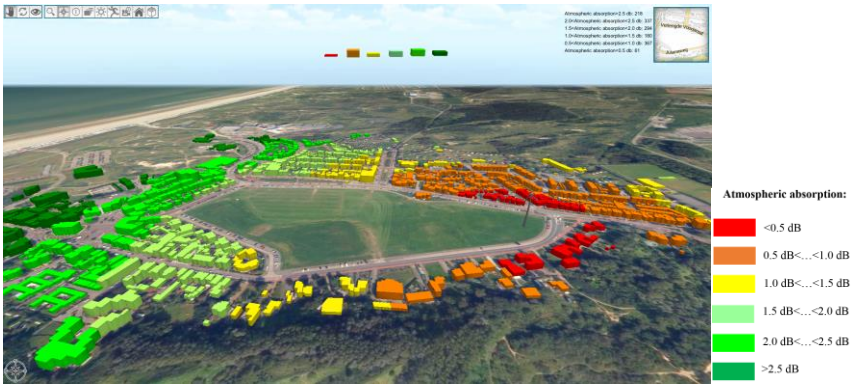

a

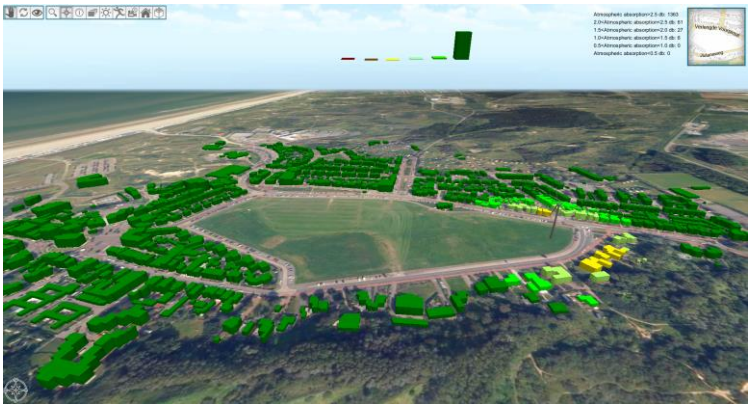

b

Figure 10. Implementation of atmospheric absorption sub-module for a) current humidity situation estimated by hourly humidity data (80.6%) and b) adjusted humidity (20%)

https://video.vu.nl/media/Developing+a+wind+turbine+planning+platform_Film3/1_uxhqbcmt

Film 3. Real-time calculation/feedback of atmospheric absorption module upon the movement of the wind turbine as well as the humidity alteration.

~~3.7.~~3.3.7. *Effect of wind*

Formatted: Heading 2, Space Before: 0 pt, After: 0 pt, Outline numbered + Level: 3 + Numbering Style: 1, 2, 3, … + Start at: 1 + Alignment: Left + Aligned at: 0 cm + Indent at: 1,27 cm, Tab stops: Not at 3,97 cm

As mentioned in Section 3.2.2.5, at specific distances and directions, the sound pressure level declines suddenly, forming so-called "shadow zones", where direct sound rays cannot penetrate. We have calculated the radius of the shadow zone based on Equation (14).

By placing a wind turbine in the scene, the wind properties of the location vicinity are extracted from the mean hourly wind data provided by KNMI to calculate the radius of the shadow zone. The direction of the shadow zone is defined according to the dominant (or actual) wind direction of the region.

Once the shadow zone radius and the direction are calculated for the specific location of the wind turbine, based on the location and height of each building and the turbine, it can be checked whether it falls within the shadow zone or not (Equation (17)). Unlike all the other sub-modules in which the calculations are performed for the buildings within 1 km of the wind turbine, the computations of this sub-module are implemented for buildings within 3 km of the wind turbine. This is due to the greater distances where weather effects have an impact.

The mean hourly wind data, the wind turbine data and the 3D building models are the underlying data for the wind sub-module (see Table 1). The real-time calculation/feedback of the wind effect module is illustrated in Film 4. This film presents the buildings falling within the wind shadow zone (in black) into which no direct sound ray can enter. These buildings are located approximately 1.6 km from the wind turbine.

https://video.vu.nl/media/Developing+a+wind+turbine+planning+platform_Film4/1_qdyhqp5p

Film 4. Real-time calculation/feedback of wind effect module.

~~4.~~3.4. Results

Formatted: Heading 1, Space After: 0 pt, Outline numbered + Level: 2 + Numbering Style: 1, 2, 3, … + Start at: 2 + Alignment: Left + Aligned at: 0 cm + Indent at: 0,95 cm

The performance of our developed system and the underlying sound model are analysed for different urban configurations and different climatic situations using the nationwide data accessed via Falcon.

Users can access the tool via an internet browser and have at their disposal different datasets of the whole Netherlands. They can be "teleported" to a specific location by typing its address or navigate to any location through the pan, rotate and zoom functionalities (Figure 11). The first upper left button in the toolbar is the pan button, the second button is the free rotation and the third one is the rotation from a fixed observer point. Zooming in/out is performed through mouse scroll, zoom in/out buttons in the interface, or pinch in touch interface.

Figure 11. The user can query a specific location by typing its address or navigate to different locations through pan, zoom and rotate buttons.

3D models of different wind turbines can be added to the scene as explained in Figure 7. Upon the placement of a wind turbine in the scene, its location, geometrical and technical information are retrieved and dispatched to all the sub-modules. For the ease of use, only the total sound module is exposed to users by default. The other sound sub-modules can be added by the users for a more detailed analysis (Figure 12).

Figure 12. The tool allows the separate implementation of each sound sub-module, as well as the total sound.

3.4.1. ~~4.1.~~ *Test cases*

Formatted: Heading 2, Space Before: 0 pt, After: 0 pt, Outline numbered + Level: 3 + Numbering Style: 1, 2, 3, … + Start at: 1 + Alignment: Left + Aligned at: 0 cm + Indent at: 1,27 cm

The Falcon environment provides the scope for an enhanced insight into the noise from wind turbines in a real-world-related virtual environment. The instant feedbacks, provided through real-time sound model calculations, enable the user to uninterruptedly explore various scenarios of turbine positioning. To illustrate both the performance and the usability of the software, we have performed a number of test cases with different environmental settings and turbine specifications. The visual and numeric outcomes of these test cases are then discussed and compared. Table presents the numeric configuration of each test case. The game interface client application, performing the analysis, is accessed using an Intel Core i7-4790 CPU with an NVIDIA GeoForce GTX 970 graphics card.

Table 3. Numeric configuration of test cases.

Settings		**Test Case 1**		**Test Case 2**		**Test Case 3**		**Test Case 4**	
Wind turbine	Height (m)	76		45		76		76	
	Blade length (m)	48		44		48		48	
	Overall SPL (dB (A))	119		118		119		119	
Urban Environment	Building height (m)	min	2	min	2	min	2	min	2
		max	15	max	15	max	37	max	37
		mean	6	mean	6	mean	5	mean	5
Climate	Temperature (°C)	15		15		15		15	
	Wind Speed (m/s)	4		4		4		4	
	Dominant wind	West–East		West–East		West–East		West–East	
	Humidity (%)	80%		80%		80%		40%	
Distance	Building–Wind Turbine (m)	min	103	min	76	min	122	min	122
		max	849	max	837	max	981	max	982
		mean	472	mean	458	mean	595	mean	597

3.4.1.1. ~~4.1.1.~~ *Test Case 1*

Formatted: Heading 3, Space Before: 0 pt, After: 0 pt, Line spacing: single, Outline numbered + Level: 4 + Numbering Style: 1, 2, 3, … + Start at: 1 + Alignment: Left + Aligned at: 0 cm + Indent at: 1,27 cm

~~The off-shore wind energy potential is greater than the on-shore potency~~ The potential for wind energy is greater off-shore then on-shore, due to the undisturbed sea surface, which allows for the development of a stable wind field with greater velocities at smaller heights. Near-shore locations require less expensive foundations than off-shore sites. Moreover, the costs of installation, maintenance and decommissioning are generally lower. Yet, only a limited number

of near-shore sites are employed for the exploitation of wind farms, mainly because of the visual disturbance of the environment.

In this test case, the near-shore wind turbine noise propagation on the surrounding buildings is explored. The study area is Urk, a town in the central part of the Netherlands, adjacent to the IJsselmeer. This town is located within the *Noordoostpolder* wind farm, the largest wind park in the Netherlands to date. The wind turbines are placed within 1.5 km of the town, and are therefore influential on the built area. The farm contains both on-shore and near-shore sections, for which, respectively, Enercon E-126 and Siemens SWT-3.0-108 wind turbines are installed.

Figure 13 visualizes the simulation of the wind turbine noise propagation on the buildings within 1 km distance. Selecting this distance was due to the very low sound level at the further buildings, mainly due to geometrical attenuation. However, this radius can be adjusted differently for different applications. In this simulation a wind turbine with 76 m height and 48 m blade length with nearly 800 kW rated power capacity and 119 dB (A) noise level is chosen. This wind turbine is located in the IJsselmeer, in the vicinity of the built area. This location was chosen to illustrate the working of the sound radiation tool, rather than to represent the positioning of an actual wind turbine. The temperature is set to 15°C and the wind speed and the humidity, derived from KNMI hourly data, are 4 m/s and 80%, respectively. As seen in the figure, the distance between the buildings and the wind turbine is the main deriving factor in the noise received from the turbine. However, the impact of obstruction can be clearly seen on the lower buildings behind the higher ones. The noise distribution is depicted visually, through colourized buildings and the chart, and numerically on the top right of the UI. The measured total sound calculation time is around 600 millisecond for this test case.

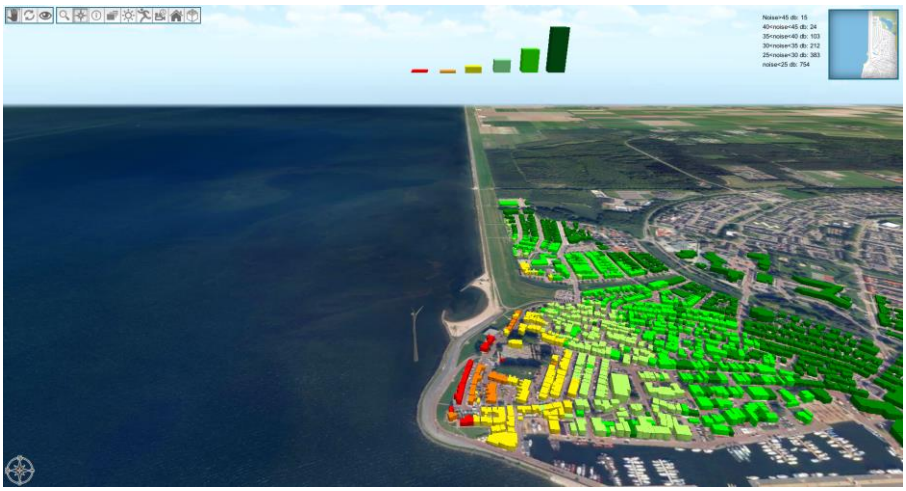

Figure 13. Wind turbine noise propagation in Test Case 1.

Within the focus area, the majority of buildings (754) receive less than 25 dB (A) noise from the wind turbine, while there are 15 buildings which receive more than 45 dB (A). These distribution results are presented in Table 4.

Table 4. Noise distribution in Test Case 1.

Noise level (dB (A))	Number of buildings affected
L_{pA} <25	754
25< L_{pA}<30	383
30< L_{pA} <35	212
35< L_{pA} <40	103
40< L_{pA} <45	24
L_{pA} >45	15
~~Noise level (dB (A))~~	~~Number of buildings affected~~
~~L_{pA} <25~~	~~754~~
~~25< L_{pA} <30~~	~~383~~
~~30< L_{pA} <35~~	~~212~~
~~35< L_{pA} <40~~	~~103~~
~~40< L_{pA} <45~~	~~24~~
~~L_{pA} >45~~	~~15~~

3.4.1.2.~~4.1.2.~~ Test Case 2

Formatted: Heading 3, Space Before: 0 pt, After: 0 pt, Outline numbered + Level: 4 + Numbering Style: 1, 2, 3, … + Start at: 1 + Alignment: Left + Aligned at: 0 cm + Indent at: 1,27 cm

The turbine characteristics are one of the influential factors on the generation and propagation of wind turbine noise. The hub height, rotor length, drive train and rotational speed are examples of such characteristics. Therefore, different wind turbines in the same landscape settings and climatic conditions induce a different noise distribution.

This test case examines the impact of the characteristics of a wind turbine on the distribution of the noise; the location, urban configuration and climatic conditions are kept the same as in Test Case 1. Here, however, a hub height of 45 m and a blade length of 44 m is selected from the wind turbine list in the Falcon UI. The selected turbine has nearly 900 kW rated power and its sound level is 118 dB (A), which is approximately the same as the sound level of Test Case 1. Figure 14 presents the noise received at the surrounding buildings.

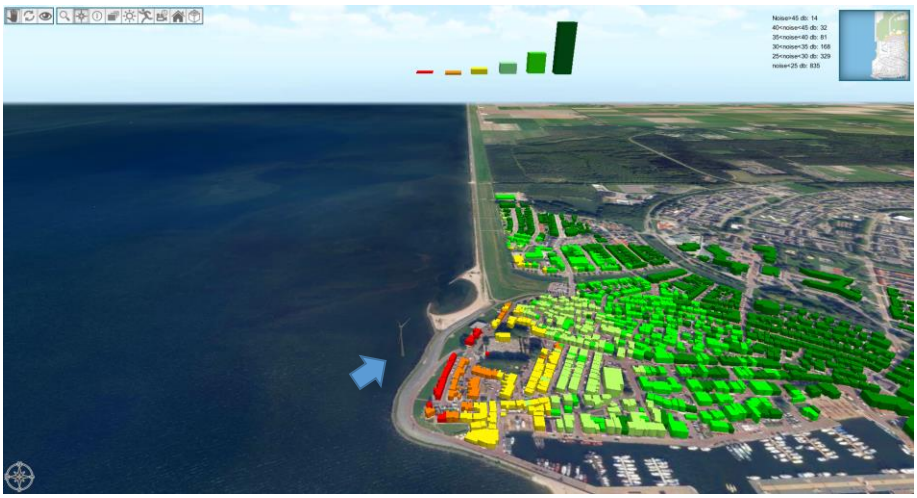

Figure 14. Wind turbine noise propagation in Test Case 2.

While for high noise levels (nearby buildings) the number of buildings remains comparable to Test Case 1, for the more distant buildings, the number which receive a lower sound level (<25dB(A)) increases compared to Test Case 1. This is due to the different wind turbine–building line-of-sight geometrical configuration. In the case of a lower wind turbine (this test case) there are more buildings whose lines of sight are obscured by the higher surrounding buildings than in Test Case 1 with the higher wind turbine and therefore experience greater obstruction attenuation. Table 5 presents the number of buildings affected by different sound levels.

Table 5. Noise distribution in Test Case 2.

Noise level (dB (A))	Number of buildings affected
L_{pA} <25	835
25< L_{pA}<30	329
30< L_{pA} <35	168
35< L_{pA} <40	81
40< L_{pA} <45	32
L_{pA} >45	14
~~Noise level (dB (A))~~	~~Number of buildings affected~~

~~L_{pA}<25~~	~~835~~
~~25< L_{pA}<30~~	~~329~~
~~30< L_{pA}<35~~	~~168~~
~~35< L_{pA}<40~~	~~81~~
~~40< L_{pA}<45~~	~~32~~
~~L_{pA}>45~~	~~14~~

Figure 15 compares the results of the similarly-situated Test Cases 1 and 2. In this figure the percentage of buildings within each noise level is illustrated for each test case.

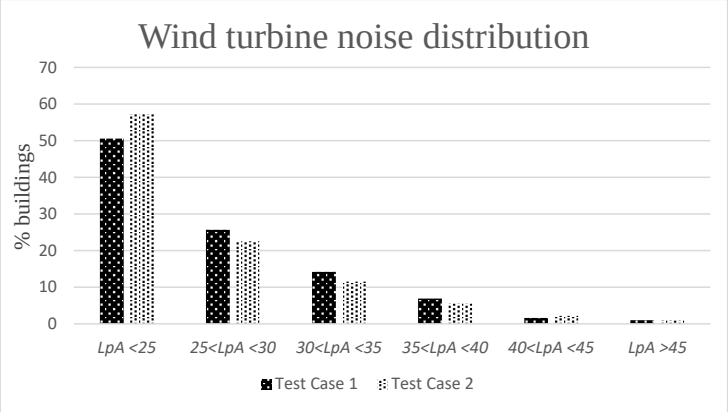

Figure 15. Comparative results between Test Cases 1 and 2.

3.4.1.3.~~4.1.3.~~ Test Case 3

Formatted: Heading 3, Space Before: 0 pt, After: 0 pt, Outline numbered + Level: 4 + Numbering Style: 1, 2, 3, … + Start at: 1 + Alignment: Left + Aligned at: 0 cm + Indent at: 1,27 cm

The vast majority of the wind turbines in the Netherlands are positioned on-shore. Moreover, based on the 2020 target, the on-shore wind power production will increase during the coming years. This test case explores the noise propagation of an on-shore wind turbine towards the neighbouring buildings in an urban area. The study area for this test case is an area in Haarlem. This city is located in the province of Noord-Holland, in the northwest of the Netherlands, where 685.5 MW of on-shore wind energy by 2020 is targeted. A wind turbine with a hub height of 76 m, blade length of 48 m, and 119 dB (A) sound level (the same as Test Case 1) is selected and placed in an agricultural area in the vicinity of the urban area. Figure 16 presents the sound simulation of the wind turbine noise distribution in this landscape configuration and the same climatic conditions as Test Cases 1 and 2.

Figure 16. Wind turbine noise propagation in Test Case 3.

The different urban configuration of this test case compared to Test Case 1 leads to a different noise propagation pattern. The tall buildings in this area block the lines of sight of a large number of buildings, which results in higher sound attenuation due to obstruction. The distribution of the number of buildings experiencing different noise levels is presented in Table 6.

Table 6. Noise distribution in Test Case 3.

Noise level (dB (A))	Number of buildings affected
L_{pA} <25	2178
25< L_{pA}<30	510
30< L_{pA} <35	380
35< L_{pA} <40	223
40< L_{pA} <45	21
L_{pA} >45	23
~~Noise level (dB (A))~~	~~Number of buildings affected~~
~~L_{pA} <25~~	~~2178~~
~~25< L_{pA}<30~~	~~510~~

~~30< L_{pA}<35~~	~~380~~
~~35< L_{pA}<40~~	~~223~~
~~40< L_{pA}<45~~	~~21~~
~~L_{pA}>45~~	~~23~~

3.4.1.4.~~4.1.4.~~ Test Case 4

Formatted: Heading 3, Space Before: 0 pt, After: 0 pt, Outline numbered + Level: 4 + Numbering Style: 1, 2, 3, … + Start at: 1 + Alignment: Left + Aligned at: 0 cm + Indent at: 1,27 cm

The propagation of sound is affected by the climatic conditions. As the meteorological parameters are temporally dynamic, the sound distribution from a turbine alters annually, daily and even hourly. In this case, the impact of alteration of the humidity on the wind turbine sound distribution is illustrated. To perform this analysis, the configurations of the wind turbine and the landscape remain unchanged with respect to Test Case 3. Only the humidity parameter is set differently. While in the other three test cases, the humidity is derived from the hourly mean humidity observation dataset of KNMI, in this test case the humidity is defined manually through the *humidity slider* in the Falcon UI. In this case, the humidity is set to 40%. The wind turbine noise simulation with the adjusted humidity parameter is illustrated in Figure 17.

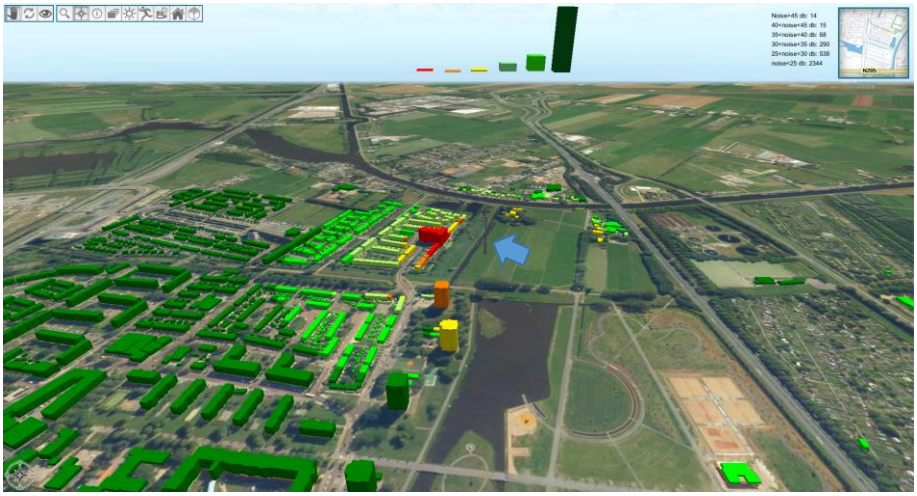

Figure 17. Wind turbine noise propagation in Test Case 4.

Comparing the results with Test Case 3, slight changes in the noise distribution can be observed due to altering the humidity from 80% (Test Case 3) to 40% (Test Case 4). In this test case, more buildings receive a noise level below 25 dB compared to Test Case 3. This is the result of sound attenuation due to atmospheric absorption, as discussed in Section 3.2.2.3. This change

occurs mainly for the buildings at relatively great distances from the wind turbine (Equation (10)). The numeric distribution of this test case is presented in Table 7.

Table 7. Noise distribution in Test Case 4.

Noise level (dB (A))	Number of buildings affected
L_{pA} <25	2344
25< L_{pA}<30	538
30< L_{pA} <35	290
35< L_{pA} <40	68
40< L_{pA} <45	15
L_{pA} >45	14
~~Noise level (dB (A))~~	~~Number of buildings affected~~
~~L_{pA} <25~~	~~2344~~
~~25< L_{pA} <30~~	~~538~~
~~30< L_{pA} <35~~	~~290~~
~~35< L_{pA} <40~~	~~68~~
~~40< L_{pA} <45~~	~~15~~
~~L_{pA} >45~~	~~14~~

The comparative sound propagation results of Test Case 3 and Test Case 4 are presented in Figure 18.

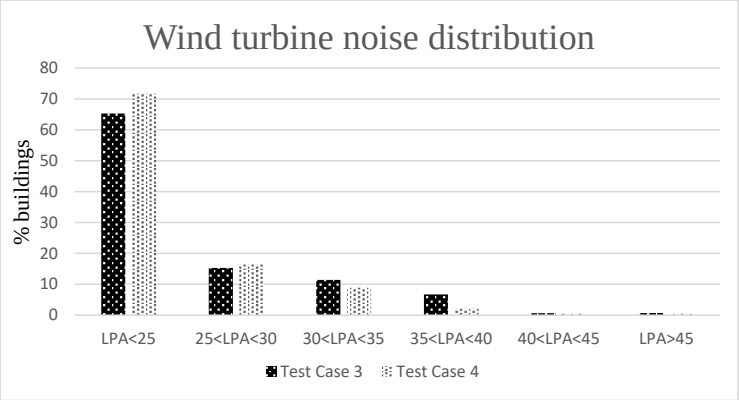

Figure 18. Comparative results between Test Cases 3 and 4.

~~5.~~3.5. Conclusion

Formatted: Heading 1, Outline numbered + Level: 2 + Numbering Style: 1, 2, 3, … + Start at: 2 + Alignment: Left + Aligned at: 0 cm + Indent at: 0,95 cm

This study describes the conceptual design and implementation of an integrated environmental information system for the support of the wind turbine planning process. The developed system is an integration of three major components, namely game engine, GIS and sound model. The easy-to-use interface of the platform allows for the contribution of users with different ~~[~~technical~~]~~ backgrounds, and its interactivity, provided through the game engine, has the potential to attract a broader age range, including the very young citizens, who are often absent from the planning process. This transparency of the interaction is considered as one of the most important requirements of a support tool (Geertman and Stillwell, 2012).

Various geospatial data are presented through this platform to the participants, who can interactively build and explore various plan scenarios, in any location in the Netherlands, and see their design impact in real time. Massive geospatial data are served from the cloud and incorporated through the integration of GIS tiling techniques and OGC standard protocols into the game engine via the Unity API. The cloud-based architecture of the framework eliminates the need for local storage and the embedded standard protocols for the data transfer through the web make this platform compatible for accessing and loading various available open data through the internet. This broadens the data accessibility and interoperability and the latter (i.e. interoperability) eliminates the need for data preparation, which leads to considerable efficiency, as in many projects a great amount of time and energy is spent on data preparation and formatting. This is of great importance for a system with several components and inter-related modules, where different data types from different domains and providers must be integrated and be able to interoperate. This can also help the further development of the software by providing the basis for an evolving Spatial Data Infrastructure (SDI) and eliminating the requirement for a whole new geospatial framework construction (Strobl, 2006). Standardization

supports the loose coupling of services and their reuse in different software systems (Goodall et al., 2011).

The developed framework provides the possibilities of assessing the aesthetic impact of the wind turbine on the landscape as well as evaluating its noise impact on the surrounding buildings. The aesthetic evaluation is performed subjectively through the 3D model of the existing geospatial data and the 3D wind turbine model. The impact of the wind turbine sound on the surrounding buildings is assessed through sound propagation models integrated into our developed framework and is displayed both numerically and through colour variation. The integration of the sound model provides the users with a more accurate estimation and makes the framework appealing for different domains, such as noise experts and legislation authorities. The system provides real-time sound calculations and feedbacks for each design scenario to intertwine the discussion process. We have accomplished this through the game operations as well as the GIS functionalities integrated in Falcon.

While the real-time sound calculations can offer great benefits in a discussion process, it should be noted that some simplifications have been carried out on the sound models for their adaptation to the performance speed. The estimation simplification for combining the direct and reflected waves as well as the modelling of the wave reflection between buildings can be mentioned here. Improving the accuracy of the sound model with the cost of a longer calculation time, would first require a further development of the sound models themselves, an aspect that is not within the scope of this research.

The integration of all the aforementioned separate components into one environment results in a fortified platform with no dependencies on external analytical software. This untangles the game engine disintegration from GIS analytical tools, mentioned by Bishop and Stock (2010) as the limitation of game engines (Bishop and Stock, 2010).

While this platform is presented for the case of a single wind turbine in this study, due to the emphasis on the explanations of the underlying models, simultaneous analysis of multiple wind turbines is also possible. This supports the wind turbine scenario formation in larger scales (e.g. wind farms) where the target energy is aimed to be yielded through multiple wind turbines (of different types). This innovative new platform has the potential to make a great contribution to planning processes. However, to evaluate the different benefits and the potential of this framework in a planning process, analysis of the usability and effectiveness should be performed. Further enhancement of this framework can embrace other wind turbine externalities, such as shadow effects, as well as wind turbine energy yield models.

~~References~~

~~Al-Kodmany, K. (1999). Using visualization techniques for enhancing public participation in planning and design: process, implementation, and evaluation. *Landscape and Urban Planning, 45*(1), 37-45.~~

Arezes, P. M., Bernardo, C. A., Ribeiro, E., and Dias, H. (2014). Implications of wind power generation: exposure to wind turbine noise. *Procedia Social and Behavioral Sciences,109*, 390-395.

Attenborough, K. (1992). Ground parameter information for propagation modeling. *The Journal of the Acoustical Society of America*, *92*, 418-427.

Attenborough, K., Taherzadeh, S., Bass, H. E., Di, X., Raspet, R., Becker, G. R., Güdesen, A., Chrestman, A., Daigle, G. A., L'Espérance, A., Gabillet, Y., Gilbert, K. E., Li, Y. L., White, M. J., Naz, P., Noble, J. M., and Van Hoof, H. A. J. M. (1995). Benchmark cases for outdoor sound propagation models. *The Journal of the Acoustical Society of America*, *97*, 173-191.

Attenborough, K., Li, K. M., and Horoshenkov, K. (2007). *Predicting outdoor sound*. New York, CRC Press.

Bakker, R. H., Pedersen, E., van den Berg, G. P., Stewart, R. E., Lok, W., and Bouma, J. (2012). Impact of wind turbine sound on annoyance, self-reported sleep disturbance and psychological distress. *Science of the Total Environment*, *425*, 42-51.

Bass, H., Sutherland, L., and Zuckerwar, A. (1990). Atmospheric absorption of sound: Update. *The Journal of the Acoustical Society of America*, *88*, 2019-2021.

Bishop, I. D. and Stock, C. (2010). Using collaborative virtual environments to plan wind energy installations. *Renewable Energy*, *35*(10), 2348-2355.

Bishop, I. D. (2011). Landscape planning is not a game: Should it be? *Landscape and Urban Planning*, *100*(4), 390-392.

Chessell, C. (1977). Propagation of noise along a finite impedance boundary. *The Journal of the Acoustical Society of America*, *62*, 825-834.

Daigle, G., Piercy, J., and Embleton, F. (1978). Effects of atmospheric turbulence on the interference of sound waves near a hard boundary. *The Journal of the Acoustical Society of America*, *64*, 622-630.

Daigle, G. (1979). Effects of atmospheric turbulence on the interference of sound waves above a finite impedance boundary. *The Journal of the Acoustical Society of America*, *65*, 45-49.

Deal, W. F. (2010). Wind power: an emerging energy resource. *Technology and Engineering Teacher*, *70*, 9-15.

de La Beaujardière, J. (2002). *Web Map Service Implementation Specification, OpenGIS® Implementation Specification, 1.1.1, OGC 01-068r3*. Open Geospatial Consortium, Inc., https://portal.opengeospatial.org/files/?artifact_id=1081&version=1&format=pdf

Formatted: English (United States)

Field Code Changed

Delany, M. and Bazley, E. (1970). Acoustical properties of fibrous absorbent materials. *Applied Acoustics*, *3*(2), 105-116.

Embleton, T., Piercy, J., and Daigle, G. A. (1983). Effective flow resistivity of ground surfaces determined by acoustical measurements. *The Journal of the Acoustical Society of America*, *74*, 1239-1244.

EU Directive (2009). Directive 2009/28/EC of the European Parliament and of the Council of 23 April 2009 on the promotion of the use of energy from renewable sources and amending and subsequently repealing Directives 2001/77/EC and 2003/30. *Off. J. of the EU, European Commission*, *5*, 16-62.

EWEA (2015). European Wind Energy Association: Wind in power: 2014 European statistics. (Retrieved 2014-11-05).

Evans, A., Vladimir, S. and Evans, T. J. (2009). Assessment of sustainability indicators for renewable energy technologies. *Renewable and Sustainable Energy Reviews*, *13*(5), 1082-1088.

Filios, A. E., Tachos, N. S., Fragias, A. P. and Margaris, D. P. (2007). Broadband noise radiation analysis for an HAWT rotor. *Renewable Energy*, *32*(9), 1497-1510.

Forrest, T. G. (1994). From sender to receiver: propagation and environmental effects on acoustic signals. *American Zoologist*, *34*(6), 644-654.

Geertman, S. and Stillwell, J. (Eds.). (2012). *Planning support systems in practice*. Springer Science & Business Media.

Goodall, J. L., Robinson, B. F., and Castronova, A. M. (2011). Modeling water resource systems using a service-oriented computing paradigm. *Environmental Modelling & Software*, 26(5), 573-582.

Gregory, J. (2009). *Game engine architecture*, *2nd edn*. CRC Press, pp. 28-38.

Grosveld, F. W., Shepherd, K. P., and Hubbard, H. H. (1995). Measurement and prediction of broadband noise from large horizontal axis wind turbine generators. *Wind Turbine Technology*, *1*, 211-220.

Groth, T. M. and Vogt, C. (2014). Residents' perceptions of wind turbines: An analysis of two townships in Michigan. *Energy Policy*, *65*, 251-260.

Hall, N., Ashworth, P., and Devine-Wright, P. (2013). Societal acceptance of wind farms: Analysis of four common themes across Australian case studies. *Energy Policy*, *58*, 200-208.

Herwig, A. and Paar, P. (2002). Game engines: tools for landscape visualization and planning. *Trends in GIS and Virtualization in Environmental Planning and Design*, *161*, 172.

Formatted: English (United States)

Jallouli, J., and Moreau, G. (2009). An immersive path-based study of wind turbines' landscape: A French case in Plouguin. *Renewable Energy*, *34*(3), 597-607.

Jobert, A., Laborgne, P., and Mimler, S. (2007). Local acceptance of wind energy: Factors of success identified in French and German case studies. *Energy Policy*, *35*(5), 2751-2760.

Johnson, M., Raspet, R., and Bobak, M. (1987). A turbulence model for sound propagation from an elevated source above level ground. *The Journal of the Acoustical Society of America*, *81*(3), 638-646.

Kurze, U. and Anderson, G. (1971). Sound attenuation by barriers. *Applied Acoustics*, *4*, 35-53.

Kurze, U. (1971). Noise and vibration control. Noise and vibration control. Ed. by Beranek, L.L. McGraw-Hill.

Maekawa, Z. (1968). Sound attenuation by screens. *Applied Acoustics*, *3*(1), 157-173.

Manwell, J., McGowan, J., and Rogers, A. (2002). *Wind energy explained: Theory, design and application*. West Sussex, UK, John Wiley.

Masó, J., Pomakis, K., and Julià, N. (2010). *Web Map Tile Service Implementation Standard*, *OpenGIS® Implementation Standard*, *1.0.0: OGC 07-057r7*. Open Geospatial Consortium, Inc., http://portal.opengeospatial.org/files/?artifact_id=35326

Moriarty, P., Guidati, G., and Migliore, P. (2005). Prediction of turbulent inflow and trailing-edge noise for wind turbines. *Proceedings of the 11th AIAA/CEAS Aeroacoustics Conference (Monterey, Canada)*. AIAA Paper 2881.

Nicolas J., Berry, J., and Daigle, G. (1985). Propagation of sound above a finite layer of snow. *The Journal of the Acoustical Society of America*, *77*, 67-73.

O'Coill, C. and Doughty, M. (2004). Computer game technology as a tool for participatory design. In: *eCAADe2004: Architecture in the Network Society, Copenhagen, Denmark*.

Oerlemans, S., Sijtsma, P., and Méndez López, B. (2007). Location and quantification of noise sources on a wind turbine. *Journal of Sound and Vibration*, *299*(4), 869-883.

Oerlemans, S. and Schepers, J. (2009). Prediction of wind turbine noise and validation against experiment. *Acoustics*, *8*, 555-584.

Pedersen, E. (2011). Health aspects associated with wind turbine noise—Results from three field studies. *Noise Control Engineering Journal* *59*(1), 47-53.

Piercy, J. E., Embleton, T. F. W., and Sutherland, L. C. (1977). Review of noise propagation in the atmosphere. *The Journal of the Acoustical Society of America*, *61*(6), 1403-1418.

Pierpont, N. (2009). Wind turbine syndrome: A report on a natural experiment. *Santa Fe, NM, USA: K-Selected Books*.

Field Code Changed

Prospathopoulos, J. M. and Voutsinas, S. G. (2007). Application of a ray theory model to the prediction of noise emissions from isolated wind turbines and wind parks. *Wind Energy*, *10*, 103–119.

Saidur, R., Rahim, N. A., Islam, M. R., and Solangi, K. H. (2011). Environmental impact of wind energy. *Renewable and Sustainable Energy Reviews*, *15*(5), 2423–2430.

SER (2013). Energieakkoord voor duurzame groei, http://www.ser.nl/~/media/files/internet/publicaties/overige/2010_2019/2013/energieakkoord-duurzame-groei/energieakkoord-duurzame-groei.ashx

Stock, C., Bishop, I. D., O'Connor, A. N., Chen, T., Pettit, C. J., and Aurambout, J. P. (2008). SIEVE: Collaborative decision-making in an immersive online environment. *Cartography and Geographic Information Science*, *35*(2), 133–144.

Strobl, J. (2006). Visual interaction: Enhancing public participation. *7th International Conference on Information Technologies in Landscape Architecture: Trends in Knowledge-Based Landscape Modelling*.

Tadamasa, A. and Zangeneh, M. (2011). Numerical prediction of wind turbine noise. *Renewable Energy*, *36*, 1902–1912.

Tippett, J. (2005). The value of combining a systems view of sustainability with a participatory protocol for ecologically informed design in river basins. *Environmental Modelling & Software*, 20(2), 119–139

Vitolo, C., Elkhatib, Y., Reusser, D., Macleod, C. J., and Buytaert, W. (2015). Web technologies for environmental Big Data. *Environmental Modelling & Software*, 63, 185–198.

Vretanos, P. A. (2005). *Web Feature Service Implementation Specification. OpenGIS® Implementation Specification, 1.1.0, OGC 04-094*. Open Geospatial Consortium, Inc. (2005), https://portal.opengeospatial.org/files/?artifact_id=8339

Wagner, S., Bareiss, R., and Guidati, G. (1996). *Wind Turbine Noise*. Berlin, Germany, Springer.

2020 climate & energy package (2009). *European Commission, Climate Action, package*. http://ec.europa.eu/clima/policies/strategies/2020/index_en.htm (last accessed 11.02.16).

Formatted: English (United States)

Field Code Changed

Chapter 4: Interactive 3D Geodesign Tool for Multidisciplinary Wind Turbine Planning[19]

Abstract

Wind turbine site planning is a multidisciplinary task comprising of several stakeholder groups from different domains and with different priorities. An information system capable of integrating the knowledge on the multiple aspects of a wind turbine plays a crucial role on providing a common picture to the involved groups. In this study, we have developed an interactive and intuitive 3D system (Falcon) for planning wind turbine locations. This system supports iterative design loops (wind turbine configurations), based on the emerging field of geodesign. The integration of GIS, game engine and the analytical models has resulted in an interactive platform with real-time feedback on the multiple wind turbine aspects which performs efficiently for different use cases and different environmental settings. The implementation of tiling techniques and open standard web services support flexible and on-the-fly loading and querying of different (massive) geospatial elements from different resources. This boosts data accessibility and interoperability that are of high importance in a multidisciplinary process. The incorporation of the analytical models in Falcon makes this system independent from external tools for different environmental impacts estimations and results in a unified platform for performing different environmental analysis in every stage of the scenario design. Game engine techniques, such as collision detection, are applied in Falcon for the real-time implementation of different environmental models (e.g. noise and visibility). The interactivity and real-time performance of Falcon in any location in the whole country assist the stakeholders in the seamless exploration of various scenarios and their resulting environmental effects and provides a scope for an interwoven discussion process. The flexible architecture of the system enables the effortless application of Falcon in other countries, conditional to input data availability. The embedded open web standards in Falcon results in a smooth integration of different input data which are increasingly available online and through standardized access mechanisms.

4.1. Introduction

Formatted: Heading 1, Left, Space After: 0 pt, No bullets or numbering

Wind energy, as a rich energy source in the Netherlands, has been applied for hundreds of years through wind mills and recently through wind turbines. Aligned with the *EU climate and energy package*, the EU aims to achieve a 20% share of energy from renewable energy sources (2020 climate & energy package, 2009), the on-shore wind power of the Netherlands is intended to

[19] This chapter is published in Journal of Environmental Management as: Rafiee, A., Van der Male, P., Dias, E., & Scholten, H. (2018). Interactive 3D geodesign tool for multidisciplinary wind turbine planning. Journal of environmental management, 205, 107-124.

increase to 6000 MW in 2020, forming 11 national wind parks (Ontwerp-structuurvisie Windenergie op land, 2013).

Wind turbine site suitability depends on environmental, technological, economic, social and political aspects (Mekonnen and Gorsevski, 2015), making it a complicated decision process for which multiple criteria should be taken into account (Grassi et al., 2012; Tegou et al., 2010). While developers are mainly concerned about economic issues as acquisition, development and operation costs (Grassi et al., 2012; Dvorak et al., 2010), residents and local communities struggle with the environmental externalities, especially noise, shadow flicker and aesthetic influences (Righter, 1996; Swofford and Slattery, 2010; Warren et al., 2005; Aydin et al., 2010; Devine-Wright, 2005; Harding et al., 2008). In spite of large public acceptance (Toke, 2002; Firestone and Kempton, 2007; Mulvaney et al., 2013), these negative impacts result in the resistance of local communities against employing a wind turbine in their neighborhood (Jones and Eiser, 2010; Jobert et al., 2007). Such conflicts can lead to the wind turbine project delay or even complete cancellation (Agterbosch et al., 2009; Mari et al., 2011) which are problematic for attaining the national wind energy target.

Research has shown that carefully considering public participation in projects reduces the citizens' oppositions and smooths public acceptance (Khan, 2003; Strachan and Lal, 2004; Aitken, 2010). Wolsink (2007) emphasized the statement of Pasqualetti and Energy (2002) for the Netherlands, that the success of the wind power depends on the public's participation both in information distribution concerning wind power as well as the public's contribution in debates and decisions regarding wind turbines locations. A transparent flow of information to the local citizens from the starting phase of a wind power project and their involvement in the planning process increases their acceptance (Maillebouis, 2003). Therefore, a participatory planning system, which can present the multi-aspect information of a wind turbine site planning, can be of great benefit.

GIS[20] as a system capable of managing geospatial data from acquisition and storage to analysis and presentation (Longley et al., 2001), has been a popular approach in many environmental planning and land allocation decision processes (Malczewski, 1996; Thomas, 2002; Arampatzis et al., 2004; Chang et al., 1997), as there are many geospatial components in such an analysis. In the case of wind turbine planning, there have been several researches on GIS-based assessments and decision support systems on wind turbine impact analysis and site allocation (Mekonnen and Gorsevski, 2015; Aydin et al., 2010; Mari et al., 2011; Ramírez-Rosado et al., 2008; Nobre et al., 2009; Malczewski, 1996; Rodman and Meentemeyer, 2006; Ouammi et al., 2012; Gorsevski et al., 2013; Minelli et al., 2014; Lejeune and Feltz, 2008; Janke, 2010; Simao et al., 2009) verifying the potency of GIS in such decision processes.

The final location of a wind turbine should be usually negotiated among the different participants of the planning process with different, and sometimes conflicting interests. This makes wind turbine site planning a multi-agent decision making process, which should be applied in a multi-criteria planning tool (Ramírez-Rosado et al., 2008; Mari et al., 2011). Such a tool should be an interface between all the components of a participatory plan process from

[20] Geographical Information System

the problem definition to the design, the evaluation and the final decision, introducing geodesign as a proper underlying method for the tool (Warren-Kretzschmar, et al., 2012). Geodesign is defined as the set of techniques for planning built and natural environments in an integrated process where the creativity of the design is integrated with impact models of the science (Flaxman, 2010; Dias et al., 2013). Within this iterative framework participants receive feedback during each design step rather than a final feedback when much effort and time have been spent. Iterating through these steps and receiving real-time feedbacks on each step, the final design will be developed more efficiently (Warren-Kretzschmar et al., 2012; Flaxman, 2010). This is a suitable framework for different participatory planning processes, for instance landscape planning, wherein the planners stimulate and evaluate different future landscape settings in the form of scenarios. A geodesign approach which enables the rapid formation, alteration and evaluation of such alternative scenarios improves the participation of the involved parties in the planning process (Albert and Vargas-Moreno, 2012). To make this framework beneficial in practice, new tools for the agile generation and evaluation of design concepts are required (Flaxman, 2010) in which complex analysis can be handled quickly (Warren-Kretzschmar et al., 2012).

In this study we have developed an interactive system to implement the geodesign framework for wind turbine site selection. This system, called "Falcon 3D Geodesign Tool" (will be called Falcon throughout the paper), is developed upon a game engine to conduct the fast interactions required for real-time feedbacks of the geodesign process. This system is an extension to the currently developed Falcon for wind turbine site planning, focusing on the noise (Rafiee, et al., 2017) which is now further developed to a multidisciplinary geodesign platform. State-of–the-art GIS techniques have been applied in this tool for serving and querying massive 2D/3D nationwide data. This is in line with the "big data era" which supports performing the geodesign practice at multiple scales (Li and Milburn, 2016). We have implemented complex environmental models into this tool for the impact estimation of wind turbines on the built-up areas as well as the turbine generated power.

4.2. Methodology: Geodesign-based System Architecture

Formatted: Heading 1, Left, Space After: 0 pt, No bullets or numbering

Though the outline of a specific geodesign study is formed by the planning participants, a general geodesign framework is posed by Carl Steinitz (1990) (Steinitz, 2012; Steinitz, 1990). This framework comprises six models which will be reviewed at least three times during the geodesign process (Steinitz, 2012). Each geodesign step is implemented separately in Falcon and yet form an integrated decision supporting system. Every step might consist of several modules which can have inter-relations or be independent from each other. Following is a more detailed explanation on the models presented in Steinitz framework and their contributions to our developed system.

4.2.1. Representation models

Formatted: Heading 2, Left, Space After: 0 pt

Representation models define how the study area should be described in content, space and time (Steinitz, 2014), in which data collection and presentation form the core

In this study, we have developed a digital platform for the geodesign process within which we have used various techniques to serve large datasets and support real-time interactions. These datasets can be visualized in the 2D or 3D representation modes. Users can be directed to a specific location by typing an address, or navigate manually through view pan, zoom and rotate functionality.

While 2D representation is a familiar and preferred environment for some participants, 3D representations provide the scope for a more intuitive perception of the scenes which equips the user with an easier link between the information and reality (Al-Kodmany, 2002; Dias et al., 2003). Furthermore, this representation is in line with the 3D nature of the different [wind turbine] impact models, such as noise, shadow and visibility.

Representation models are presented to the geodesign team through Falcon platform. The architecture of this platform, concerning only representation models, is depicted in Figure 1.

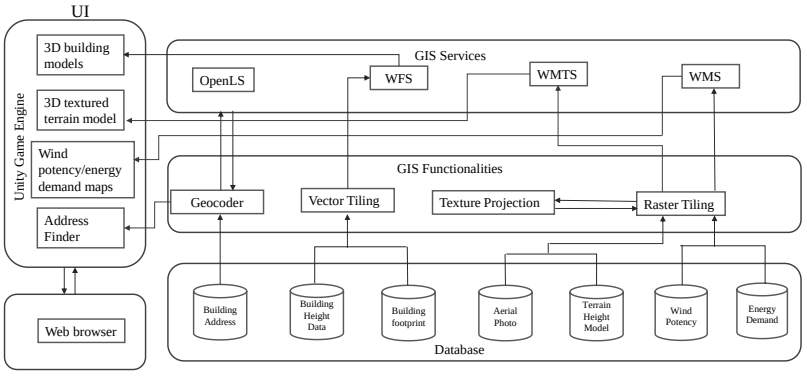

Figure 1. Architecture of the representation models.

The main features of this architecture are explained as follows:

- *Web-based platform*

A web-based system has several advantages over traditional stand-alone systems, among which are the cross-platform capability, easier update deployment and maintenance (db net Solutions, 2007). Assimilation of representation models into a web-based system supports the provision of the common picture of the study area to different users from different locations and platforms.

- *Game Engine*

Game engines provide an interactive platform for the navigation in spatial environment depicted through graphical presentation. Different graphical and geometrical optimization techniques

support a graphically rich presentation of a spatial environment in different levels of detail (Freudenberg et al., 2001). A game engine often consists out of three main components, namely, a 3D engine, behavior and a network component. While the *3D engine* is responsible for real-time rendering and generation of a constant frame rate for animation, *behavior* is a set of rules for i.a. dynamic simulations and collision detection and *network* assists in multi-player interactions (Freudenberg et al., 2001).

- *Integration of GIS into a game engine*

Integration of geospatial data and GIS functionalities into the interactive environment of a game engine provides the scope for optimized visualization of various georeferenced data, efficient interaction with the data and performing real-time environmental analysis. However, scale is an important issue when geospatial data are involved. While a particular functionality performs well in a neighborhood level, it might not perform the same at regional or national level/at neighborhood level. In larger scales, [massive] geospatial data cannot be handled through traditional data processing systems. Tiling is a technique used to serve large geospatial data in small parts to client. WMS[21], WMTS[22] and WFS[23], as OGC[24] standard protocols, are integrated in our platform to serve the raster and vector information of each tile through internet, respectively. In addition to the feasibility of serving large datasets, implementing these standard protocols support the data interoperability through which data from different resources can be served into the platform without any preceding preparations. Geocoder functionality, which is built through the incorporation of OpenLS[25] service, provides the possibility of navigating to a specific address, is a useful component for a system which operates on a national level.

Integration of GIS techniques and the standard protocols into the game engine enabled us to serve large geospatial data of the whole of the Netherlands from different resources into the interactive environment where optimized visualization and various interactions are its two key features (Rafiee et al., 2017).

- *Data*

The study area is described by the 2.5D terrain model which is textured through the aerial photo of the region as well as the extruded 3D building models. 2.5D terrain model and 3D building models are generated using detailed height model of the Netherlands (AHN2[26]) using LIDAR[27] technique. The accuracy of this dataset is 5 centimeter in both horizontal and vertical planes and the density of the dataset is 6-10 points per square meters (Van der Zon, 2013). The terrain

[21] Web Map Service
[22] Web Map Tile Service
[23] Web Feature Service
[24] Open Geospatial Consortium (http://www.opengeospatial.org/)
[25] [OpenGIS®] Open Location Service
[26] AHN2 was collected and made available by the Dutch Water Boards and Rijkswaterstaat, part of the Ministry of Infrastructure and the Environment (http://www.ahn.nl/).
[27] Light Detection And Ranging

and building models are served into the game engine using 3D vector tiling and the aerial photo is served using raster tiling techniques.

Electricity demand map on the neighborhood level (generated through combining the yearly average electricity consumption data[28] and postcode 6 digits boundary map of the Netherlands) as well as the wind potency map of the Netherlands at 100 meter height (SenterNovem, 2005)[29] are served as WMS in Falcon. The former provides an indication of the suitable areas for wind turbine positioning when a local energy supply/consumption target is aimed and the latter provides a useful overview on the proper locations for wind turbines from wind power harvest perspective. The input data of the wind potency computations are the long-term statistic of wind speeds at KNMI[30] stations and the hourly wind speed at KNMI stations within one year are used for the wind turbine power estimations (see Section 2.5.1).

4.2.2. Process models

Formatted: Heading 2, Left, Space After: 0 pt

Process models attempt to seek how the study area operates and find out the functional and structural relationships among the elements as well as their interaction behavior (Steinitz, 2014; Reynolds, 2014). These models determine the scope of the project and indicate what should be included (Steinitz, 2012).

The location of exiting wind turbines in the study area influences the positing of new wind turbines in the region due to different factors such as energy distribution and wind turbulence caused by the wind turbines. In this study, we have integrated the location and characteristics of the existing wind turbines of the whole of the Netherlands in Falcon. For presenting the existing wind turbines a standard 3D wind turbine model has been chosen and scaled for each turbine based on its geometrical characteristics obtained from the wind turbine dataset. Figure 2 presents an instance of existing wind turbines.

[28] This dataset has been provided as open data through grid operator Liander (https://www.liander.nl/over-liander/innovatie/open-data/data)
[29] This map has been developed by KEMA Nederland B. V. under the assignment of SenterNovem (a former agency of the Ministry of Economic Affairs)
[30] the Royal Dutch Meteorological Institution

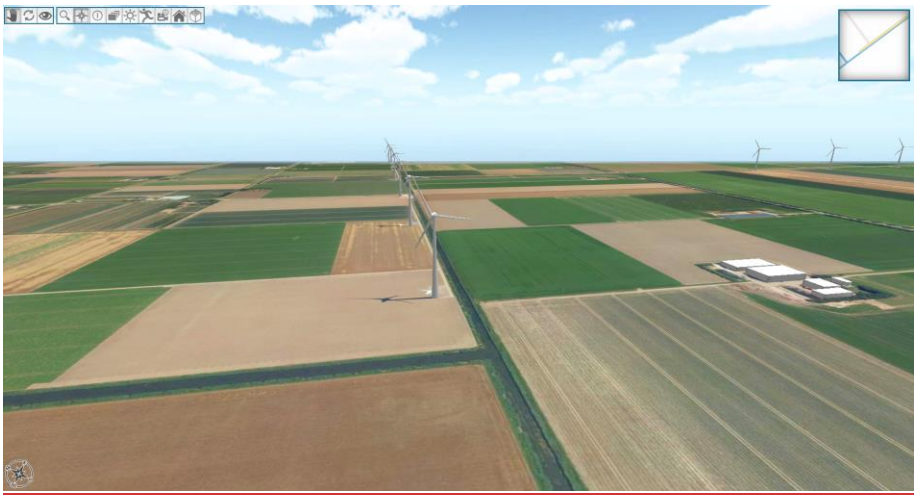

Figure 2. Existing wind turbines

One of the affecting issues on the wind turbine locations are the regulations posed by the national and/or local government regarding the wind turbine positioning. These regulations should be identified in the process models (Steinitz, 2012).

In this study we have used the Dutch national rules extracting from Risk Zoning Wind Turbines Manual[31] (Faasen, et al. 2013). This document is set up by DNV GL[32] and commissioned by Netherlands Enterprise Agency[33] and provides the uniform method for the quantitative risk analysis of wind turbine operation on the environment and tests the results against the acceptance criteria. This results in the estimated risk distance around buildings, roads, railways, power line, pipeline, primary dike and water.

The risk distance criteria depends on the wind turbine capacity, hub height and rotor diameter. Therefore different distance criteria should be applied for different wind turbines. In this study we have defined the distance criteria for all the wind turbine types in Falcon library and subsequently generated constrained areas' map for each wind turbine type through applying spatial buffers around the aforementioned objects (e.g. buildings). The generated restricted area map is served as WMS in Falcon.

Figure 3 presents the generated map of the restricted area for two wind turbines. The first one is a 800kW wind turbine with 50 meter hub height and 48 meter rotor diameter and the second one is a 4200 kW wind turbine with 135 meter hub height and 127 meter rotor diameter.

[31] Handboek Risicozonering Windturbines
[32] https://www.dnvgl.nl/
[33] Rijksdienst voor Ondernemend Nederland

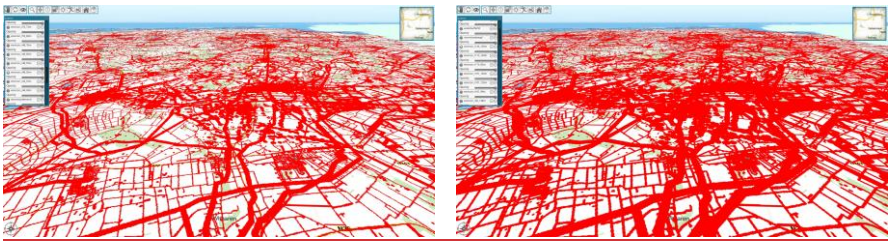

a b

Figure 3. Restricted area map for a) 48R-50 H wind turbine and b) 127R-135 H wind turbine. The buffer radii are the distance criteria derived from the regulations (tables 1 and 2) which are dependent on the wind turbine capacity, hub height and rotor diameter.

In addition to the visualization, the generated regulation web map services are used as inputs in the *Regulation Control* module for an automated real-time regulation conformity control. Upon placing a new wind turbine or moving it in the game scene, the relevant regulation map will be defined automatically based on the wind turbine type and its relevant WMS layer will be queried. Subsequently, the land allowance status for the wind turbine location will be queried using GetFeatureInfo Request and presented by the interface. The mentioned national regulations are applied in this system for the generation of the restricted area and does not contribute in other decision support processes. Figure 4 shows the implemented process models.

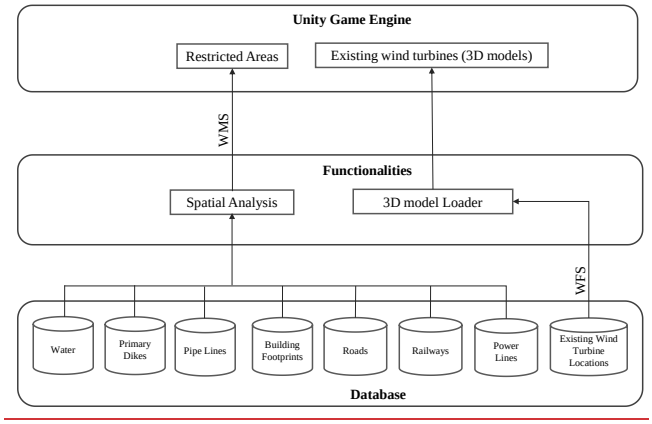

Figure 4. Process models.

4.2.3. *Evaluation models*

Formatted: Heading 2, Left, Space After: 0 pt

Evaluation models consist of objective or subjective evaluation approaches and criteria to assess the performance of the current situation of the study area. Local inhabitants and stakeholders consider different performance components to evaluate the appropriateness of the current situation. Attractiveness, vulnerabilities, existing risks and poor performances of the area are clarified in this step which defines what should be changed and what should be preserved.

Therefore evaluation models have great influence on the decision-making process (Campagna and Di Cesare, 2014).

The location and distribution of the existing wind turbines and their total generated power, when compared with the target power (the total desired power for the region), provides an initial outline to the planning group about the proper number, location and specifications of new wind turbines.

National and local regulations on wind turbine locations also play important role on the evaluation of the current situation of the study area. When the location of an existing wind turbine is in conflict with the regulations, e.g. due to wind turbine construction prior to a specific legislation, an orientation towards relocating and replacing it with a new and more efficient wind turbine might arise. Figure 5 presents the components of the evaluation model.

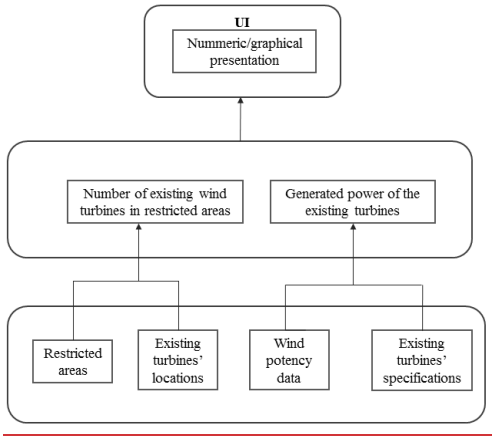

Figure 5. Components of the evaluation model for the case study.

4.2.4. *Change models*

Formatted: Heading 2, Left, Space After: 0 pt

Change models peruse how the study area might be altered through posing different scenario's and alternatives (Steinitz, 2014; Nedkov et al., 2014) which form the first step of a concrete design (Campagna and Di Cesare, 2014). These changes can be propounded by citizens, designers or local authorities (Nedkov et al., 2014). An interactive and collaborative design platform supports a multi-disciplinary planning process in which various participants from different domains can work together.

Altering the amount of the generating power from the wind turbines requires the increase/reduction of the number of wind turbines or replacing the old turbines with new ones. Planning for such an alternation requires the knowledge about the landscape and cannot be performed irrespective of the characteristics of the study area. Therefore the design platform should contain the information of the landscape. An interactive design environment in which the information from different domains is integrated, plays a great role in a multi-disciplinary

planning process. Fast performance of the design platform speeds up the discussion procedure and eases the creation of the different scenarios to converge to the ultimate design. Figure 6 presents the architecture of this design environment.

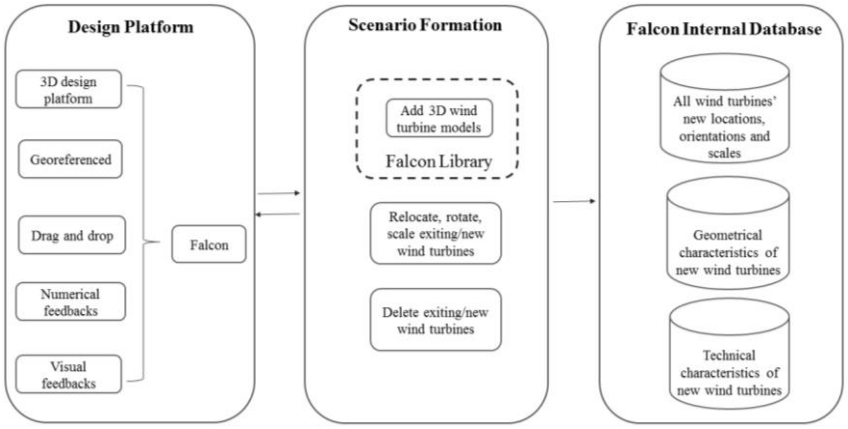

Figure 6. Architecture of the design platform developed in this study.

This platform contains a library of 3D models of different wind turbines encompassing their geometric and technical information, delivered by the suppliers. Users can insert different turbines into the design environment through a simple drag and drop act and relocate them with a simple drag and move one (Figure 7). Once a wind turbine is added to the scene, different technical information of the turbine is presented to the user (Rafiee, et al., 2017). Geometric information (e.g. wind turbine hub height and rotor diameter) and other technical specifications (e.g. wind turbine power capacity and sound power level) will be further used in impact analysis step in which both visual and numerical feedbacks are provided to the designers.

Figure 7. Falcon 3D design platform; designers can add different types of wind turbines into the scene. Once a specific wind turbine is added, its technical information will be queried for further analysis. This information can also be observed by clicking the wind turbine.

4.2.5. *Impact models*

Formatted: Heading 2, Left, Space After: 0 pt

A design cannot be finalized regardless of its nearby environment. Each time a scenario is designed, its impact on the environment should be assessed. Likewise, the impact of the existing elements of the environment on the design might be considerable. Therefore, a new design should be evaluated within its spatial context and environment.

Impact models intend to explore the consequences of the alteration proposed by a specific design scenario. The range of the sequels caused by the change might be broad and overlay different domains.

Environmental impacts of a wind turbine can be grouped in two categories of benefits and externalities. The environmental benefits of a wind turbine include the replacement of fossil energy with a clean renewable energy source which leads to CO_2 reduction and the global warming mitigation. The negative externalities of a wind turbine, as the second environmental impact group, comprises of wind turbine noise, shadow and aesthetic impacts, which are, as mentioned in Section 1, the main concerns of local communities and citizens rather than

developers. The environmental impacts of a wind turbine depend on the wind turbine specifications, as well as the configuration of the built-up area.

We have implemented analytical models in the 3D design environment of Falcon to present the consequences of a design scenario to the geodesign team. These consequences comprise of wind turbine generated power and the negative environmental impacts which are quantified through sound, shadow and visibility models. Figure 8 presents the applied impact models in Falcon 3D geodesign tool. Upon the placement of a wind turbine in a specific location, all these impacts are calculated real-time and presented to the team both numerically, as well as visually, by using variant colors and charts.

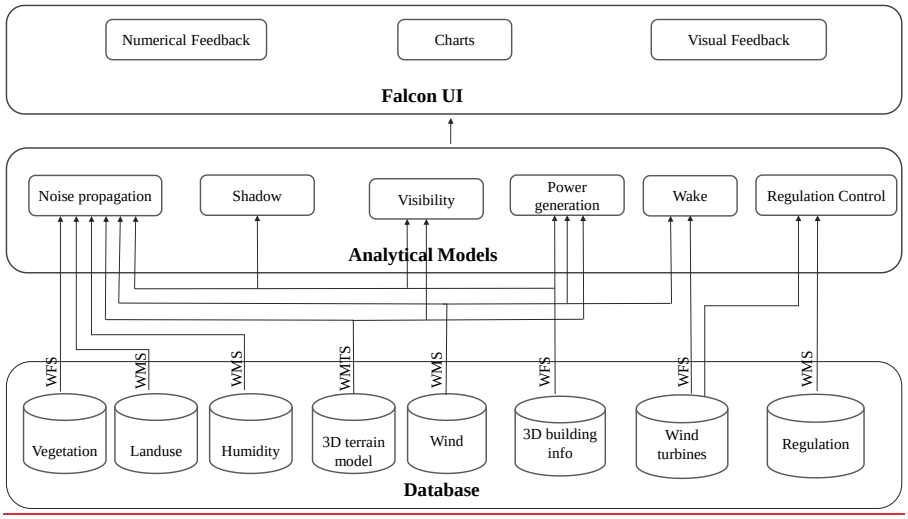

Figure 8. Components of the impact models applied in this study.

Table 1 presents the constituent modules for these impact models as well as the applied technique types and domains and the employed data. Once a new configuration is designed, the different impacts of the design are evaluated real-time through the embedded models of our geodesign environment.

Table 1. Components of the impact model sub-module together with the applied technique types/domains and the employed data.

Module	**Technique**		**Data**
	type	**domain**	
Sound			
Geometrical Spreading	3D Distance	Game engine	3D Building models
			Wind turbine characteristics
Atmospheric Absorption		GIS	Temperature

	GetFeatureInfo Request		Humidity
Vegetation	3D Distance	Game Engine	Landuse
	3D Line Casting	Game Engine	Wind turbine Characteristics
	GetFeature Request	GIS	3D Building models
Ground Reflection	3D Distance	Game Engine	Landuse
			Wind turbine Characteristics
	GetFeatureInfo Request	GIS	3D building models
Turbulence Disturbance	3D Distance	Game Engine	Landuse
	GetFeatureInfo Request	GIS	Wind
			Wind turbine Characteristics
			3D building models
Obstruction	3D Distance	Game Engine	Wind turbine Characteristics
	3D Line casting	Game Engine	3D building models
	3D Collision Detection		
Weather Effects	3D Distance	Game Engine	Wind
			Temperature
	GetFeatureInfo Request	GIS	3D building models
Shadow			
3D Shadow Model Generation	Mesh Filter/Mesh Renderer	Game Engine	Wind turbine geometrical characteristics
Shadow Model Interaction With Buildings	3D Collision Detection	Game Engine	3D building models
	GetFeatureInfo Request	GIS	
Visibility			
Line-of-Sight Analysis	GetFeatureInfo Request	GIS	3D building models
			2.5D terrain model
	3D Collision Detection	Game Engine	Wind turbine geometrical characteristics
Power Generation			
Yearly Average Generated Wind Power	GetFeature Request	GIS	Wind
			2.5D terrain model
			Wind turbine geometrical and technical characteristics

Regulation Control			
Regulations Conflict Control	GetFeatureInfo Request	GIS	Restricted Areas
Wake Control			
Wake Conflict Control	Mesh Filter/Mesh Renderer	Game Engine	Wind turbine geometrical characteristics
	3D Collision Detection	Game Engine	

4.2.5.1. Power Generation

In accordance with Justus et al. (1976), the average generated wind power of a wind turbine $\overline{P}_T$ can be estimated as follows:

$$\overline{P}_T = \int_{-\infty}^{\infty} P_T(u)\, f(u)\mathrm{d}u \qquad (1)$$

Here, $P_T(u)$ is the generated power as a function of the wind velocity and $f(u)$ the probability density distribution of the wind velocity u. This probability density distribution can reasonably well be described by the Weibull function:

$$f(u) = \frac{k}{a}\left(\frac{u}{a}\right)^{k-1} e^{-\left(\frac{u}{a}\right)^{k}} . \qquad (2)$$

The actual shape of the Weibull function is determined by the scale factor *a* and the shape factor *k*, determining the skewness of the distribution. Wieringa and Rijkoort (1983) considered the application of the Weibull distribution for the Dutch wind climate. They found limited variation of the shape factor and suggested values of $k = 1.74 \pm 0.06$ for onshore locations and $k = 2.0$ for coastal areas. The scale factor can be estimated from the mean yearly wind velocity $\overline{U}$. Realistic normalized values for the scale factor in the Netherlands vary from $a = 1.123\overline{U}$ for onshore locations to $a = 1.128\overline{U}$ for coastal areas. These values are normalized to a height z_0 =10 m above open terrain. Once the coefficients *a* and *k* are known for this reference height, their values for the desired altitude can easily be determined (Justus et al., 1978).

The power curve is specific to wind turbine characteristic, but in general, the following expression can be adopted (Akpinar and Akpinar, 2004):

Formatted: Heading 3, Left, Space After: 0 pt, No bullets or numbering

Field Code Changed

Field Code Changed

Field Code Changed

Field Code Changed

Field Code Changed

Field Code Changed

Field Code Changed

Field Code Changed

Field Code Changed

Field Code Changed

Field Code Changed

Field Code Changed

$$P_T(u) = \begin{cases} 0 & , \text{ for } u \le U_{ci} \\ P_{TR}\dfrac{u^k - U_{ci}^k}{U_R^k - U_{ci}^k} & , \text{ for } U_{ci} < u \le U_R \\ P_{TR} & , \text{ for } U_R < u \le U_{co} \\ 0 & , \text{ for } u > U_{co} \end{cases} \quad (3)$$

In this expression, U_{ci} and U_{co} are the cut-in and cut-out wind velocity of the turbine, respectively, while U_R is the rated wind velocity. P_{TR} represents the generated power at rated wind velocity, and k is the shape factor from the adopted Weibull distribution.

A similar model has been applied in the studies done by Lu et al. (2002) and Celik (2004). The presented model is applicable for flat terrains without too much atmospheric disturbance from buildings and vegetation. The model could be extended to account for the presence of buildings (Kastner-Klein and Rotach, 2004, Grimmond and Oke, 1999, MacDonalds et al., 1998) and vegetation (Dellwik et al., 2014), respectively.

The hourly wind data is extracted from KNMI. For each station, we have calculated the mean wind velocity probability density distribution through a Weibull function (Equation (2)). Once a wind turbine is added to the scene, the nearest station to the turbine will be queried and the corresponding wind velocity probability density distribution parameters will be retrieved. Linking the wind turbine characteristics with the wind velocity density distribution, we have determined the mean power production of the wind turbine (Equation (1)).

Since the goal of a wind turbine siting project is to fulfill a target energy amount, in each design stage an overview of the produced and residual power supports the stakeholders with a better orientation on the more proper distribution and characteristics of the remaining wind turbines.

4.2.5.2. Noise

The noise of a wind turbine, as perceived by a receiver, originates from the combination of the noise generation at the turbine and the noise propagation towards this receiver (Wagner et al., 1996). At the turbine, the noise is generated mechanically or aerodynamically. Several detailed models have been developed for the prediction of this noise (Filios et al, 2007, Oerlemans and Schepers, 2010, Tadamasa and Zangeneh, 2011). As a rule of thumb, the generated noise can be estimated from the rotor diameter and the blade tip speed (Manwell, 2002):

$$L_{WA} = 50(\log_{10} V_{tip}) + 10(\log_{10} D) - 4, \quad (4)$$

where L_{WA} is the overall A-weighted sound power level, V_{tip} the blade tip speed and D the diameter of the rotor.

Ray tracing models are commonly applied for the prediction of the propagation of the noise from a single sound source (Lamancusa and Daroux, 1993, Attenborough et al.,(1995),

Field Code Changed
Field Code Changed
Field Code Changed
Field Code Changed
Field Code Changed
Field Code Changed
Formatted: Heading 3, Left, Space After: 0 pt, No bullets or numbering
Field Code Changed
Field Code Changed
Field Code Changed
Field Code Changed

Attenborough et al. (2006), and Prospathopoulos and Voutsinas, 2007). Given the sound pressure level L_{p_0} at unit distance from a source, the sound pressure L_{p_r} at a receiver location can be obtained from:

$$L_{p_r} = L_{p_0} - \sum A_i \,, \qquad (5)$$

where A_i represents the excess attenuation that may result from geometrical spreading, ground reflection, atmospheric turbulence, atmospheric absorption, absorption through vegetation and diffraction.

The attenuation from the geometrical spreading of a single wave can be found from the inverse square law, where the reflection from the ground can be accounted for via the superposition of the direct and the reflected waves (Piercy et al., 1977). This approach accounts for the wave incidence angle, path length for the direct and the reflected waves, the sound frequency and the impedance of both air and ground. For the estimation of the latter, several empirical results relations exist (Delany and Bazley, 1970, Chessell, 1977, Nicolas et al., 1985, Embleton et al., 1983, and Attenborough, 1992).

The effect of atmospheric turbulence can be included on the basis of the models from Daigle (1978) and Daigle (1979). These models allow for the estimation of the long-term average of the mean square of the sound pressure, where the effect of different weather conditions is accounted for, through the index of reflexion and a specific turbulence length scale (Johnson et al., 1987).

Atmospheric absorption is caused by sound energy scattering due to viscous losses and relaxation process, and can be expressed in terms of an absorption coefficient. Bass et al. (1990) presented an empirical relation for the absorption coefficient as a function of the sound frequency, the temperature and the humidity. The absorption is shown to be higher for high frequencies, while the absorption generally decreases for increasing humidity. Regarding the dependency on temperature, the absorption coefficient shows a peak at a specific temperature, the value of which increases for increasing frequency and decreasing humidity (Harris, 1966). Attenuation through vegetation results from scattering, reflection and refraction, from leaves and trunks. As an approximation, the attenuation can be calculated from the sound frequency and the crossing distance (Kurze and Beranek (1971)).

In order to predict the sound level behind an obstruction, such as a building, the diffraction model of Kurze and Anderson (1971) is adopted. This engineering model uses the Fresnel number to estimate the attenuation.

Apart from diffraction, refraction due to the wind and temperature conditions is considered. Both wind and temperature gradients affect the sound wave pattern, potentially resulting in sound shadow zones – areas with a sudden decrease in the sound pressure. Such shadow zones may occur at a certain distance from the source in the upwind direction, as a result of the

Field Code Changed
Field Code Changed
Field Code Changed
Field Code Changed

curvature of the sound wave paths. The distance at which a shadow zone may appear can be predicted with the model described by Wagner et al. (1996). The applied sound models of Falcon are explained in details in Rafiee, et al., 2017).

The different sound model components, namely, geometrical spreading, atmospheric absorption, vegetation effect, ground reflection, air turbulence, diffraction due to obstacles and refraction due to shadow zones are implemented in Falcon as separate noise modules which can be presented detachedly in Falcon. The total resulting sound from the turbine on the surrounding buildings, as the integration of all the aforementioned components, is implemented in Falcon geodesign tool (for a detailed explanation see (Rafiee, et al., 2017)).

Figure 9 presents the wind turbine total noise calculation in Falcon. The different noise components, resulting from the turbine noise emission and propagation, are included in this calculation. Upon the placement of a wind turbine in the scene, its sound impacts on the surrounding buildings (within 1km distance) are calculated and presented real-time both visually (through building colorization and relevant-colored chart) and numerically.

Figure 9. Wind turbine noise impact calculation in Falcon. The wind turbine noise impact is presented real-time both visually (colorized buildings and chart) and numerically (top).

Falcon contains a simplified sound module, next to the above mentioned detailed sound module, which takes only the geometrical spreading (as the major defining component) into account for a faster performance. For the area depicted in Figure 9, the performance duration of the advanced sound module is around 980 millisecond versus 10 millisecond for the simple sound module.

In addition to the sound propagation prediction of the current climatic situation, Falcon provides the possibility for different climatic scenario analyses. This can support the seasonal or extreme climates impact analyses on the propagated sound, for instance. Wind speed, humidity and temperature values can be adjusted through the employed sliders in the interface (Figure 9). By altering the value of each slider, all the relevant sub-modules are triggered and updated real-time.

4.2.5.3. Shadow

Formatted: Heading 3, Left, Space After: 0 pt, No bullets or numbering

For the reconstruction of the objects' shadows at a specific moment, the position of the sun, expressed in solar azimuth and altitude should be known. We have calculated the solar azimuth and altitude for a specific time on a specific location based on the orbital algorithms (Vallado, 2001). Once the azimuth and altitude of the sun is known the shadow vertices for each object can be calculated using an affine transformation.

While the instantaneous shadow analysis is helpful for a specific time, stakeholders may also be interested in a broader view on the shadow impact of a wind turbine. They might want to have an insight on the average shadow impact in summer when they sit in their garden or winter when the shadows are longer. Furthermore, different stakeholders have different priorities and purposes based on which a flexible shadow analysis is required. Therefore, in addition to the 3D model reconstruction of the instantaneous shadow, we have implemented the algorithm for real-time reconstruction of the yearly average, seasonal and monthly shadow models. For this purpose, the minimum and maximum solar azimuth and the average of the elevation within a whole year, season and month are calculated through the orbital algorithms and applied in the shadow model, replacing the momentary solar azimuth and altitude.

To spot the affected buildings by the shadow volume of the wind turbine, we have performed the collision detection analysis in Falcon. Beside the visualization possibility, we have implemented the numerical feedback in Falcon, through displaying the total number of affected building by the shadow in the scene. This can orient the geodesign team in an optimized positioning of the wind turbine where less buildings will be influenced by its shadow.

4.2.5.3.1. Instantaneous shadow

Formatted: Heading 4, Left, Space After: 0 pt, No bullets or numbering, Tab stops: Not at 3,97 cm

The instantaneous 3D shadow model is generated based on the instantaneous solar azimuth and elevation of the arbitrary time, day, month as well as the wind turbine location and geometry. Figure 10 presents the wind turbine instantaneous shadow implementation in Falcon. Effected buildings by the turbine's shadow are displayed in black. The total number of affected building are displayed on the top of the image. The shadow slide is shown on the top left of the image. The user can alter the time, day and month values and the 3D shadow model will be constructed real-time.

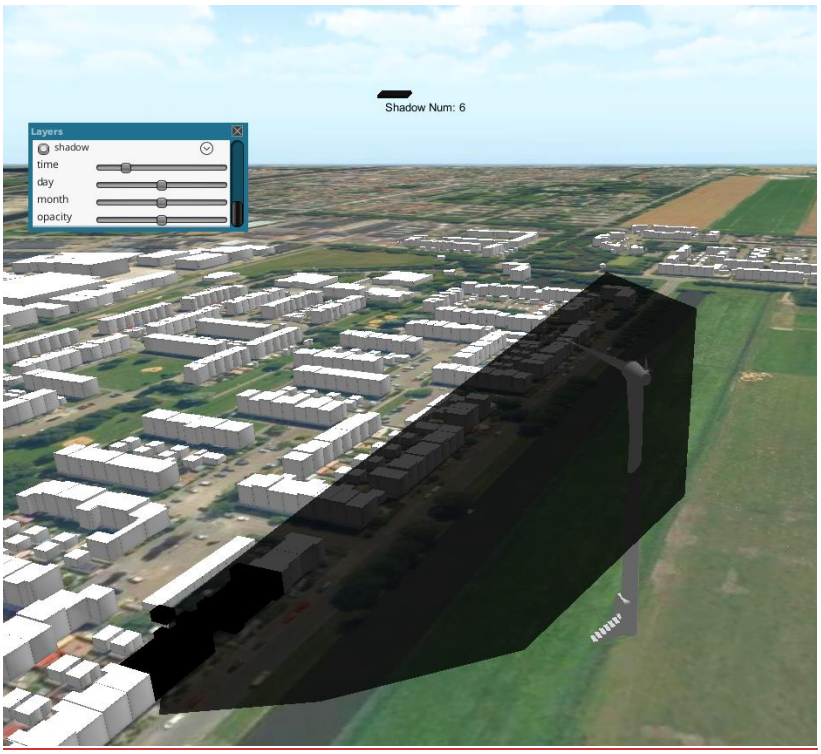

Figure 10. 3D wind turbine instantaneous shadow model implementation in Falcon. Upon the time/day/month alternation (top left slider) updated shadow model is reconstructed real-time.

4.2.5.3.2. Average shadow

Formatted: Heading 4, Left, Space After: 0 pt, No bullets or numbering, Tab stops: Not at 3,97 cm

The average shadow sub-module contains yearly, seasonal and monthly average 3D shadow models. Figure 11 presents the wind turbine average shadow reconstruction in Falcon.

a b

c

Figure 11. Wind turbine average shadow a) yearly average, b) seasonal average (winter) and c) monthly average (February).

The real-time performance of the wind turbine shadow is depicted in Film 1.

https://video.vu.nl/media/Interactive+3D+geodesign+tool_Film1/1_rrodfdb1

Film 1. Real-time performance of wind turbine shadow

The optimized performance of the game engine in collision detection, together with the implementation of real-time solar calculations and 3D shadow algorithm, resulted in a real-time shadow impact analysis. At the moment, this analysis cannot be implemented real-time in a conventional GIS system, as the intersection operation is a computationally demanding and time-consuming process. On the other hand, loading the georeferenced objects of the whole country into a game engine and the following analysis would be hardly possible without the optimization GIS techniques, such as vector tiling. Therefore, an integration of GIS objects and techniques into a game engine can greatly support interactive and real-time shadow analysis.

4.2.5.4. Visibility

Formatted: Heading 3, Left, Space After: 0 pt, No bullets or numbering

The wind turbine visibility from each building is estimated through the optimized line casting/collision detection possibility of Falcon, based on Unity game engine. A line of sight is defined between the target point (center point of each building) and the wind turbine hub location and height. Subsequently, the obstruction of the line of sight by other buildings is controlled through the collision detection between the sight line and the surrounding 3D building models. If there are any obstacles colliding the line of sight between the wind turbine and the target point, the wind turbine is considered as “not visible” and otherwise “visible” (Figure 12).

Figure 12. Visibility analysis performed in Falcon. The wind turbine is visible from taller buildings whose line of sight is not blocked by other buildings (pink) while not visible from lower buildings hidden behind taller buildings (blue).

The agile performance of the wind turbine visibility module is presented in Film 2.

https://video.vu.nl/media/Interactive+3D+geodesign+tool_Film2/1_gact83yj

Film 2. Agile performance of the wind turbine visibility module.

The optimized performance of the game engine on line casting/collision detection speeds up this procedure, which is a computational demanding task and cannot be performed real-time in a conventional GIS system.

4.2.5.5. Wake area

Formatted: Heading 3, Left, Space After: 0 pt, No bullets or numbering, Tab stops: Not at 3,97 cm

The flow disturbance from wind turbines in the upwind segment of the area, reduces the energy yield of the neighboring wind turbines (Limpo, 2011). To minimize the effect of flow disturbances, a minimum spacing between the wind turbines should be accounted for. In line with previous studies, for an array loss less than 10%, we have applied a spacing of 8-10 and 5-7 times the rotor diameter in the prevailing and crosswind directions, respectively (Lissaman et al., 1982; Manwell et al., 2010). This forms two elliptic areas around a wind turbine, called wake areas, into which no other wind turbines should be placed. The major axis should be chosen towards the prevailing wind direction, which for the Dutch wind climate corresponds with the south-west to north-east direction.

These wake areas around each turbine, are presented in Falcon. Each time a wind turbine is added to the scene, its rotor diameter will be retrieved from the database and its wake ellipses

will be constructed, rotated towards the dominant wind direction and displayed real-time in the viewer.

In addition to the visual analysis, the interference between the wake areas of the inserted wind turbines are inspected using the game engine collision detection functionality. Upon the insertion or movement of a wind turbine in the scene, the collision of its inner and outer ellipses with the other wake area ellipses of the scene is detected separately. As a result, the total number of wake area conflicts for the inner and outer ellipses are calculated and presented real-time through the interface. Figure 13 illustrates the numeric feedback regarding the inner and outer wake area interference of multiple new and existing wind turbines (top right). *Vacant area conflict first ring* attribute depicts the total number of the inner ellipse collisions with each other and *vacant area conflict second ring* attribute presents the total collision numbers between the outer ellipses as well as the inner-outer ones.

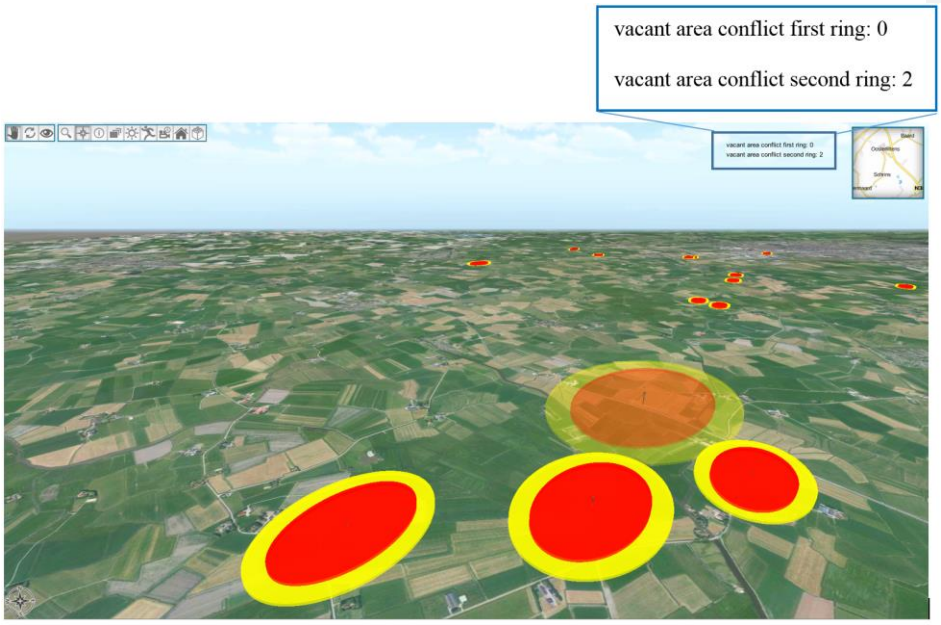

Figure 13. Numeric feedback regarding the wake area interference between the new (transparent) and existing wind turbines

4.2.6. *Decision models*

Formatted: Heading 2, Space After: 0 pt

The purpose of decision models is to determine the preferences among all the feasible scenario's and alternatives to converge to the final decision. The final decision can be influenced by the local knowledge as well as the design scenario's impacts presented at impact models.

Since in such a decision process several [conflicting] influential criteria and preferences play a role, a multi-criteria decision analysis (MCDA) can help the stakeholders and decision makers in converging to the best alternative. This, alongside the local knowledge of local inhabitants helps the decision team in approaching the final decision.

In this framework, we have applied Weighted Linear Combination (WLC) for defining the decision function. This function is specified as the overall combinatory value in location i defined as $V(A_i)$ in Equation 6.

$$V(A_i) = \sum_{k=1}^{n} w_k v(a_{ik}) \quad (6)$$

where w_k is the assigned weight to the k^{th} criteria, a_{ik} is the value of the k^{th} criteria in location i and v is the value function, which converts the raw criteria values into a standardized one (Malczewski and Rinner, 2015) (Equation 7).

$$v(a_{ik}) = \left(\frac{a_{ik} - \min\{a_{ik}\}_i}{\max\{a_{ik}\}_i - \min\{a_{ik}\}_i}\right)^{\rho} \quad (7)$$

for the k^{th} criterion intended to be maximized and

$$v(a_{ik}) = \left(\frac{\max\{a_{ik}\}_i - a_{ik}}{\max\{a_{ik}\}_i - \min\{a_{ik}\}_i}\right)^{\rho} \quad (8)$$

for the k^{th} criterion to be minimized. The shape of these functions is determined by ρ (Malczewski and Rinner, 2015).

To estimate the criteria weights (w_k), as the relative importance of a criterion compared to other criteria, we have applied two approaches, namely rating and pairwise comparison methods. Figure 14 presents our proposed decision model.

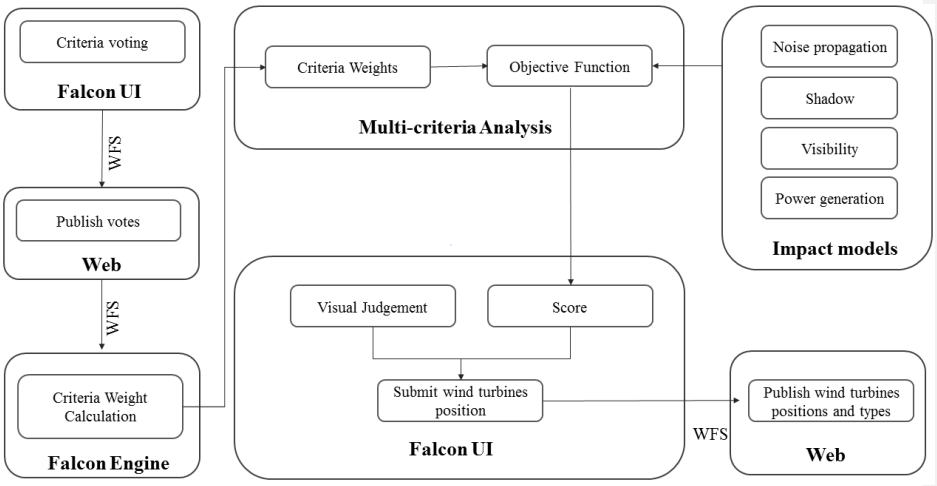

Figure 14. The applied decision model in Falcon.

4.3. Results and discussion

Formatted: Heading 1, Left, Space After: 0 pt, No bullets or numbering

This research focuses on the integration of different aspects regarding wind turbine siting. The remaining of this section contains the implementation results of how the different aspects are combined in the system in order to best inform the user. In addition, it contains the discussion on how the system can be potentially applied in an international context.

4.3.1. Multi-criteria analysis

Formatted: Heading 2, Left, Space After: 0 pt, No bullets or numbering, Tab stops: Not at 3,97 cm

While each particular wind turbine impact (noise, shadow, visibility and power generation) can be of importance for a specific target group, the additional information on the overall impact of a wind turbine provides a collective indicator for the stakeholders. Therefore, we have integrated all the impact modules into a single component which, upon a wind turbine placement in the scene, calculates and integrates all the wind turbine effects simultaneously. While it is still possible for the stakeholders to choose a single (or multiple arbitrary) impact module(s) for wind turbine influence investigation, the overall impacts offers a better scope for

a multi-criteria analysis. The real-time simultaneous performance of the sound (simple), shadow, visibility and power generation is depicted in Film 3.

https://video.vu.nl/media/Interactive+3D+geodesign+tool_Film3/1_uzl1vw6g

Film 3. The real-time simultaneous performance of the sound (simple), shadow, visibility and power generation modules.

4.3.1.1. Scoring

Formatted: Heading 3, Left, Space After: 0 pt, No bullets or numbering

In this implemented multi-criteria analysis, we have defined a decision function which takes wind turbine sound, shadow, visibility and power generation into account (Equation (6)). The [scaled] value of this function, called "score" in this study, is an auxiliary information which can potentially orient the stakeholders towards a more convergent decision.

The applied criteria in the decision function includes the number of buildings receiving above 35 dB(A) noise, the number of buildings affected by the turbine(s)' shadow, the number of buildings which have a view on wind turbine(s) and the amount of the yearly produced power by the turbine(s). The quantity of these criteria is standardized through value functions to be used in the decision function. For all the criteria we have applied a maximizing value function (Equation (7)) so that all the criteria can be added together and the final "score" becomes ascending with the direct relation to the appropriateness of the scenario configuration. The value functions of the decision criteria are considered linear, in line with most of the GIS-MCDA[34] approaches (Malczewski and Rinner, 2015; Malczewski, 2006).

The applied weights of a decision function can have significant impact on its final value. In the case of a planning process consisting of participants with different domains and roles, the preferences of the decision agents with respect to the criteria significance often differ and conflict. For instance, in the case of wind turbine planning, developers assign more weights on the produced power while local communities might allocate higher weights to the wind turbine sound, shadow and visibility. This conflict of vision on the assigned weights might lead to contradictory *score* values. Therefore it is important that these weights are defined collaboratively by the different participating stakeholders. In our system, there are two ways for collaborative determination of criterion weights of the objective function, namely collective and individual collaboration. The former refers to the case where all the participants use a single device for scenario design whereas in the latter case, stakeholders are participating through individual devices. Two weighting methods, namely, Rating and Pairwise Comparison are implemented in Falcon (see Section 2.6), which can be used separately or for the comparison of the resulting scores.

In a collective process, the weight for each criteria can be discussed among the stakeholders in person and will be assigned to the objective function through Falcon *weight sliders*. Each time

[34] GIS-based Multicriteria Decision Analysis

the weight of a criteria is altered by a user through its slider, the weights of the other criterion, in the Rating method, will be updated automatically and are displayed seamlessly through their sliders. The added/subtracted value for the other criterion equals to one third of the difference between the old and new value for the altered criteria so that the total summation of the weights remains equal to 1. For an individual collaboration process, we have developed a voting system where each participant can vote for the criteria weights. Voting is a reliable approach in supporting a group decision making (Laukkanen et al., 2002). In our system, this is performed by defining weights through *weight sliders* and submitting them to the system. Each submitted vote will be sent to the server and added to an existing web feature service, which holds the voted weights of all other participants. For each criteria, the average of all weights are then calculated and applied in the decision function (as implemented by Laukkanen et al. (2002) and Andrienko et al. (2003)). Film 4 presents Falcon *weight sliders* which is used for score weight assignment in a collective or individual collaboration. It presents the sliders for Rating method as well as Pairwise Comparison approach where the relative preferences of mutual criteria is defined by the user(s).

https://video.vu.nl/media/Interactive+3D+geodesign+tool_Film4/1_3egimwlo

Film 4. Weight sliders for Rating as well as Pairwise Comparison methods applied in the multi-criteria analysis

The impact of different assigned criteria weights on the final score is depicted in Figure 15. Increasing the energy yield criterion weight (Figure 15 (a)) leads to a low score. This is due the low produced power with regard to the total power target. Increasing the number of wind turbines, keeping all other parameters and weights the same (high energy yield criterion weight), results in an increased score (Figure 15 (b)). By decreasing the energy yield criterion weight and increasing the shadow criterion weight, keeping all other parameters (wind turbine types and configuration) the same as (b), the final score decreases to 89.65 (Figure 15 (c)). This is due to the combination of high number of affected buildings by shadow and shadow criterion weight.

Score: 54.84 Score: 99.6

a b

Score: 89.65

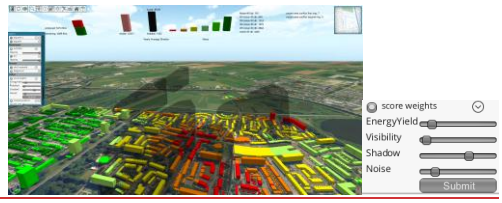

c

Figure 15. The impact combination of criteria weight and configuration on the final score; the higher number of wind turbines in (a) compared to (b), in combination with a high energy yield criterion, with all other parameters the same, results in a higher score. The higher shadow criterion weight (and the lower energy yield weight) in (c), with the same wind turbines' configuration as (b), leads to a decreased score.

In each scenario design stage, the total score is presented which can potentially orient the stakeholders towards a more efficient scenario (re)design. The applied decision function can be used together with the knowledge of the local inhabitants as well as the participants' judgements about the turbines visual effects and other impacts (noise, shadow, visibility and power generation), provided through numbers and charts in Falcon interface, to orient towards a decision. The final decision will be taken after multiple iterations through the geodesign steps.

While the previously developed decision support systems have focused on important aspects of wind turbine site selection, the implementation results of Falcon demonstrates the advancement of this system regarding the interactivity, flexibility and multidimensionality which makes it a suitable decision support tool for a wide range of participants. Mari et al., (2011) designed a web-oriented decision support system to help public operators in preliminary determination of proper wind turbine locations. This system provides the information as map layers (comprising wind data, wind power maps, exclusion maps and background layers) which can be overlaid by the users for an easier navigation through the region. While these map layers provide useful information to the user, the incorporation of numerical impact models in Falcon provides the means for an objective evaluation of the different environmental effects of a wind turbine on its surroundings. Aydin et al., (2010) considered different wind turbine environmental impacts in their developed decision support system. These impacts were indicated as the fuzzy objectives of the decision problem which were quantified with different criteria. The applied criteria were the buffer zones defined through Turkish legislations as well as previous studies

which were used to define the membership functions of the acceptability fuzzy sets aimed for the final estimation of priority sites. In another study, Ramírez-Rosado et al., (2008) have created different criteria maps for different user groups followed by the creation of tolerance maps using GIS techniques. The resulting tolerance maps of the decision support system are used for the selection of the best locations of wind turbines. While the presentation of the suitable locations of wind turbines through these indicators are useful, the explicit and detailed numerical feedbacks on each environmental impact for each adjusted scenario, as in Falcon, offers a deeper view and can open up a more objective discussion process between the different user groups. Furthermore, the possibility of seamless wind turbine placement and movement, rather than predefined (grid) locations, and real-time update of environmental models in Falcon upon the placement/movement of each wind turbine, rather than offline (pre)calculations, supports a seamless discussion process and makes Falcon a novel decision support system for wind turbine site planning compared to the previously developed tools. The 3D environment, the possibility of straightforward integration of other map layers by the user, without the alteration in the system (provided through open standard web service incorporation in Falcon) and the integration of massive geospatial data (through tiling techniques) which expands the analysis feasibility to the extent of the whole country or more (See Section 3.2) are other privileges of Falcon compared to the previously mentioned tools.

4.3.2. *International context*

Formatted: Heading 2, Left, Space After: 0 pt, No bullets or numbering

Formatted: Font:

The choice to make Falcon compliant with geospatial web standards (Section 2.1) enables this application to be effortlessly applied in other countries eliminating data formatting inconsistencies and supporting data interoperability. The system's skeleton, namely the game engine-GIS-analytical models integration, remains unchanged and the alteration merely occurs in the input data. Naturally, the data needs to be present, but recent years have witnessed a burst of governmental and non-governmental data being published and made available online via standardized access mechanisms and often within national or international Spatial Data Infrastructure such as NSDI in the US (Federal Geographic Data Committee, 1995), ASDI in Australia (ANZLIC, 1996), Geosur in south America (Van Praag and Borrero, 2012) and INSPIRE in Europe (European Commission, 2007). In the European context, the data Falcon currently uses is in most cases prescribed within INSPIRE initiative meaning European countries are expected to collect and share most of this data in a comprehensive and standardized format. Table 2 presents the required input data for applying Falcon in other countries as well as the OGC standard data access type and the INSPIRE annexes and themes.

Table 2. The required input data and the relevant service types for the deployment of Falcon in other countries as well as their equivalent INPIRE annexes and themes (European Commission, 2007).

Input Data	Service Type	INSPIRE Theme	An-nex	comments
Building Address	WFS	Addresses	I	
Building Footprint	WFS	Buildings	III	
Building Height Data	WFS	Elevation	II	in combination with the previous
Aerial Photo	WMS	Orthoimagery	II	
Terrain Height Model	WMS	Elevation	II	
Wind Velocity	WMS	Meteorogical geographical features	III	also energy resources theme
Electricity Demand	WMS		-	
Existing wind Turbine Locations	WFS	energy resources	III	
Restriction Elements	WFS		-	based on local legislation
Vegetation	WFS	Land cover	II	
Landuse	WMS	Land use	III	
Humidity	WMS	Meteorogical geographical features	III	

4.4. Conclusions

Formatted: Heading 1, Left, Space After: 0 pt, No bullets or numbering

The involvement of the stakeholders with different, and sometimes contradictory, viewpoints in wind turbine site planning calls for the presentation of clear and easy to use information on the multiple aspects of a wind turbine. This recapitulates the importance of having a system in the process that embeds the information regarding the different attributes involved in a wind turbine planning. In line with this, we have developed an interactive multidisciplinary wind turbine planning platform. It enables a geodesign approach, which supports a design attitude of drawing, (immediate) evaluating and redrawing (Albert and Vargas-moreno, 2012). The adaptation of the geodesign framework in the system enabled the structuring of the multidisciplinary process where the design and impacts are clearly intertwined and linked. In this platform, we have integrated game engine, GIS and different analytical models for real-time environmental analyses regarding wind turbines siting in the Netherlands.

The implementation of raster and 2D/3D vector tiling techniques in the system was a solution for data volume issues, through which different 2D/3D geospatial datasets of the whole of the Netherlands could be loaded on-the-fly in the game engine based platform. Through the incorporation of OGC standard protocols and web services in our system, many diverse datasets from different resources can be loaded to Falcon. This can untangle the data accessibility knot, which is mentioned as an impediment for the widespread application of a planning support system (Vonk et al., 2005). Furthermore, these datasets are interoperable and can be used directly, since the data formatting is no longer an issue.

Receiving real-time feedbacks at each design phase is considered an ideal geodesign instance (Flaxman, 2010). By integrating different analytical models in our system, the participants receive feedback of the different environmental impacts continuously during scenario design and with every adjustment. The long processing time required for running a such models is often a problematic issue. While in an offline system, this might be less a problem (e.g. commissioned environmental impact reports), in a live design procedure, where the participants should receive quick responses and real-time feedback of the design impact, the processing time plays a crucial role. To overcome this issue, we have applied different game engine functionalities (e.g. physical simulations through the game engine's physics engine) and GIS techniques for the real-time performance of the impact models.

Such a real-time impact analysis can inform the participants of the influence of their alteration each time a change model is proposed, during the design process rather than a final indication after the completion of the whole scenario design. This instantaneous impact assessments provides a seamless exploration scope and an intertwined discussion process.

The integration of the whole geodesign models, processes and impact evaluations into one platform, which is understandable for participants from different domains is mentioned as a privilege for a geodesign process (Albert and Vargas-morento, 2012). Such a unified platform splices the design process and omits the dependency for external software. The public accessibility of this platform through internet offers an easier way for public participation in planning processes (Batty, 1998; George, 1997; Albert and Vargas-moreno, 2012).

We believe that this 3D game engine-based and GIS integrated platform has great value in a participatory planning process and can be applied in wind turbines site selection. However, the usability and participants' experience of this tool should still be assessed in an applied geodesign workout.

Chapter 5: Analysing the impact of spatial context on the heat consumption of individual households[35]

Abstract

The heating of houses comprises a considerable share of the total energy consumption in many developed countries in temperate and colder climates. While most of the factors affecting space heating depend on individual choices (e.g. occupants' behaviour, interior building design, heating system efficiency) that are difficult to influence through urban planning, spatial context of individual housing units is within the sphere of influence of planners. Yet the impact of spatial context has hitherto received limited research attention due to the lack of geospatial data and the massive computer processing required to capture the shape and surroundings of individual housing units.

Regression analysis was performed in this study to explain the yearly gas consumption of all individual housing units in the city of Amsterdam, the Netherlands. The analysis focused on the impact of spatial context variables at two complementary scales: housing unit and postal code level. State-of-the-art 3D Geographic Information System (GIS) techniques were applied for the efficient processing of massive 3D geospatial data for all buildings in the city. Two- and three-dimensional spatial context of individual housing units was described using spatial data processing routines that characterised building shape and its surroundings.

The local housing unit level results highlighted the benefits of compact, dense urban forms: denser neighbourhoods with less open space and buildings with higher numbers of housing units and less exposed perimeters have lower heating demand. Trees are found to limit energy consumption when they are located on the colder northwest side of building units. The more aggregate postal code level results showed the importance of demographic composition: (larger) households with children consume most energy. Size and age of the housing unit are important determinants of energy at both scale levels: older houses have a higher energy consumption, but a rebound effect was found for the newest dwellings.

5.1. Introduction

The continuing increase in global energy consumption is still largely reliant of fossil fuels (Agency IE, 2011; Say and Yücel, 2006; Aydin, 2014). Under current policies, energy demand is expected to grow by 51% between 2009-2035 (Agency IE, 2011), especially because of economic growth, population growth, urbanization and energy prices (Agency IE, 2011; Feng and Zhang, 2012; Aydin, 2015; Köne and Büke, 2010). The resulting carbon emissions are estimated to increase by 2.4% per year between 2009 and 2035 (Aydin, 2014).

[35] This chapter is published in Renewable & Sustainable Energy Reviews journal as: Rafiee, A., Dias, E., & Koomen, E. (2019). Analysing the impact of spatial context on the heat consumption of individual households. Renewable & Sustainable Energy Reviews, 112, 461-470.

Formatted: Font: 16 pt, English (United States)

Formatted: Font: 16 pt, English (United States)

Formatted: English (United States)

Formatted: Heading 1, Space After: 0 pt, Line spacing: single, Outline numbered + Level: 2 + Numbering Style: 1, 2, 3, … + Start at: 1 + Alignment: Left + Aligned at: 0 cm + Indent at: 0,63 cm

The households (or residential) sector accounts for a substantial share of the total national energy consumption in many developed countries. This share is estimated to be around 22% in the USA (Energy Data Facts) and 25% in the European Union (Eurostat, 2018). In many countries space heating is the single most important contributor to household energy consumption, accounting for approximately 20%-80% of total household energy use in European countries depending on their climatic conditions (Eurostat, 2018). Reducing heat consumption in space heating has, subsequently, considerable potential in limiting the overall energy consumption and can be an important contribution to climate change mitigation.

5.1.1. The factors influencing household heat consumption

In order to develop strategies for reducing household heat demand, it is important to understand which factors influence heat consumption. The literatures consulted indicated four major groups of factors influencing heat consumption: occupants' behaviour, (interior) building design, system's efficiency and spatial context (Ratti et al., 2005; Rode et al., 2014; Chalal et al., 2016).

In the seventies, studies showed a significant contribution of behavioural changes on energy conservation (Donovan and Fischer, 1976) and that most variation in consumption (up to 71%) derives from occupant's behaviour (Sonderegger, 1978). More recently, Santin et al. (2009) demonstrated that occupants' behaviour and characteristics have a significant role on the used energy (4.2% for heating), but building characteristics and efficiency have a dominant share (42% for heating). However, the occupants' characteristics contribution may be actually larger as it also relates to dwelling type and heating system used which may increase its share when accounting for the relation. In Denmark, Gram-Hanssen (2010) applied quantitative measurements as well as qualitative interviews to explore the variation within socio-technical homogeneous groups living in similar buildings and showed that occupants' behaviour can lead to three times higher heat consumption. Guerra-Santin and Itard (2010) researched the relationship between energy usage and occupants' behaviour, household characteristics and their heating, ventilation and air conditioning systems. This research uncovered amongst others that the presence of manual thermostats and mechanical ventilation contributed more to energy conservation than having programmable thermostats and balanced ventilation. In addition, it showed that the presence of elderly people also had significant impact through increasing the number of hours the heating system was on. It is clear that homes and systems are becoming more efficient and smart technology support the efficient use of energy for heating spaces. However, studies have shown that the energy efficiency increase may not achieve full benefits since consumption behaviour adapts to the new efficiency (and decreased costs) by increasing consumption. This is known as the rebound effect and is described extensively by Berkhout et al. (2000).

In addition, several studies found that building design and system efficiency contribute to heat demand in existing house stock. Hong et al. (2006) studied the impact of energy efficiency refurbishment on space heating of residential buildings in the United Kingdom uncovering that insulation (cavity wall and loft insulation) leads to significant (up to 17%) impact on fuel consumption. Smeds and Wall (2007) and De Boeck et al. (2015) analysed how the energy

Formatted: Heading 2, Space After: 0 pt, Line spacing: single, Outline numbered + Level: 3 + Numbering Style: 1, 2, 3, … + Start at: 1 + Alignment: Left + Aligned at: 0 cm + Indent at: 1,27 cm

Formatted: English (United States)

performance of residential buildings can be improved through more efficient heating and ventilation systems and building design features, such as area to volume ratio, thermal insulation, air tightness of building envelope and the positioning of window areas and shading devices. Pacheco et al. (2012) confirmed these aspects, but also indicated that the influence of spatial context on energy performance of urban buildings is important and should be included in future research.

5.1.2. Spatial context and heat demand

Formatted: Heading 2, Left, Space After: 0 pt, Line spacing: single, Outline numbered + Level: 3 + Numbering Style: 1, 2, 3, … + Start at: 1 + Alignment: Left + Aligned at: 0 cm + Indent at: 1,27 cm

While numerous studies focused on the importance of occupants' behaviour, interior building design and system's efficiency for explaining building heat demand, limited attention has been paid to the spatial configuration of buildings and their surroundings. Some studies reflected on the role of local urban context on buildings' heat consumption using engineering models. Sanaieian et al. (2014) reviewed studies on the impact of urban block form on the energy performance of individual buildings. They listed several modelling approaches that calculate potential energy consumption based on assumed and theoretical relationships. Also Ratti et al. (2005) investigated the impact of the local urban context on energy consumption of buildings using an engineering-based energy consumption model. Their results suggested that about 10% of the annual energy usage for non-residential buildings can be explained by urban morphology. Rode et al. (2014) investigated the theoretical heat demand of different urban form types using samples of dominant building typologies and applying engineering-based models for their heat demand predictions. Their results indicated that higher surface-to-volume ratios (tall buildings) and increased building density values reduce heat demand. However, their analysis applied a limited number of fairly small case study areas and the authors call for further analysis to be expanded to the scale of full metropolitan areas.

Engineering models apply detailed building physical characteristics for the prediction of building energy demands based on known thermodynamics relations (Chalal et al., 2016). Energy and Environmental Prediction (EEP), Building Research Establishment Housing Model for Energy Studies (BREHOMES) and Digital Elevation Models/ Lighting and Thermal (DEM/LT) are often applied methods for energy predictions at the urban level (Sanaieian et al., 2014). Though these models can provide accurate energy performance estimates at building level, applications are limited to relatively small case studies due to their computational load as well as limited availability of the required detailed building data as input (Buffat et al., 2017; Fumo and Biswas, 2015; Zhao and Magoulès, 2012). Furthermore, engineering models mainly focus on simulating the impact of building physical characteristics and the applied systems on the energy performance, rather than unravelling the actual influence of neighbourhood conditions. In fact, Sanaieian et al. (2014) conclude in their review of studies applying engineering models that it is difficult to apply these to study the impact of urban block form and related micro-climate on energy consumption because of the complexity of properly describing the impact of all contributing factors simultaneously. Nouvel et al. (2015) applied engineering as well as statistical models for heat demand predictions and energy saving analysis in a specific neighbourhood in Rotterdam, the Netherlands (around 1000 buildings). Multi-linear regression analysis was used for the prediction of buildings' gas consumption at the city scale on zip-code zone level. This allowed for understanding how different variables such as

Formatted: English (United States)

house type (e.g. row house), floor area, number of occupants and construction period aggregated to zip-code level explained the variation of measured gas consumption.

Statistical approaches offer the opportunity to analyse actual variation in dwellings' energy behaviour and allow for the inclusion of a broader set of energy consumption related explanatory factors (Chalal et al., 2016; Frayssinet et al., 2018). These techniques have been applied in several studies investigating, for instance, the impact of dwelling type, surface area, construction year, number of occupants and characteristics of the inhabitants such as age and income (Mastrucci et al., 2014; Theodoridou et al., 2011; Santin et al., 2009). Only a few studies looked at the impact of building shape on heat demand. Steadman et al. (2014), for instance, explored the relationship between buildings' geometrical form and energy usage for the non-residential sector of London. They used energy consumption data aggregated at lower and medium level, containing around 300 and 1500 buildings, respectively. Their results showed a strong correlation between exposed surface area (outer walls and roofs) and energy use (gas and electricity). Such aggregated analyses on the neighbourhood and coarser scales provide valuable insights into the general relationships between energy consumption and urban form. Analysis at the individual housing unit level may provide more specific estimations of the impact of local characteristics of urban morphology on energy consumption.

The aim of this paper is to study the combined impact of building shape and surroundings on the energy consumed in space heating. The study is novel in the sense that highly detailed spatial data sources were applied to capture the characteristics of individual buildings units and their direct spatial context in addition to coarser data that captures more aggregate neighbourhood conditions.

5.1.3. Applying GIS in household heat demand analysis

Formatted: Heading 2, Left, Space After: 0 pt, Line spacing: single, Outline numbered + Level: 3 + Numbering Style: 1, 2, 3, … + Start at: 1 + Alignment: Left + Aligned at: 0 cm + Indent at: 1,27 cm

Geographical Information Systems (GIS) manage the acquisition, storage, analysis and presentation of geospatial data (Longley et al., 2005). GIS allows extracting the information required for energy demand analysis, from geospatial data sources. Most studies applying GIS in energy demand analysis are limited to relatively small areas or coarser scales or restricted to aggregate building types rather than studying individual housing units. Therefore, the full capacity of GIS has not been used in building stock analysis (Rode et al., 2014; Buffat et al., 2017). While 2D GIS has been explored in heat demand assessments, the use and extent of 3D GIS is much more limited. This may partly be due to limited availability of 3D geospatial data as well as computational limitations.

In this study, a quantitative assessment of the spatial context influence on the household heat consumption was performed for a complete city at two complementary scales: housing unit and postal code level. 2D and 3D geospatial data and advanced GIS technologies were applied to automatically extract spatial characteristics of all individual housing units and their surroundings in the city of Amsterdam, the Netherlands. State-of-the-art 3D GIS techniques supported the efficient processing of massive geospatial data and broadened our analysis extent to the whole city and individual housing unit level. Dedicated spatial data processing routines, through which spatial context of buildings have been characterised, are described in detail in the next section. The applied routines employed massive geospatial datasets and mathematical

algorithms for the automated extraction of buildings' shape characteristics including building height, area, roof shape and exposed perimeter, as well as variables characterizing the surrounding of buildings. These urban configuration variables were applied in a regression analysis together with other building characteristics (such as construction year), as well as the measured gas consumption data per housing unit, to explore the relationship between household heat consumption and its spatial context. In addition to individual housing unit level, a separate regression analysis has been performed on the postal code level to study the influence of the aforementioned urban configuration elements on heat consumption at different scales. At this coarser level we were also able to include demographic data, which allowed analysing the relative contribution of demographic variables compared to spatial context variables on heat consumption.

5.2. Methodology

5.2.1. Regression analysis

Statistical approaches have been widely used in household energy consumption studies. Especially multi-linear regression has been applied because of its ability to disentangle the contribution of diverging factors and performance simplicity (Fumo and Biswas, 2015; Aydin, 2014).

In general, a multi-linear regression has the following basic form (Equation 1):

$$Y = \beta_0 + \beta_1 X_1 + \beta_2 X_2 + \cdots + \beta_n X_n \quad \text{(Equation 1)}$$

where Y is the dependent variable, $\beta_0 - \beta_n$ are the regression coefficients and $X_1 - X_n$ are the independent variables. In this study, the dependent variable was the measured yearly heat consumption at household level, whereas the independent variables related to micro-scale characterisations of *building shape*, its *surroundings*, and *basic building characteristics*.

Building shape is foremost characterised by two straightforward indices that determine the volume of the residential space that needs to be heated: the surface area and height of the building units. Building design is further captured by the number of housing units in a building (assuming that multiple story buildings consume less heat through shared walls and floors) the shape of its roof (as skewed or slanted roofs are expected to be more prone to heat loss due to open attic spaces and the type of insulation (Davidson et al., 2010)) and the exposed perimeter (that directly links to the part of the building where heat is lost to the surroundings). The impact of the *surroundings* on a buildings heat consumption are expected to follow from its exposure to sun (that may limit the need for heating) and wind (that will result in heat loss). The sky view factor (SVF) expresses how much sky is visible from a particular location and can be used as proxy to investigate microthermal impacts of urban geometry (Oke, 1981; Chen et al., 2012). To specifically study the impact of trees on neighbouring housing units, the volume of trees in various wind directions is included. The more general urban context is, furthermore, described with an urbanization degree indicator that is based on the share of built-up elements within a

Formatted: English (United States)

Formatted: Heading 1, Space After: 0 pt, Line spacing: single, Outline numbered + Level: 2 + Numbering Style: 1, 2, 3, … + Start at: 1 + Alignment: Left + Aligned at: 0 cm + Indent at: 0,63 cm

Formatted: Dutch (Netherlands)

Formatted: Heading 2, Left, Space After: 0 pt, Line spacing: single, Outline numbered + Level: 3 + Numbering Style: 1, 2, 3, … + Start at: 1 + Alignment: Left + Aligned at: 0 cm + Indent at: 1,27 cm

3km radius. This variable is included to test whether compacter, denser neighbourhood indeed results in lower heat consumption of individual households as suggested in Rode et al. (2014). Finally, *Basic building characteristics*, are proxied by the construction year that is expected to reflect the state of thermal insulation for instance. More detailed descriptions of the way the buildings are insulated, the number and types of windows, the efficiency of the heating system are unfortunately not available.

These variables and the automated extraction approaches for characterising each individual building in the whole city, are explained in the following sub-sections.

5.2.2. Defining building shape and surroundings

Formatted: Heading 2, Space After: 0 pt, Line spacing: single, Outline numbered + Level: 3 + Numbering Style: 1, 2, 3, … + Start at: 1 + Alignment: Left + Aligned at: 0 cm + Indent at: 1,27 cm

The variables to describe the spatial context of all buildings in the city of Amsterdam were derived automatically through the application of algorithms on detailed spatial data sources related to the built environment. The input data for these algorithms were obtained from open geospatial 2D/3D data and prepared through advanced GIS operations. The integration of these algorithms in a GIS allowed to use GIS standard spatial data manipulation and spatial analysis routines in combination with the developed dedicated algorithms. The variable processing operations and mathematical calculations were scripted in C# or Python (using ESRI's ArcPy package) and SAGA GIS (for SVF calculations) to efficiently handle the large amounts of data and large number of operations. All data was available in the Dutch national projected coordinate system RD New (see: https://epsg.io/28992). Figure 1 provides an overview of the different components of the geospatial routines developed for this study to describe the spatial context in our analysis. The different components of the routines, comprising the employed data and mathematical models, are explained in detail in the following sub-sections.

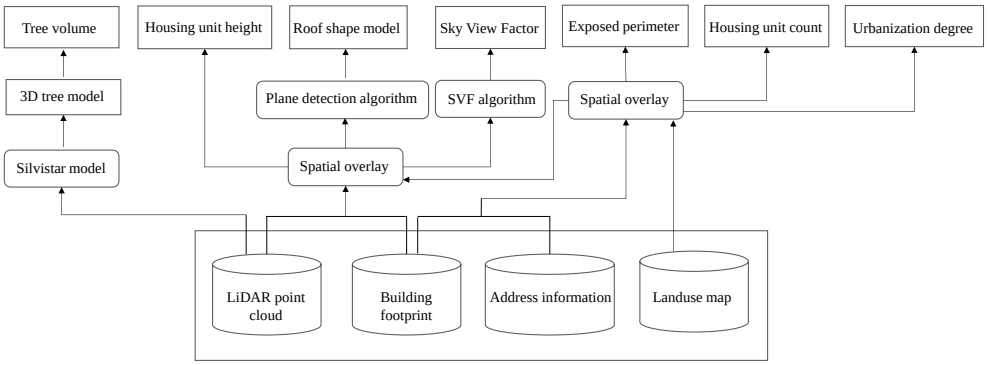

Figure 1. Overview of the components in the automated extraction of spatial context variables for all individual buildings at the city scale.

5.2.2.1.Data

LiDAR 3D point cloud

3D point cloud data of the surface of the Netherlands was acquired through airborne LiDAR technology and is openly available from a group of Dutch Governmental organisations (www.ahn.nl). The data set was initially developed to provide an accurate assessment of the ground level, but it can also be used to map the heights of buildings and other objects such as trees (see, for instance, (Koomen et al., 2009; Rafiee et al., 2016)). For this study the raw data that is composed of 3D points was used (in the LAS file format created for the interchange of 3-dimensional point cloud data between users, see www.asprs.org). This dataset has an average density of 6 to 10 points per m^2 and 5cm horizontal and vertical accuracy (van der Zon, 2013).

Building footprint and address information

Building footprints and address information of the Netherlands were derived from the highly detailed cadastral database that describes the location, shape and age of all individual buildings in the country. The dataset distinguishes individual units (called objects) within buildings that usually have a separate address and that are described in terms of their size and function. For this analysis we mainly use the objects classified as housing units. This data is collected by municipalities and managed by the national cadastre. It is the official registration of addresses and buildings and openly available through a web portal (https://bag.basisregistraties.overheid.nl/). The data is available in vector format (as shapefile) and has a positional accuracy of 28cm (Kooij et al., 2018).

Land-use

Information about local land use is obtained from the land use database of Statistics Netherlands (CBS, 2008). This dataset is based on the detailed geometry of digital topographical maps meant for 1:10,000 scale applications (Van Leeuwen, 2004). In this study we apply the vectorised land-use data referring to 2010 available in shapefile format to calculate an urbanization degree around buildings.

5.2.2.2.Models

3D tree model

For the automatic extraction of individual 3D tree models of the entire city, LiDAR 3D point cloud data was used in combination with the Silvistar tree model (Koop, 1989). This process has been performed by the Wageningen University & Research to produce individual tree models for the whole country (available from http://www.boomregister.nl). Silvistar is an asymmetric 3D single tree model, which is composed of horizontal quarter ellipses and vertical crown curves. The horizontal crown sections are described by sets of quarter ellipses at each height level and the vertical crowns are computed through quadratic equation of an ellipse with a varying exponent (Equation 2):

$$x^E/a^E + y^E/b^E = 1 \quad \text{(Equation 2)}$$

Formatted: Heading 3, Space After: 0 pt, Line spacing: single, Outline numbered + Level: 4 + Numbering Style: 1, 2, 3, … + Start at: 1 + Alignment: Left + Aligned at: 0 cm + Indent at: 1,27 cm

Field Code Changed

Field Code Changed

Formatted: Heading 3, Space After: 0 pt, Line spacing: single, Outline numbered + Level: 4 + Numbering Style: 1, 2, 3, … + Start at: 1 + Alignment: Left + Aligned at: 0 cm + Indent at: 1,27 cm

where x and y are the coordinates of the interpolated points and *a* and *b* are the axis halves of the ellipse and the variant exponent *E* is applied to depict a broad range of tree crown shapes (Koop, 1989).

Silvistar requires eight tree points, as a minimum, for fitting a 3D model. These points are tree crown top and base locations, tree base and fork locations as well as the locations/heights of the tree four periphery points. The coordinates of tree base as well as the locations/heights of periphery points have been extracted through LiDAR observations and the coordinates of the tree fork and crown top/base are estimated from the tree base eccentricity in the crown projection (Koop, 1989). Figure 2 depicts the process of 3D tree model and volume estimation of individual trees for the whole Netherlands. This 3D dataset was processed to calculate the volume of the individual trees and subsequently the volume of trees surrounding each building on each direction separately (northwest, northeast, southwest or southeast). This algorithm was implemented in C# coding language. The resulting variables are the total tree volumes at each quadrant for each buildings.

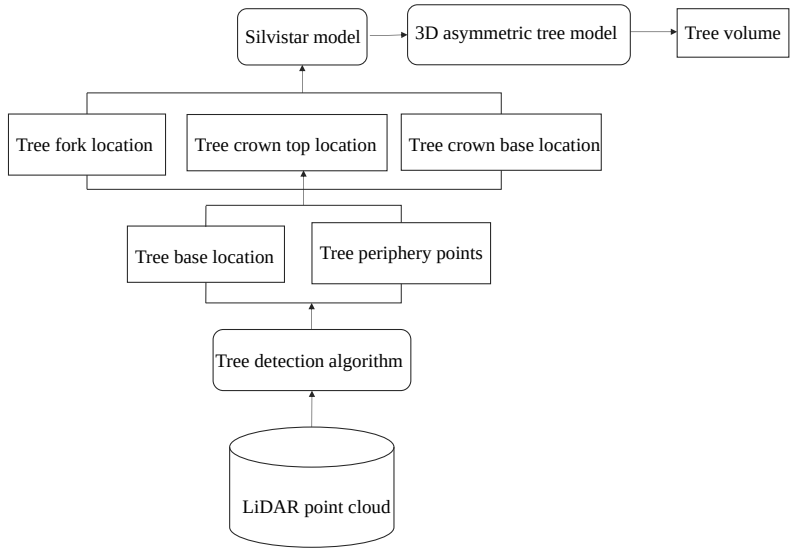

Figure 2. The applied algorithm for automated 3D tree volume estimation of all the individual trees of Amsterdam.

Roof shape model

Roof shape have been extracted automatically from LiDAR 3D point cloud using the Random Sample Consensus (RANSAC) algorithm (Fischler and Bolles, 1981). This algorithm is an iterative model fitting technique which can estimate mathematical model parameters on

observed data containing gross error (Fischler and Bolles, 1981). In our study, the RANSAC algorithm was implemented in C# language and it allows to detect mathematical 3D planes from the 3D point cloud observations. For each building, its point clouds were extracted from the LiDAR point cloud dataset through spatial overlay techniques. Subsequently, based on the RANSAC algorithm, three random points (from the building point clouds) were chosen through which a unique 3D plane was fitted. The distance between all other points to this plane was then estimated. The points with a distance less than a defined threshold (10cm) were assigned to the plane. The number of points lying on the plane was calculated. This process was iterated (based on a predefined number of iterations) and the plane with the highest number of supporting points was selected as the first detected roof plane. A convex hull was defined around the supporting points of the plane which formed the plane polygon for which the area was calculated. If this area was above a defined threshold (i.e. if the plane is large enough), the plane was selected. The threshold was defined as 0.1 for the ratio between each convex hull and the largest found roof segment. If the slope of the plane was below 5°, the plane segment was labelled as flat and otherwise as slated (sloped) plane. The supporting points of the selected plane were deleted from the point cloud data and the whole process was repeated until the maximum number of detected plane or minimum number of points per plane criteria was reached. The flat/slanted roof label of the whole building was assigned based on the status of all the detected roof plane segments. Figure 3 describes the applied roof shape modelling procedure in this study.

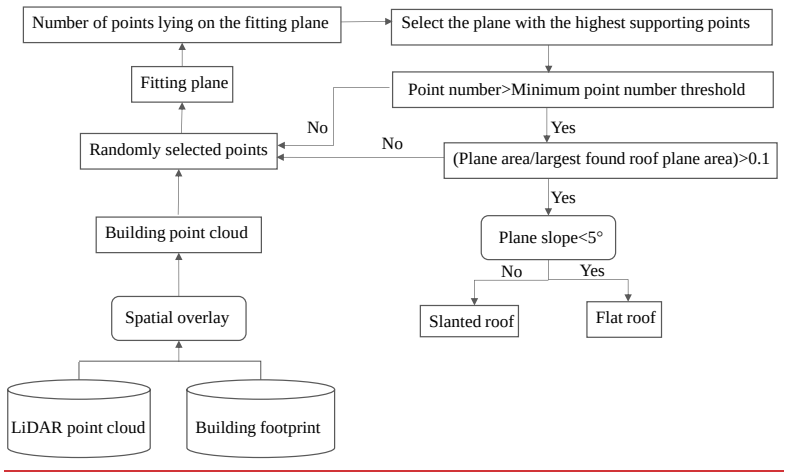

Figure 3. The applied roof shape modelling algorithm

Sky view factor (SVF)

Based on Johnson and Watson (1984) the SVF for a non-symmetrical canyon with finite length can be defined as (Equation 3):

$$\psi_s = 1 - (1/2\pi\{(\gamma_2 - \gamma_1) + \cos\beta[tan^{-1}(\cos\beta\ \tan\gamma_1) - tan^{-1}(\cos\beta\ \tan\gamma_2)]\}) \quad \text{(Equation 3)}$$

where γ_1 and γ_2 are the azimuth angles of the wall ends, β is the elevation angle of the wall top from the line parallel to the wall which passes through the surface element and ψ_s is SVF expressed a dimensionless value between 0 (sky completely blocked) to 1 (sky fully visible). In this study, the rasterized 3D LiDAR point cloud was used for the calculation of SVF on each grid cell using the SAGA-GIS software. The resulting SVF raster was subsequently used to calculate the aggregated SVF surrounding each building. Due to the high values of SVF on buildings' rooftops, which were not expressive for the dwellings, the SVF grid cells belonging to buildings were excluded through a spatial overlay on the building footprint dataset.

Exposed perimeter

The cadastral building dataset provides spatial descriptions of the two-dimensional shape of the buildings and point locations for individual housing units (addresses) it comprises. The exposed perimeter of each individual housing unit was estimated based on the cadastral footprint of the building and the following calculation that accounts for the fact that multiple housing units can be located inside a larger building (Equation 4):

Formatted: English (United States)

$$e_i = L_f \times \frac{\sum_{i=1}^{n} S_i}{n \times S_p} \quad \text{(Equation 4)}$$

where S_i is the surface of the i^{th} unit (address) within the building footprint, S_p is the surface area of the building footprint, n is the number of housing units within a building footprint, L_f is the building exposed perimeter and e_i is the exposed perimeter of the i^{th} unit within the building footprint. The building footprint exposed perimeter, L_f, was derived through a spatial overlay in GIS, through scripting in Python (ESRI ArcPy package). By intersecting the footprint borders with all the surrounding building borders (iteratively) the shared boundaries of each building to all other buildings were determined. Then the shared border lengths for each building were summed and the information was added to each building. The difference between the total perimeter and the shared border length is the exposed perimeter (Figure 4).

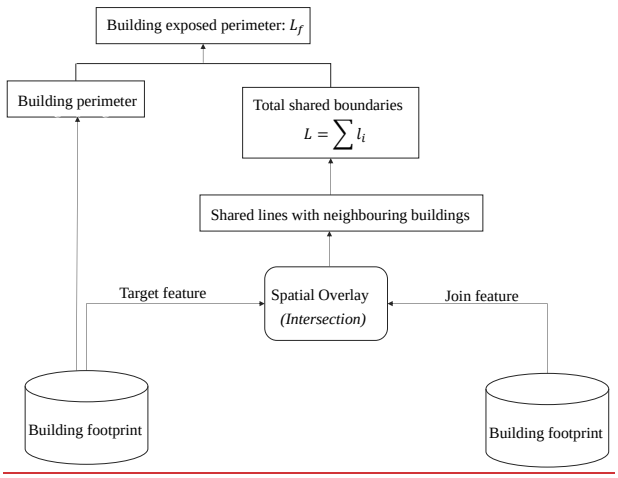

Figure 4. Estimation of building exposed perimeter variable, L_f.

Urbanization degree

The urbanization degree was estimated for each building and expressed the share of built-up elements within a 3km radius. Its calculation was based on the land-use map of the Netherlands that was classified into urban and non-urban elements such as green space and water bodies. See Rafiee et al. (2016) for a detailed description of this indicator.

Housing unit height

Housing unit height was derived through a spatial overlay between LiDAR 3D point cloud and building footprints. For apartment units, an average floor-to-ceiling height was assigned for their housing unit height.

Housing unit count

Housing unit counts was derived through a spatial overlay between the point locations of address information and building footprint datasets.

5.3. Results and discussion

The geospatial routines described in the preceding section, allowed a detailed characterisation of all individual housing units for the complete city of Amsterdam. Figure 5 depicts a small subset of the extracted 3D buildings and tree models for illustration purposes. These models were subsequently used to capture various aspects of building morphology, such as building exposed perimeter, illustrated in Figure 6.

Formatted: English (United States)

Formatted: Heading 1, Space After: 0 pt, Line spacing: single, Outline numbered + Level: 2 + Numbering Style: 1, 2, 3, … + Start at: 1 + Alignment: Left + Aligned at: 0 cm + Indent at: 0,63 cm

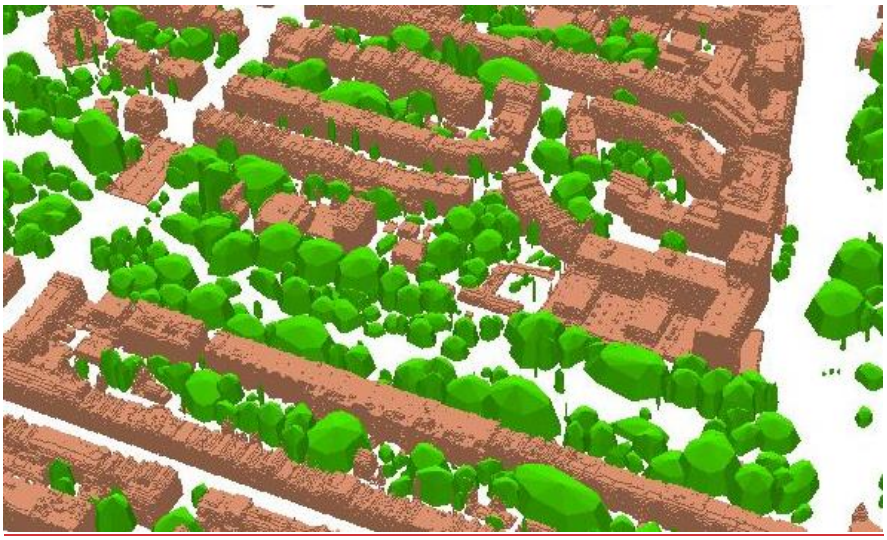

Figure 5. 3D building and 3D tree models extracted from airborne LiDAR point cloud data, visualized in ESRI ArcScene viewer.

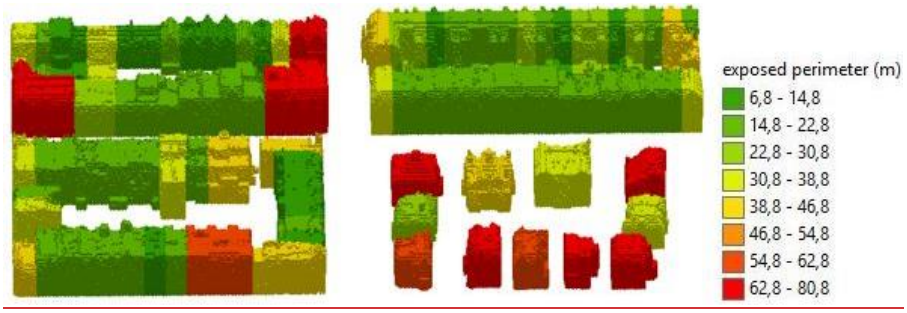

Figure 6. The estimated exposed perimeter of the individual units, visualized in ESRI ArcScene viewer.

The variables related to building shape, characteristics and surroundings were applied in a regression analysis to explain household heat demand relation. The measured yearly gas consumption of all individual households in Amsterdam was used as the dependent variable. The observations lower than 50 m^3 and above 10000 m^3, as well as the observations with more than 100% variation between the preceding and succeeding years, in a 5-year window (for household level), have been excluded due to the lack of knowledge on their deviant extreme values. These observations (accounting for 14% of the total number of observations) were unlikely to represent normal household behaviour and could relate to houses being empty for most of the year, houses with other heating sources, etc. Table 1 presents the descriptive statistics of the measured gas consumptions at household and postal code level and the independent variables included in our analysis.

Formatted: English (United States)

Table 1. descriptive statistics for the data used in the analysis on housing unit (N= 109727) and postal code level (N = 11326). Note that the values for individual postal code areas represent average conditions that are either based on own calculations (aggregated from individual housing units in the area) or external sources (for demographics).

Variable name	Description	Household level		Postal code level	
		Mean	Standard deviation	Mean	Standard deviation
Gas consumption	measured gas consumption	1206.41 m^3	756.20 m^3	1467.74 m^3	809.80 m^3
Building shape					
Area	surface area per housing unit	65.71 m^2	38.54 m^2	84.53 m^2	94.46 m^2
Unit height	height per housing unit	3.00 m	1.30 m	3.48 m	1.70 m
Slanted roof	dummy variable indicating whether roof is slanted (0 or 1)	0.69	0.46	0.68	0.35
Housing unit count	number of housing units per building	11.73	23.41	5.90	8.23
Exposed perimeter	exposed perimeter per address	14.74 m	7.0 m	16.10 m	7.83 m
Surroundings					
SVF	Sky View Factor (mean) in building vicinity	0.78	0.11		
NE tree volume	total tree volume northeast of building (*0.0001)	0.42 m^3	0.68 m^3	-	-
NW tree volume	total tree volume northwest of building (*0.0001)	0.40 m^3	0.66	-	-
SE tree volume	total tree volume southeast of building (*0.0001)	0.43 m^3	0.78 m^3	-	-
SW tree volume	total tree volume southwest of building (*0.0001)	0.40 m^3	0.73 m^3	-	-
Urban degree	urbanization degree (0-1)	0.09	0.09	0.1	0.14
Building characteristics					
Build year<1900	dummy variable indicating whether building is built before 1900 (0 or 1)	0.15	0.35	0.21	0.41
1900<Build year<1930	dummy variable indicating whether building is built between 1900 and 1930 (0 or 1)	0.32	0.47	0.31	0.46
1930<Build year<1950	dummy variable indicating whether building is built between 1930 and 1950 (0 or 1)	0.13	0.34	0.14	0.34
1950<Build year<1970	dummy variable indicating whether building is built between 1950 and 1970 (0 or 1)	0.23	0.42	0.17	0.38
1970<Build year<1990	dummy variable indicating whether building is built between 1970 and 1990 (0 or 1)	0.11	0.315	0.086	0.28
1990<Build year<2000	dummy variable indicating whether building is built between 1990 and 2000 (0 or 1)	0.04	0.20	0.060	0.24
2000<Build year<2010	dummy variable indicating whether building is built between 2000 and 2010 (0 or 1)	0.01	0.087	0.017	0.13

Build year>2010	dummy variable indicating whether building is built after 2010 (0 or 1)	0.001	0.039	0.006	0.078
Demography					
0<Age<15	ratio of occupants with age between 0 and 15 (0-1)	-	-	0.14	0.090
15<Age<25	ratio of occupants with age between 15 and 25 (0-1)	-	-	0.12	0.082
25<Age<45	ratio of occupants with age between 25 and 45 (0-1)	-	-	0.37	0.16
65<Age<75	ratio of occupants with age between 45 and 65 (0-1)	-	-	0.065	0.063

The result of the regression analysis on housing unit level is included in Table 2.

Table 2. Regression analysis results on housing unit level. Heat consumption at individual household level is used as the dependent variable. The independent variables comprise housing unit characteristics as well as spatial context related elements at household level (r^2=0.212).

The results show that floor area has the highest impact on the dwellings' heat consumption. Unit height, as the other dwelling size variable has the second highest influence. This is due to the prominent relationship between space heating and dwelling dimension. Our results present 4.9m^3 and 111.3 m^3 heat consumption increase for 1m^2 and increase in area and 1m increase in unit height, respectively. Exposed perimeter also presents prominent positive relationship with heat consumption. This is due to the high association between a building heat consumption and its heat loss through walls. Based on our results, 1 meter increase in the household exposed perimeter leads to 21.4 m^3 increase of the gas consumption. Housing unit count shows a high negative relationship to household consumption. This clarifies the well-known fact that households in apartments with more number of units consume relatively less heat than other building types (e.g. detached and semi-detached buildings), due to the heat transfer from the shared walls and floor/ceilings. Based on our results, every added housing unit within an apartment leads to 3.4m^3 household heat consumption reduction.

Directional impact of tree volume around the buildings, is explored by allocating the surrounding 3D tree models into their corresponding quadrants, namely at northwest, northeast, southwest and southeast of each building. The results indicate that only the trees at the northwest have an impact on the dwellings' heat consumption and tree volume variables on other directions were not statistically significant. We expect that the impact of trees at the northwest on household heat consumption is caused by their wind blocking effect. Due to the dominant western wind and colder northern wind stream in the Netherlands, trees northwest of buildings have the highest influence on blocking wind around buildings. Our results show that a 10000 m^3 increase in tree volume leads to 18.4 m^3 heat consumption reduction. Based on the Amsterdam typical tree size definitions by Rafiee et al. (2016), one small, one medium and one large tree can reduce a dwellings' heat consumption by 1.3 m^3, 6.2 m^3 and 27 m^3, respectively. Trees south of buildings have a dual impact on heat consumption as they block both wind as

Formatted: English (United States)

well as sunlight. This dual effect of is reflected in the high p-values (therefore insignificant variables) for southwest and southeast tree volume in Table 2. While the former can reduce the heat consumption, the latter increases that. To the authors' knowledge the directional impact of trees on dwellings' heat consumption at a city scale has not yet been studied.

SVF shows a positive relation with dwellings' heat consumption. High SVF values indicate the presence of open space around a dwelling and may link to higher heat consumption through lower heat gains from neighbouring buildings and higher heat loss through the surrounding open space. Although high SVF around buildings has also positive impact on their solar gain, at high latitude locations with scant solar gain, heat conservation plays a more dominant role than sunlight gain as also discussed by Ratti et al. (2005). Urbanization degree shows a negative impact on the household heat consumption. This can be due to the higher compactness, smaller building size and occupants' behavior in higher urbanized city fragments. The positive relationship between slanted roofs and heat consumption might be due to the heat loss in open attic spaces or insulation types (these are known causes from energy efficiency homes practice Davidson and Heinberg, 2010).

Formatted: English (United States)

Building construction year was categorized into seven dummy classes with building years before 1900 as the reference class. The results indicate that for the classes starting at the class *1900<building year<1930*, until the class *2000<building year<2010* newer the building, the less energy it consumes (except for class *1950<Build year<1970* explained below). The last class, the newest buildings built or fully renovated after 2010, have a positive coefficient indicating they consume more energy than the reference class. This can be explained by the rebound effect (Berkhout et al., 2000), a well-known effect where consumers adapt their behaviour to the perceived increased efficiency and consume more (for instance using automatic thermostats that actually led to more hours of peak temperature (Guerra-Santin and Itard, 2010)). Another exception to the increase in energy conservation for younger buildings, occurs for the *1950<building year<1970* class where the positive beta indicates a higher energy consumption than the reference class. This can be due to the building characteristics of this period: the years after the World War II, with high dwelling demands and lack of building material, from one hand, and massive and fast reconstruction using cheap building material and not considering insulation, from the other hand. From 1975, building insulation became mandatory in the Netherlands. Furthermore, older buildings might have been renovated by now, while the relatively newer buildings (50s-70s) are more probable to have remained in their original state. *1930<building year<1950* class was not statistically significant.

The statistical model explains a substantial share (21%) of the variance in household heat demand from spatial context and building year variables only. This implies that urban planning and building regulations can have a considerable impact on the total energy consumption for residential heating of the city. This is in line with the study performed by Ratti et al. (2005) for Toulouse and Berlin. Using an engineering-based energy consumption model they explained 10% of the variation in energy consumption from urban texture. Obviously, a large part of the variation in energy consumption of individual households remains unexplained. This is not surprising as this variation is fairly large and dependent on erratic individual preferences and housing conditions. There will be differences in the time spent at home, preferred temperatures,

efficiency of the heating system etc. Data on these conditions either does not exist or is unavailable due to privacy restrictions. Not having this type of data is not a major constraint as the focus is on the factors that can be influenced by policy (e.g. housing density, design of the public space surrounding houses) and building regulations (e.g. building layout).

In addition, the heat demand analysis was performed on postal code level to investigate the relationship between dwellings' heat consumption and urban configuration elements at a more aggregated scale. Furthermore, due to the availability of demographic information on postal code level, we could include household composition in the regression analysis to explore their relative impact on heat consumption compared to spatial context elements.

Table 3 presents the results on postal code level with aggregated household heat consumption as the dependent variable and aggregated dwelling characteristics, spatial context elements and demographic data as independent variables.

Table 3. Regression analysis results on postal code level (dependent variable is household heat consumption aggregated at postal code). The independent variables comprise aggregated dwellings' characteristics, spatial context related elements and demographic data at postal code level (r^2=0.315).

Variable	**Beta Coefficient**	**Standardized Beta Coefficient**	**p-value**
(Constant)	747.627		0.000
Building shape			
Area	2.408	0.281	0.000
Unit height	116.674	0.245	0.000
Slanted roof	173.201	0.075	0.000
Housing unit count	-4.968	-0.051	0.000
Exposed perimeter	17.886	0.173	0.000
Surroundings			
Urban degree	-246.138	-0.044	0.000
Building characteristics			
1900<Build year<1930	-293.980	-0.168	0.000
1930<Build year<1950	-404.196	-0.171	0.000
1950<Build year<1970	-441.869	-0.206	0.000
1970<Build year<1990	-574.018	-0.198	0.000

1990<Build year<2000	-815.306	-0.240	0.000
2000<Build year<2010	-851.896	-0.135	0.000
Build year>2010	-520.677	-0.050	0.000
Demography			
0<age<15 (%)	729.010	0.081	0.000
15<age<25 (%)	584.030	0.059	0.000
25<age<45 (%)	-273.170	-0.053	0.000
65<age<75 (%)	447.513	0.035	0.001

Results on postal code level confirm the strong impact of housing unit area and height on heat consumption. The impacts of the other variables related to the physical characteristics of the house (number of housing units in a building, roof type and exposed perimeter) are very much in line with household level results.

The relative impacts on different building year categories is generally in line with those of housing unit level, that is, buildings of more recent periods consume less energy than the reference class (buildings<1900). Yet, there are differences in *1950<building year<1970* and *building year>2010*. While the former, showed a positive beta coefficient at housing unit level, it has a negative beta coefficient at postal code level. This might be due to the interrelation with occupants age range of 65-75, as a fair share of the occupants of buildings from 1950-1970 belong to that age group. Controlling for the positive impact of this occupant age range on heat consumption, seems to lead to better explanation of the relation between this building age category and their consumed heat. The lower beta coefficient of *building year>2010* compared to the previous class *2000<building year<2010*, considering the consistent pattern from 1900 to 2000 of higher energy conservation, is again an indication of the rebound effect (although milder at this scale), wherein occupants tend to increase their heat consumption upon better insulation or a more efficient system (Khazzoom, 1987).

The demographic composition of the postal code area is also an important determinant of residential heat demand. The 0-15, 15-25 and 65-75 age classes show a positive influence and 25-45 age class presents a negative impact on heat consumption. The relatively large and positive impact of 0-15 and 15-25 age classes is expected to be related to the presence of children at home. This indicates that the higher number of occupants, i.e. household size, has a positive impact on heat demand, which is also shown in previous studies (Santin et al., 2009), as a larger number of rooms needs to be heated. In addition, households with younger children are likely to spend more time at home increasing the total heat consumption.

The 25-45 age class indicates a contribution to heat conservation, in opposition to the 65-75 age class that shows a positive influence (more energy is consumed in areas with mainly

inhabitants of this age class). This might be related to differences in the occupants' presence at home as well as the preference of older occupants for higher temperature, which is in line with other studies (Day and Hitchings, 2009; Yamasaki and Tominaga, 1997) and specifically Guerra-Santin and Itard (2010) for Dutch occupants. As the directional impact of tree volumes and SVF differ strongly for individual buildings, these factors are not used to characterise the more aggregate postal code areas and they are thus excluded from the regression analysis.

The analysis at the more aggregate postcode level yields a higher r^2 (0.31) than the household level analysis. We expect this to be related to the inclusion of demographic data at the postal code level and the fact that the most extreme variation related to erratic individual behaviour and specific building characteristics is suppressed at this more aggregate level of analysis. Yet, also in this case a large part of the variation remains unexplained.

It is worth noting that the influence of spatial context elements on household heat consumption at the two different scales seems relatively stable (with comparable standardized beta coefficients) across the two different scales studies (household and postal code aggregation), which indicates robustness in the variables and methods chosen. The possibility of including certain variables at specific scales, for instance in this study directional tree and SVF at housing unit level and demographic variables at postal code level, suggests a complementary role of the analysis at these two scales.

The advantage of multi-variate linear regression analysis is that it produces robust results that are easily interpretable: one unit change in any of the explanatory variables (e.g. 1m more exposed perimeter) has a direct link to a change in heat consumption that can be read from the coefficients. Such direct interpretation is not possible from black-box type of artificial intelligence techniques such as support vector machines or artificial neural networks. However, these machine learning techniques provide more flexibility and perform better in explaining variance (Dreiseitl and Ohno-Machado, 2002). The flexibility of these techniques, compared to multi-variate linear regression, lies in their ability to address nonlinear relationships (Zhao and Magoulès, 2012). This is especially relevant for short-term forecasting, however, multi-linear regression is shown to yield efficient results in the long-term predictions (Wang and Srinivasan, 2017).

5.4. Conclusions

A quantitative assessment on the relationship between household heat consumption and its spatial context at a city scale was performed. This analysis has been performed at two scales, namely housing unit and postal code level. At housing unit scale, the measured heat consumption of each individual household for the whole city of Amsterdam was applied in a regression analysis together with a set of explanatory factors that characterise building shape, surroundings and basic building characteristics. At postal code level, these heat consumption measurements and explanatory factors were aggregated and applied in a separate regression analysis that also contains reference to the demographic composition of the postcode areas. The results at both scales confirm the dominance of housing unit surface area and height on heat

Formatted: English (United States)

Formatted: Heading 1, Space After: 0 pt, Line spacing: single, Outline numbered + Level: 2 + Numbering Style: 1, 2, 3, … + Start at: 1 + Alignment: Left + Aligned at: 0 cm + Indent at: 0,63 cm

demand. Exposed perimeter also shows high positive impact at both scales. Number of housing units per building, presents a higher impact on the housing unit level compared to postal code level. The presence of a slanted roof and urbanization degree present a consistent impact at both scales. The local housing unit level analysis allowed assessing the directional impact of tree volume and indicates that only the trees northwest of building had a significant and negative impact on household heat consumption. The inclusion of demographic data on the postal code level revealed the impact of occupants' age classes on the heat demand. The consistency on the impact of urban settings elements at both scales indicates the robustness of the results. The capability of including certain variables at specific scales (for instance directional impact of tree volume and SVF at individual housing unit scale and the demographic variables at postal code scale), makes the two scales complementary.

Formatted: English (United States)

The positive impact of exposed perimeter and SVF and the negative influence of number of housing units within a building and urbanization degree confirms the benefits of compact urban morphology for a lower heat demand. Although compact urban form reduces solar gain, for the countries with lower sunlight during winter, the influence of heat conservation of dense urban form plays a more prominent role on dwellings' heat demand. The results of this study can be applied in urban policies for quantitative assessment of sustainability of neighbourhood (re)design, considering urban settings, aiming at heat consumption reduction.

Spatial data processing has been described for the automated extraction of 2D and 3D urban morphology elements for each individual building for the whole Amsterdam. These routines integrate different mathematical algorithms into a Geographical Information System where massive geospatial data can be accessed and managed efficiently. The availability/accessibility of detailed geospatial data, in combination with state-of-the-art GIS technologies for the efficient management of the data, serve these mathematical models an optimized procedure for expanding their extent and level of detail. This integration enabled us to broaden our analysis to a city extent and even beyond that. Furthermore, the application of open geospatial data, rather than proprietary, commercial data, in our dedicated routines broadened the scope of the analysis and enabled us to include more explanatory factors in our analysis. The applied Geographic Information System plays an important role in the efficient and updated accessibility to open geospatial datasets.

Beyond this study, this geospatial data processing procedure can be applied in other energy related studies where spatial context information at a local level is required for a large extent. This is applicable in both energy demand and energy supply studies where location matters.

Chapter 6: From BIM to geo-analysis: view coverage and shadow analysis by BIM/GIS integration[36]

Abstract

Data collection is moving towards more details and larger scales and efficient ways of interpreting the data and analysing it is of great importance. Building Information Model (BIM) includes very detailed and accurate information of a construction. However, this information model is not necessarily geo located but uses a local coordinate system hampering environmental analysis. Transforming the BIM to its corresponding geo-located model helps answering many environmental questions efficiently. In this research, we have applied methods to automatically transform the geometric and semantic information of a BIM model to a georeferenced model. Two analysis, namely view and shadow analysis, have been performed using the geometric and semantic information within the georeferenced BIM model and other existing geospatial elements. These analysis demonstrates the value of integrating BIM and spatial data for e.g. spatial planning.

6.1. Introduction

A Building Information Model (BIM) contains very detailed and semantically rich information of a construction. The model is usually not integrated with its surrounding information. For example, when planning a new building in an existing environment, information from BIM models is generally not integrated with environmental information to calculate shadowing of neighboring buildings or to carry out view coverage analysis. Geographic Information Systems (GIS), on the other hand, are capable of performing spatial analysis using the physical and functional spatial representations of an environment.

It is expected that integration of BIM in a GIS environment results in a much more comprehensive system that can be used to improve decision making during spatial planning. Adding environmental information to BIM in GIS automates many analysis due to the complementary nature of the detailed construction information from the BIM and the information about the surrounding area.

There have been several researches and investigations on the integration of BIM and GIS. These researches have focused on different domains and applicability of BIM and GIS integrations. Examples of research are: modeling interior utilities (Hijazi et al., 2011), water utility network (Hijazi et al., 2009), low-disturbance construction (Sebastian et al., 2013), transformation from IFC to GML data model (Wu and Hsieh, 2007), optimization of tower cranes' location on

[36] This chapter is published in Procedia Environmental Sciences as: Rafiee, A., Dias, E., Fruijtier, S., & Scholten, H. (2014). From BIM to geo-analysis: view coverage and shadow analysis by BIM/GIS integration. Procedia Environmental Sciences, 22, 397-402.

Formatted: Font: 16 pt, Font color: Text 1
Formatted: Font: 16 pt, Bold, Font color: Auto
Formatted: Centered
Formatted: Font: 14 pt, Font color: Auto
Formatted: Font color: Auto
Formatted: Heading 1
Formatted: Font: 14 pt
Formatted: Font: 14 pt, Not Bold
Formatted: Justified, Line spacing: Multiple 1,15 li

construction sites (Irizarry and Karan, 2012), CityGML GeoBIM extension (de Laat and van Berlo, 2011), site selection and fire response management (Isikdag et al., 2008), web services for the visualization and analysis of 3D building information (Hagedorn and Döllner, 2007), visual monitoring of construction supply chain management (Irizarry et al., 2013) and large scale (building) asset management (Zhang et al., 2009).

We propose a method to automatically integrate an IFC BIM model of a building in a GIS environment. This integration will enable multiple analysis opportunities for effective and efficient spatial analysis where construction details relate to its surrounding environmental information.

This paper reports on two studies integrating detailed information from BIM and spatial data in a GIS environment. The first study explores positions of windows from a BIM model to determine the view quality of these windows (the type and amount of existing physical features in the view) using spatial data (3D buildings and 3D trees). The second study uses roof segments derived from a BIM model to determine shadowing effects from surrounding 3D buildings and trees on the roof. The studies can be used for economic research (house price analysis), energy potential analysis (rooftop and window irradiation) and design quality (position of windows for best view).

6.2. Methodology

Formatted: Heading 1
Formatted: Font: 14 pt
Formatted: Font: 14 pt, Not Bold
Formatted: Justified, Line spacing: Multiple 1,15 li

In the first step, a BIM IFC format was converted to a vector geographic format using Extract Transform Load (ETL) process. This conversion is a geometric transformation from IFC geometry to the vector geographic geometry. Global ID of each object in the IFC model is allocated to its corresponding vector object as an attribute through ETL process.

The next step is to assign the semantic information from the IFC BIM model to the spatial information model. Within this process we developed a semantic conversion from BIM to GIS. This semantic conversion automatically relates object semantics within IFC data model to the corresponding object in geographic vector model, using the common Global ID. These semantic information appear in the form of vector attributes.

The resulting geographical dataset is not yet georeferenced, meaning the model is still in a local coordinate system and not in a geographical coordinate system. In order to transform or georeference the local coordinate system to a geographic coordinate system we developed a transformation mechanism including scaling, rotating and translation. The attributes from the IFCSite class “refLongitude”, “refLatitude” as well as “NorthDirection” in “IFCProject” class (IFCRepresentationContext) are used for this process. The centroid of the entire BIM model is taken as the reference point of the IFC model. In this way the BIM model is converted automatically to a georeferenced object that can be used in geospatial analysis and visualization in GIS tools.

6.2.1. *View analysis*

The translated semantic properties of the IFC model are used to select all windows from the geographical dataset. Based on the geographical location of each window, 3D fields of view are defined. These fields of view are 3D solids which are originated from windows and extended outwards for a specific distance. The FOV solid of each window might contain (portions of) one or more objects, e.g., buildings. Once the georeferenced 3D models of such objects are available, the content of each window FOV can be determined.

Accurate 3D building and tree models of the Netherlands have been developed using accurate and detailed national height data of the country, called AHN. The second version of this dataset, called AHN2, with 5 centimeter planar and vertical accuracy and the point density of 8-20 points per square meter is used for developing 3D models of existing buildings and trees.

For each window FOV solid, all 3D building and tree solids which fall within the FOV are determined using an "intersection" function of a GIS tool. The outputs of the intersection function are the 3D solids of building and tree portions. Calculating the volume of the intersected building and tree portions, for each window FOV we have estimated the ratio between the intersected buildings volume and trees volume. This ratio indicates the grayness/greenness of a view field.

6.2.2. *Shadow analysis*

The 3D representations of the buildings and trees are used to calculate shadow volumes for a specific date and time. From the integrated BIM-GIS information the real-world location of the roof top segments are derived. By intersecting 3D shadow solids of buildings and trees with the georeferenced BIM rooftop, the total area of the rooftop portions lying in the shadow at the specific date and time is determined.

6.3. Results

A BIM model of a residential building in IFC format was chosen for BIM-GIS integration experiment (Figure 1). This model has been developed by Zeep Architects in the Netherlands (Zeep-Architecten, 2013).

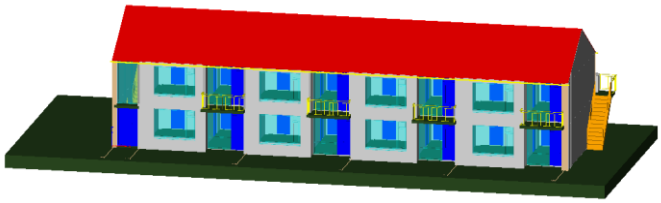

Figure 1. BIM model in IFC format.

Formatted: Heading 2, No bullets or numbering
Formatted: Justified, Line spacing: Multiple 1,15 li
Formatted: Heading 2, No bullets or numbering
Formatted: Justified, Line spacing: Multiple 1,15 li
Formatted: Heading 1
Formatted: Font: 14 pt
Formatted: Font: 14 pt, Not Bold
Formatted: Justified, Line spacing: Multiple 1,15 li
Formatted: Line spacing: Multiple 1,15 li
Formatted: Centered, Line spacing: Multiple 1,15 li
Formatted: Font: 11 pt
Formatted: Font: 11 pt
Formatted: Line spacing: Multiple 1,15 li

Geometric and semantic conversion to geographic vector format was performed on the IFC BIM model through ETL process and self-developed semantic mapping conversion, respectively. The absolute coordinates of the reference point from the IFCSite class are transformed (rotated, scaled and translated) from the local coordinate system to the geographic coordinate system. The result of this georeference process is presented in Figure 2. Next to the georeferenced building model, the surrounding environment is represented in 3D by the building blocks and trees derived from spatial data (see 2.1).

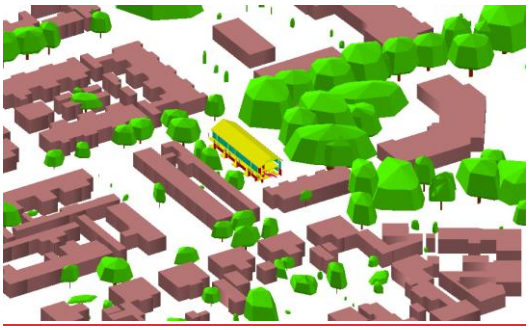

Figure 2. Georeferenced BIM model in geographic vector format among accurate 3D building and tree models

6.3.1. Quality of view analysis

Semantic information from the BIM model has been transformed into the attributes of the geospatial vector model. In the GIS these attributes can easily be queried to select specific spatial elements. For example in the GIS environment roofs, ceilings, doors and windows can be selected by querying on these terms. In the case of the view analysis the windows are selected in the GIS tool as depicted in Figure 3. The selected windows are positioned on their exact location on earth.

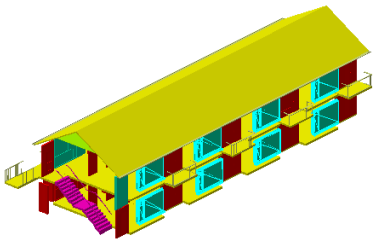

Figure 3. Selecting windows from the BIM model integrated in spatial data through a GIS attribute query. Elements whose "IFCTYPE" attribute field equals to "IFCWINDOW" are selected (blue)

From each georeferenced window a 3D field of view is formed to specify its view composition. Each window field of view is intersected with the neighboring 3D building and tree models (Figure 4).

Formatted: Justified, Line spacing: Multiple 1,15 li

Formatted: Centered, Line spacing: Multiple 1,15 li

Formatted: Heading 2, No bullets or numbering

Formatted: Justified, Line spacing: Multiple 1,15 li

Formatted: Centered, Line spacing: Multiple 1,15 li

Formatted: Font: 11 pt

Formatted: Font: 11 pt

Formatted: Justified, Line spacing: Multiple 1,15 li

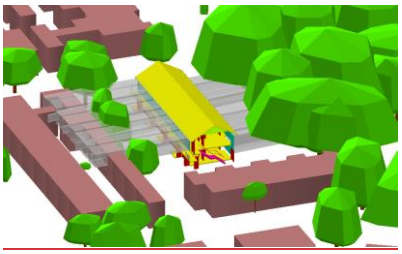

Figure 4. 3D windows' FOV and 3D geographical objects

Figure 5 shows the portions of the 3D building and tree models falling within the 3D field of view of each window. For each field of view, the ratio of total intersected building volumes to tree volumes is calculated.

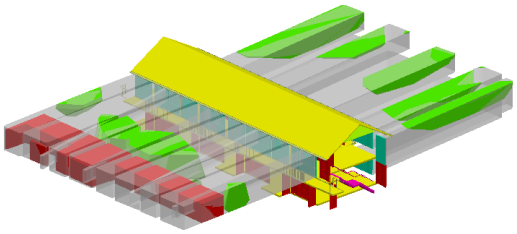

Figure 5. 3D building and tree model portions falling within windows' field of view

6.3.2. Shadow volume analysis

For the second analysis, rooftop elements were selected from the building model integrated in the geographical vector model by querying these elements from the building attributes.

The 3D building and tree models were used to calculate the 3D shadow models for a specific date and time. Shadow solids are developed based on the 3D object geometry, solar azimuth and solar altitude for a specific moment.

Figure 6a presents the georeferenced building model and the calculated 3D shadow of buildings and trees. The selected/queried rooftop elements of the building were intersected with the 3D shadow models. The surface area of the intersected rooftop portions lying in the shadow during a specific date and time were estimated relative to the total roof area (Figure 6b). This determines the rooftop area percentage which is unexposed to solar radiation.

Formatted: Centered, Line spacing: Multiple 1,15 li

Formatted: Font: 11 pt

Formatted: Font: 11 pt

Formatted: Line spacing: Multiple 1,15 li

Formatted: Centered, Line spacing: Multiple 1,15 li

Formatted: Heading 2, No bullets or numbering

Formatted: Justified, Line spacing: Multiple 1,15 li

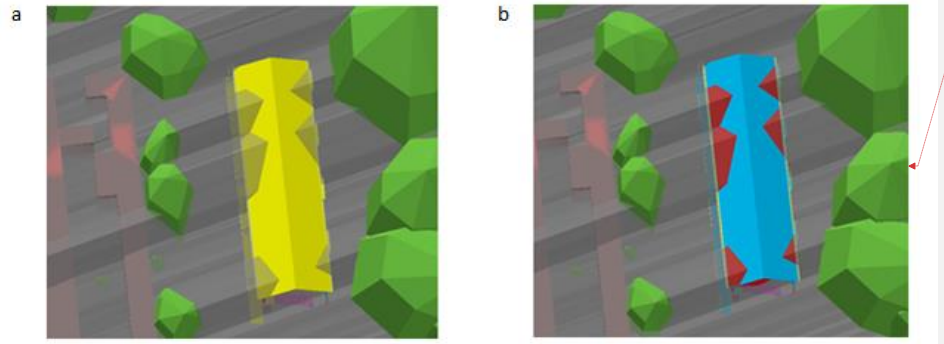

Figure 6. Shadow analysis on the building rooftop (a) georeferenced building model and 3D shadow model; (b) Rooftop portions intersecting with shadow models (red).

6.4. Discussions and conclusions

While BIM contains very detailed and semantically rich information about a construction, GIS focuses more on the real geographical coordinates and spatial analysis. Integrating these two leads to a more comprehensive system where detailed and semantically rich information is connected to its exact location.

There is a vast domain of applications where the integration of BIM and GIS plays an important role. In this research we have performed two analysis which benefits from BIM-GIS integration, namely, view and shadow analysis. Detailed geometry and semantic information of the BIM model was converted to a georeferenced vector graphic model and GIS functionalities were applied to the resulting model for the mentioned geospatial analysis. The process has been automated using self-developed scripts as well as existing tools.

Calculating the view contents of a window can help urban planners, architects, etc for different analysis purposes, like house pricing. Once the whole process is being automated, one can benefit from fast and accurate analysis on a large scale.

Shadow analysis plays important roles for different purposes, for example in energy sector. Solar panels, as important renewable energy sources, are becoming more popular in the world. Geometrical characteristics of a building are important for an optimal energy gain from solar panels mounted on its rooftop(s). In the case of non-flat roofs, the horizontal orientation, steepness angle and rooftop area are important factors for, among others, calculating the gain potential of a solar panel. This information can be extracted from a BIM model. However, the potency of a building or a solar panel is not restricted to the building characteristic alone. Shadowing effects on the rooftop play an important role on the solar energy potential. This information cannot be extracted regardless of its environment context. Integration of BIM and GIS makes such a comprehensive analysis possible.

Formatted: Line spacing: Multiple 1,15 li
Formatted: Font: 11 pt
Formatted: Font: 11 pt
Formatted: Font: 11 pt
Formatted: Heading 1
Formatted: Justified, Line spacing: Multiple 1,15 li

Chapter 7: Synthesis and conclusions

This study explored solutions for enhancing the performance of spatial decision support systems for environmental problems. This optimization included different aspects of a SDSS, such as [geospatial] data integration from different domains, interactivity, model development and model integration. Different approaches and techniques have been applied in this study to enable the optimization of these aspects. The chapters of this study focus on methodologies for augmenting the performance of one or more SDSS components. The core method for optimizing the performance of the different components of a SDSS was the efficient Data-Model-Technology integration.

In line with the current limitations of SDSSs for multi-disciplinary environmental decision making processes, the following research objectives for the enhanced performance of SDSSs were defined. These objectives comprise of the development/implementation of:

- Methods for efficient accessibility to massive 2D/3D open geospatial data from different resources and different domains on a large extent

- Methodologies for efficient integration and interoperability between the geospatial datasets from different domains and disciplines

- Approaches for boosted visualization from both information content as well as interactivity and scene rendering perspectives

- Experimental environmental model development on an extended (city) scale and the third dimension

- Techniques for the development of interactive and responsive 3D design platforms with augmented information content and rendering capabilities

- Methods for boosted speed and scale of implemented simulation models

This chapter reviews the research carried out in this study to fulfil the research objectives.

7.1. Geodesign framework for a multi-disciplinary decision making process

To provide a structure for pursuing the above research objectives, a geodesign framework was applied. Geodesign, as an iterative design and planning approach, provided a constructive outline for positioning each research objective in its proper location within the complete decision making process framework. This provided an insight on the complete picture and helped in defining the inter-relation between the different elements of the total framework, which in turn, boosted the efficiency in designing and developing the different modules of environmental SDSSs and supported the scalability of the designed modules to be reused in different sub-modules of the framework. The geodesign framework contains six models, related

to the current situation as well as the alterations. Different chapters of this study addressed one or more of these models, as follows. Data-Model-Technology integration has been applied for each (sub)module of the geodesign framework.

7.1.1. Representation models

Representation models portray the spatio-temporal content of the study area (Steinitz, 2014) and are of great importance in providing a comprehensive picture of the current situation. Representation models contain different modules to include the different aspects of the illustration of the study area. Data collection and its visualization are two main components of representation models. Data collection, on its own, comprises several attributes, such as data availability, accessibility, extent, level of detail and interoperability. These features can be defined for each study, based on its problem statements and objectives. In this study, all chapters deal with these data attributes, as geospatial data is the foundation for all the research conducted. More specifically, Chapter 2 employed massive 2D and 3D open geospatial data (on city extent) and processing techniques for the estimation of UHI model parameters, namely, tree volume, sky view factor and urbanization degree. Chapters 3 and 4, incorporated tiling techniques, open standards protocols and web services for the on-the-fly serving of massive 2D/3D datasets of the whole country from different domains, untangling the data accessibility and interoperability knots. Chapter 5 applied massive 2D/3D open geospatial data on a city extent to extract different urban configuration parameters (such as roof shape model, exposed perimeter and sky view factor) for each individual building through the dedicated geospatial data processing routines to estimate the impact of spatial context on household heat demand. Chapter 6 employed open 3D geospatial data along with the BIM model, in open standard IFC information model, for the automated integration of the BIM model into the GIS environment through the developed routine. This enhanced the interoperability between BIM and GIS, which originate from different disciplines and objectives and opened up a path for increased efficiency in different analyses within a SDSS.

In addition to information content, the presentation and visualization style of spatial information is an important factor for the proper perception of the decision making team of the current situation. This study contributed to the development of an enhanced interactive 3D visualization platform where massive geospatial data on a large extent and from different domains can be served on-the-fly. Chapters 3 and 4 applied game engine for optimized scene rendering and graphical presentation, resulting in an interactive 3D visualization platform. The incorporation of geospatial information and GIS functionalities into the game engine-based system, resulted in the optimized rendering of various georeferenced data and efficient interaction with the data. Integration of tiling techniques, open standards protocols and web services in the game engine environment, expanded the game engine scene capabilities on on-the-fly serving of nationwide massive geospatial data from different domains on the cloud, resolving local data storage, formatting conflictions and data update issues.

7.1.2. Process models

Process models aim to explore the functional, structural and interaction behaviour among the elements of the study area to figure out how the study area operates (Steinitz, 2014; Reynolds,

2014). These models can indicate the operational picture of the current situation in different ways. In this study, quantitative analyses were performed for the development and application of different process models to present the interactions between different geospatial elements of the study area in different domains. Different mathematical and geometrical models have been developed/applied in the delineation procedure of the process models. While many studies mainly focus on detailed analysis on a small extent or coarse analysis on a large extent, a major objective in this study was to increase the extent of process models while maintaining a high level of detail, which was fulfilled through the efficient employment of geospatial open data and technology. This provided more detailed and comprehensive insights on the inter-relations between the elements of the study area for decision making processes on a city or national extent.

Chapter 2 developed a process model on the exploration of the impact of tree volume on the nocturnal heat island of Amsterdam. For the development of this model, tree volume from 3D models of all the individual trees in Amsterdam was calculated. While in other UHI studies, a 2D vegetation surface is applied, the employment of 3D tree volume in this study provided more accurate information on the relationship between the amount of trees and UHI. For the development of this process model, another process model, namely, sky view factor, was applied. Sky view factor, associated with heat release by urban elements, was estimated through a detailed height model for the whole of Amsterdam. Chapter 5 developed a process model exploring the impact of geospatial context on household heat demand. This research applied detailed parameters (on individual households) on the whole city of Amsterdam to investigate the relationship between the geospatial context of each household and its heat demand. These parameters were modelled through dedicated spatial data processing routines, using different mathematical algorithms and open geospatial datasets. Chapter 4 modelled the restricted areas for locating wind turbines throughout the Netherlands according to Dutch national rules based on the quantitative risk analysis of wind turbine operation on the environment. As the risk distance criteria employed depends on the wind turbine capacity, hub height and rotor diameter, different restricted areas were modelled for different wind turbine types. Upon the selection of a wind turbine type, the appropriate restricted area model is served accordingly. Furthermore, in this chapter the location and characteristics of existing wind turbines for the whole of the Netherlands were integrated in the system. This process model defines the current operation of the study area, from a wind turbine distribution point of view, which has an influence on the evaluation of the current situation as well as the positioning of new wind turbines in the area. The results of these process models are served into the system through the incorporated tiling techniques. Chapter 6 developed process models for quantitative analyses on view coverage from windows as well as roof segment shadow using a BIM model as well as 3D geospatial elements, namely, 3D building and tree models. These process models reflect the interactions between the BIM model and geospatial elements.

The development and integration of the process models, together with the employed geospatial data and visualization techniques, resulting from representation models provides an insight on the content, inter-relations and operations of the current situation. These models provide scope for the evaluation of the current situation by stakeholders through the adapted evaluation

models of the planning process. Following the evaluation of the current situation, alteration scenarios are posed by stakeholders through the proposed change models.

7.1.3. Change models

Change models investigate the modality of alterations in the study area, which are determined through different scenarios. The alteration scenarios can be proposed by different stakeholders, such as designers, citizens and authorities. A multidisciplinary design platform, wherein different stakeholders from different backgrounds can interact and work collaboratively, can have a considerable impact on the competence of the alteration scenarios and the design process. The information content of the design platform is an important factor in a multidisciplinary design process, due to the presence of participants from different domains and with different insights and priorities. The interactivity of a platform can increase the stakeholders' willingness to participate in the alteration design process. The platform's responsiveness boosts the efficiency of the scenario configuration process and can lead to the conjunction in the subsequent discussion flow, regarding the proposed alterations.

In Chapters 3 and 4, interactive 3D design platforms for wind turbine site planning were developed, upon Unity game engine. The optimized 3D rendering of the game engine, as well as the interactive environment developed thereby, boosted the intuitiveness and the interactivity of the design platform. On the other hand, the incorporation of geospatial datasets and GIS functionalities enabled the rendering of existing georeferenced landscape elements and increased the extension of the platform to the whole country (as described in representation models). The feasibility of on-the-fly serving of different cloud-based geospatial data, from different domains, through the incorporation of tiling techniques and open standard protocols, augmented the information content of the design platform, which is important for a multidisciplinary design process. Configuring alteration scenarios can be enhanced when stakeholders can design new situations on existing geospatial elements and different geospatial [thematic] information, integrated in the same design platform. The platforms' responsiveness to scenario configuration was augmented through the employment of different game engine functionalities. In addition, the systems' responsiveness to the impact assessment of the configured design is boosted through the effective integration of game engine, GIS and analytical model integration. The systems' responsiveness to these elements enabled the seamless scenario configuration and analysis in any location of the country.

7.1.4. Impact models

Configured alteration scenarios cannot be investigated irrespective of their mutual impacts on their environment. Impact models aim to explore the consequences of the posed alteration scenarios on the different domains involved. Quantitative assessments of the scenario design impacts can be performed through the employment of models. The existing challenges here are, among others, model complexity, performance speed, availability of input data, dependence on third-party software and the connection of the software to the design platform. These factors are obstacles to an iterative design and planning approach, as a core part of geodesign, where the immediate feedback on the impact of a proposed design into the evolution of the design process can result in a more efficient design process and more robust design solution (Lee et

al., 2014). This study aimed to contribute to exploring solutions for the elimination of these obstacles through embedding different models into the design platform and the efficient integration of game engine and GIS functionalities for the performance enhancement of the incorporated models.

Chapter 3 has incorporated state-of-the-art sound models into the planning platform for wind turbine sound impact assessments on the surrounding buildings. In addition to sound models, Chapter 4 has embedded wind turbine shadow, visibility, generated power and wake area models to explore the multi-aspectual impacts of the configured wind turbines on their surroundings. These models were scripted into the game engine-based planning system through Unity game engine C# scripting API. The employment of different game engine functionalities, resulting from Unity physics and rendering engines, resulted in the real-time performance of these models. On the other hand, the incorporation of GIS functionalities, such as tiling techniques, enabled real-time impact assessments for any location in the country. In addition, the incorporation of cloud-based open geospatial datasets and open standard protocols enabled the accessibility to and interoperability of the input data of these models, from different domains. Through the integration of these techniques, for the (re)placement of a wind turbine in the designed scene, all the embedded impact models will be (re)calculated real-time and on-the-fly and the results will be presented graphically and numerically in the scene. This immediate design-feedback loop interlocks the scenario configuration and discussion process of the design team. The models incorporated into the design platform and the integration of game engine and GIS techniques for their performance enhancement resulted in an enhanced system where alteration scenarios can be seamlessly configured in any location of the country and the impact assessment on the different aspects of these configured scenarios can be performed in real-time with no dependencies on third-party software. This provided scope for an intertwined discussion process between stakeholders from different disciplines which can enhance the efficiency and the results within a decision making flow.

Considering the impacts of the configured scenarios in all the involved disciplines and after several iterations through the geodesign steps, the decision team can converge on the final solution through the applied decision models. Based on the applied criteria, these models define the preferences among all the posed scenarios. The final decision can be inspired by the local knowledge as well as the illustrated impacts of the posed alteration scenarios.

7.2. Answers to the research questions

1. *How can [massive] 2D/3D open geospatial data, from different domains, be efficiently served in portraying the current spatial configuration in representation and change models?*

This study applies web services and open standard protocols for accessing different interoperable geospatial data from different domains. In addition, tiling techniques have been employed for on-the-fly serving of these massive 2D and 3D datasets on a large extent. These datasets are used in all the chapters of this study, for the depiction of the current situation in

visualization platforms as well as inputs for the developed/implemented process and impact models.

2. *How can the interactivity, extent and responsiveness of a 3D spatial design platform be enhanced through the employment and integration of technology from different domains?*

The integration of technology from different domains, in this study, resulted in the performance enhancement of design platforms, regarding alteration scenario configuration as well as impact assessment of the different designs. The employment of game engine functionality, such as rendering engine and physics engine, supported the enhanced 3D scene rendering, interactivity and responsiveness of the design platform. The incorporation of GIS tiling techniques and open standards, in the game engine environment enhanced the extent of the design platform to the whole country and potentially even beyond that. This integration is addressed in Chapters 3 and 4.

3. *What is the benefit of 3D geospatial information on the development of process models?*

This study demonstrates the benefit of 3D geospatial information on the development of UHI as well as on the heat demand model, in Chapter 2 and Chapter 5, respectively. In Chapter 2, the impact of tree volume and sky view factor, as local factors influencing UHI was investigated. While other studies investigated the impact of vegetation on UHI through using vegetation surface, information on the volume, which is extracted though their 3D geometry, provides additional insight on their shading and evapotranspiration cooling characteristics. This provides a more comprehensive view on the impact of urban trees on UHI. Chapter 5 investigates the impact of the spatial context on the heat demand of individual households. In this research, 3D urban configuration related elements as well as building shape parameters, such as sky view factor, tree volume, building height and roof shape, showed to have influence on housing units heat demand. 3D geospatial information, therefore, plays an important role on the impact estimation of spatial context on the heat demand of individual housing units.

More specifically on process models, based on the defined use cases of this study, the following research questions were posed:

4. *What is the influence of tree volume on nocturnal Urban Heat Island (UHI)?*

Chapter 2 investigates the impact of tree volume on the nocturnal Urban Heat Island (UHI) of Amsterdam. To explore the maximum local impact of tree volume on UHI, buffers with varying radii around each temperature observation have been defined. For each buffer, the impact of aggregated tree volumes, derived from 3D tree models, on UHI was estimated through multi-linear regression analysis. Sky view factor, as another local parameter, and urbanization degree, as a regional parameter, have also been taken into account in each buffer as additional explanatory variables, along with tree volume, in the regression model. The results of this research show that the impact of tree volume on UHI achieves its maximum on the smallest buffer radius of 40 m and that in this radius an increase of 60,000 m^3 tree volume leads to one degree UHI mitigation. Based on the geometrical characteristics of trees in the study area, this volume is approximately equal to 90 small trees or 20 medium trees or 4 large trees.

5. *How do spatial context parameters affect household heat consumption?*

Chapter 5 carried out a quantitative assessment of the relationship between household heat consumption and its spatial context on a city extent and at two different scales: housing unit and postal code level. At housing unit scale, a regression analysis was performed to explore the relation between the measured heat consumption of each individual household, for the whole city of Amsterdam, with its spatial context. A set of explanatory factors that described building shape, surroundings and basic building characteristics were applied, together with the measured heat consumption, in the regression analysis. At postal code level, heat consumption measurements and explanatory factors, also containing demographic composition of the postcode areas, were aggregated and applied in a separate regression analysis. The results of this research at both scales revealed the dominance of housing unit surface area and height on heat demand. Exposed perimeters were also found to have a high positive impact on heat demand at both scales. The number of housing units per building showed a higher impact on the housing unit level compared to postal code level. The presence of a slanted roof and urbanization degree presented a comparable impact at both levels. Tree volume presented a directional impact on heat demand. Only trees northwest of a building had a significant and negative impact on household heat demand. Demographic data at the postal code level showed the impact of occupants' age classes on heat demand.

6. *How can geospatial information be efficiently extracted from data to be used as the inputs of the predictive analytics on the whole city extent and high level of detail?*

Chapters 2 and 5 address the efficient and automated detailed 2D/3D geospatial information extraction from raw data on a large extent to be applied as the inputs of the predictive analytics. Chapter 2 discussed the automated extraction of 3D tree models as well as sky view factor from 3D LIDAR point cloud. This research also described the automated extraction of urbanization degree indicator from land use maps. Chapter 5, in addition to tree volume and sky view factor, demonstrated the automated extraction of different spatial context elements for the whole city of Amsterdam. The spatial data processing routines developed in this research integrate different mathematical algorithms into GIS where massive geospatial data can be accessed and managed efficiently. The availability/accessibility of detailed open geospatial data, in combination with the employment of GIS functionalities for the efficient management of geospatial data, serve the mathematical algorithms an optimized procedure for increasing their extent and level of detail. This integration enabled the automated extraction of detailed spatial context elements on individual building level and at the same time enabled broadening the extent of this research to the whole city and even beyond that.

7. *How can BIM-GIS integration support the efficiency of construction-environment impact analyses?*

In Chapter 6, a pipeline for the automated integration of BIM and GIS is introduced. Two use cases for this integration are defined in this study: view coverage and roof shadow coverage analysis, which are related to liveability and energy domains. BIM-GIS integration supports the combination of the highly detailed geometrical and semantic information of the BIM model with the large-scale geospatial data on its environment, which provides the scope for efficient

construction-environment mutual impact analysis on a large extent. This is demonstrated through the applied use cases of this research. View coverage analysis can help different stakeholders, such as urban planners and architects, to perform different analyses (e.g. house pricing) on a large extent quickly and accurately. Roof shadow coverage analysis is of great benefit in, for instance, the energy sector, where the information on a building roof (horizontal orientation, steepness angle and rooftop area) from a BIM model, in combination with the shading impact of surrounding buildings and trees can be used for calculating the gain potential of rooftop solar panels.

7.3. Future perspectives

The focus of this study was to provide new insights and methods to support environmental decision making. For this purpose, different routines were developed, through efficient Data-Model-Technology integration, in a geodesign framework, for the enhancement of different components of SDSSs in different domains. While energy and liveability have been chosen as the cases of this study, the developed routines and systems are scalable to other domains with geospatial components. These results, on the one hand, from the cloud-based architecture of the developed modules and the applied technology for the accessibility to and interoperability of different datasets from different disciplines, makes them independent from specific data providers or domains. On the other hand, the developed routines for boosting the performance of each component are made of loosely-coupled geospatial and/or game engine functionalities which are scalable and can be adapted in different domains with geospatial components. While the enhanced performance of the different developed components, as presented in this study, can increase the efficiency of decision making processes in different domains, their usability and user experience should be evaluated in decision making processes.

A major focus of this study was the employment of cloud-based techniques for accessibility to and integration of different open geospatial datasets from different domains which play an important role in multi-disciplinary decision making processes. While the employment of these techniques are of great importance in broadening the decision making scope and boosting the efficiency of the data collection/presentation procedures, the differences in accuracy, scale, update and level of detail between these datasets are further challenges and should be considered in their integration. Incorporating harmonization methods for the integration of heterogeneous geospatial data, as described in different studies (von Goesseln, 2005; Butenuth et al., 2007) can contribute to overcoming this challenge.

Furthermore, integration of data from different disciplines, for instance BIM and GIS, with different objectives, information models and levels of detail, contain different geometrical and topological inconsistencies (Ohori et al., 2017). This can lead to different errors and mismatches in their conversion process. Understanding the nature and sources of these errors is an important step for their repair, aiming at improving integration. Biljecki and Tauscher (2019) constructed a framework for quality assessments of BIM and GIS interoperability. They have employed different methods and tools for error detections, such as val3dity (Ledoux, 2018) and custom

Extract-Transform-Load process. In addition to error detection, Donkers et al. (2016) presented an algorithm for automated error repair, resulting in a BIM conversion to a geometrically and semantically correct 3D GIS object. Incorporation of this error detection and repair algorithm in the framework of this study can reduce errors and mismatches between the datasets of different disciplines (BIM and GIS in this study) and enhance the multidisciplinary data integration and the subsequent analyses.

The focus of this study on the use of simulation models is their efficient integration with geospatial data and techniques for their optimized performance. These simulation models have been obtained from validated literature. However, the employment of the simulation and the developed process/impact models in actual applications should be carefully done and the applied assumptions and validations under certain circumstances should be cautiously investigated. The decision making team should be aware of the validity and applicability of these models in their case studies, considering the spatial settings and scale of their study as well as the availability and detail level of model input data.

The developed components and routines in this study can be applied in different developing platforms and processes. Digital transformation is an important on-going process wherein integration of technologies from different domains plays a crucial role. European Commission has defined different traits for Europe's digital future in European Digital Strategy, namely, the benefits for all people, creation of fair and competitive digital economy and an open and sustainable digital society. Europe's horizon for smart cities is an instance where innovative technologies and digitalization plays an important role on a city's prosperity and sustainability enhancement (European Commission, 2020). Digital twin of, which is a virtual representation of its physical reality, can be considered as the first step of digital transformation (Emerson, 2019) and has recently gained popularity in different domains. Amsterdam Smart City[37] is one of the platforms where digital twin plays an important role in providing the spatial and functional picture to the involved stakeholders (such as citizens, knowledge institutes and public authorities) for designing the future city. Two major components of a digital twin comprise of data and process models. The Smart City Operating System collect massive [geospatial] data from different resources and should in real-time extract information from them to depict the situational picture to the stakeholders. From 2017, Municipality of Rotterdam works on Digital City program wherein researches have been carried out to explore the form of the future city. In the framework of this program an Open Urban Platform is being developed through which data from different sources and domains can be shared among different stakeholders and new applications and services can be developed. The core of this platform is formed through the digital twin of the city, which depicts the current picture upon which new applications and services can be developed. Sharing data among different stakeholders via open standards, enables the better handling of more complex questions and decisions makings (Gemeente Rotterdam, 2020). These platforms emphasize on the incorporation of open standards for the integration of geospatial data from different sources. Furthermore, efficient serving of massive geospatial data in these platforms is of great importance for the digital twin of a dynamic urban environment. In addition, the integration of process and impact models into

[37] https://amsterdamsmartcity.com/network/amsterdam-smart-city

these platforms enables them to depict the functional picture of the urban area to the different stakeholders, which helps in different decision makings in the city. Regarding these attributes, the developed modules of this study can be applicable in different segments of these platforms, from techniques for massive geospatial data integration based on open standards, to enhanced visualization platforms to the large scale developed process models and efficient implementation of impact models. The scalability of the developed modules in this study enables their supple employment in such platforms.

Summary

Taking appropriate decisions for the mitigation of environmental problems and their impacts on our life is a challenging task due to their multi criteria nature, the involvement of stakeholders from different domains, and the uncertainty and complexity of environmental problems. Reliable and updated information on the current situation is the initial step, upon which proper alteration scenarios can be configured. Due to the close relationship between environmental phenomena and their locations, geospatial information plays a crucial role in the analysis of environmental problems, as well as in the configuration of mitigation solutions.

Geospatial information can be acquired from geospatial data through different techniques. This process requires the definition of a proper framework for the efficient access, maintenance, processing and presenting of geospatial datasets. During the last decades, different environmental studies have focused on the definition and/or implementation of geospatial frameworks. In line with these studies, a framework for supporting environmental decision making has been investigated in this study. Geodesign was chosen as the framework for multi-disciplinary decision making processes, due to its design-feedback loop which should be iteratively revisited by the involved stakeholders from different domains.

Geodesign contains different inter-related components whose agile performance have significant impact on the enhanced performance of the entire decision support system. These components comprise, among others, visualization, data integration, process models, design platform and impact models. The optimized performance of these components is reliant upon several factors, among which are the data availability, accessibility and interoperability, the system's performance capacity, and the accessibility and integration of process/impact models. Considering the current limitations on the performance of these elements, this study aims to enhance the [geodesign-based] decision support system components through efficient data, model and technology integration. The research conducted as part of this thesis presents the enhancement of these components for supporting environmental decision making.

Local impact of tree volume on nocturnal urban heat island: A case study in Amsterdam

Urbanization growth and the resulting development of the built environment in urban areas has led to an increase of the Urban Heat Island (UHI). One of the factors affecting UHI is vegetation cover. While different studies have investigated the impact of vegetation surface (2D) on the urban heat island, studies on the impact of tree volume on UHI on a city scale are scarce. This is due to information scarcity on the tree volume of a whole city. Chapter 2 of this thesis focuses on a quantification of tree volume impact on the nocturnal urban heat island of Amsterdam, using 3D tree models of the whole city. Sky View Factor (SVF) and urbanization degree as the local and regional urban compactness parameters, respectively, have been used in a multi-linear regression analysis, together with urban tree volume, to estimate tree volume contribution to UHI. Scale effect was investigated by examining aggregated tree volume on different radii to explore the highest impact of tree volume on UHI. The results of this study indicated that, in this case study, the highest impact of tree volume on UHI is within 40 m, where in this buffer

a 60,000 m^3 tree canopy volume increase leads to one degree UHI reduction. Furthermore, this study demonstrated how geospatial technology can be applied for automated information extraction, in high detail and for large extents, for efficient analysis of the relation between UHI and urban elements.

Developing a wind turbine planning platform: Integration of "sound propagation model–GIS-game engine" triplet

Environmental problems resulting from fossil fuel use have prompted us to consider energy production using renewable energy resources. Wind energy is a common renewable energy source which is widely used in many countries, including the Netherlands. However, despite the benefits of wind energy, wind turbine development projects face opposition from citizens due to wind turbine externalities, such as noise. A properly designed information system through which citizens, in collaboration with other stakeholders, can express their ideas and receive information on the current and designed situation can help to involve citizens, which can increase understanding in the siting of wind turbine allocation projects and make the wind turbine planning process more efficient. In Chapter 3, an interactive information system for wind turbine siting, considering its visual and sound externalities, has been developed. This system is an integration of sound propagation models, GIS and game engine embedded in a unified platform. This integration supported the optimized performance of the system and the real-time wind turbine sound calculation in any location of the whole country. Game engine-GIS integration provides a 3D virtual environment of the whole country, with existing geospatial elements, through which users can navigate, (re)place wind turbines and explore their visual impacts on the environment. The integration of sound propagation models in the game engine-GIS integrated environment, enabled the real-time calculation of wind turbine sound on its surrounding buildings in any location of the country. The game engine component supports the optimized performance for scene rendering as well as sound model calculations. The GIS component enables serving massive (on-the-fly) georeferenced data through tiling techniques as well as data accessibility and interoperability via cloud-based architecture and open geospatial standard protocols, to be applied both for visualization as well as inputs of the sound propagation models.

Interactive 3D geodesign tool for multidisciplinary wind turbine planning

Wind turbine site planning is a multidisciplinary task where stakeholders from different domains and with different interests and priorities are involved. An information system capable of integrating knowledge on the different aspects of a wind turbine can be of great importance in providing a common picture to all of the stakeholders involved. In Chapter 4 of this thesis, a multidisciplinary interactive 3D information system for planning wind turbine locations in the whole of the Netherlands was developed. The architecture developed for wind turbine planning through the game engine-GIS-sound model integration of the previous chapter, was applied as the basis architecture of this system and is further developed in this chapter to include other

aspects in wind turbine planning. The integration of GIS, game engine and the analytical models has led to the development of an interactive platform with real-time feedback on the multiple wind turbine aspects for different environmental settings. This system supports iterative design loops and has been designed based on a geodesign framework. Each of the geodesign models is implemented in this system, which together form an interactive multidisciplinary wind turbine site planning platform for seamless wind turbine configuration and real-time feedback in any location of the country. This provides scope for an interwoven discussion process. The criteria applied in this system are: wind turbine sound, shadow, visibility from buildings, energy yield, wake effects and regulations. Different analytical and geometrical models have been embedded in this game engine-GIS integrated system to calculate these process/impact models in real-time upon (re)placing wind turbines in the scene. The multi-aspectual feature of this system broadens its applications and can lead to the involvement of stakeholders from different backgrounds.

Analysing the impact of spatial context on the heat consumption of individual households

The heating of residential buildings in temperate and colder climates accounts for a significant share of the total energy consumption of a country. This, in combination with the usage of fossil fuel for home heating, leads to an increase in global warming and environmental problems. Therefore, reducing home heating consumption leads to a considerable reduction in total energy consumption. The initial step here is to explore the factors influencing household heat demand. Most of these factors depend on individual choices (e.g. occupants' behaviour, interior building design, heating system efficiency) and are difficult to influence through urban planning. However, parameters affecting household heat demand regarding the spatial context can be influenced by urban planners. Yet the impact of spatial context on household heat demand on a city scale has not been adequately studied. This is mainly due to the scarcity of geospatial data and the massive computer processing required for capturing the spatial configuration elements of each individual household for the whole city. Chapter 5 focuses on exploring the combined impact of building shape and its surroundings on the household heat consumption of Amsterdam, both at individual household level as well as postal code level, through regression analysis. The spatial context of individual housing units was described through spatial data processing routines and algorithms and using detailed 2D and 3D geospatial data. GIS techniques were employed for the efficient processing of massive 3D geospatial data for all buildings in the city. The local housing unit level results demonstrate that compact neighbourhoods with less open space and buildings with higher numbers of housing units and less exposed perimeters have lower heating demand. Trees were found to lead to heat demand reduction when they are located on the northwest side of buildings. The results at postal code level highlighted the importance of demographic composition. (Larger) households with children have the highest heat consumption. At both individual and postal code scales, size and age of housing units have important impacts on heat consumption. Older houses consume more energy, but a *rebound effect* was found for the newest housing units.

From BIM to geo-analysis: view coverage and shadow analysis by BIM/GIS integration

Environmental analysis in urban areas, regarding current processes as well as alteration scenarios, has a significant impact on the different decision making processes. For this purpose, the integration of data from different domains and disciplines plays an important role. This integration provides the scope for more comprehensive and detailed analyses regarding the on-going processes. The difference between the disciplines, detail level and information model cause challenges for this integration. The integration of the Building Information Model (BIM) and geospatial data is such an instance. BIM comprises detailed geometrical and semantic information of a construction. GIS, on the other hand, consists of the physical and functional representation of the environment. These two information sources are often not integrated, which is mainly due to the difference in their level of detail, caused by different scales. The integration of BIM and GIS provides the scope for understanding the mutual impacts of a construction and its environment and supports performing different automated detailed analyses on a large extent. Chapter 6 introduces a pipeline for the automated integration of IFC BIM in a 3D GIS environment. The BIM-GIS integration was applied in two studies: view coverage and shadow analysis. In these studies, the detailed information of windows and roofs were extracted from BIM model and were subsequently used together with 3D geospatial elements (building and tree models) and process models for the estimation of view coverage quality as well as shadow coverage on rooftop segments. These analyses revealed the added-value of integrating BIM and spatial data for, for instance, spatial planning. In addition, it demonstrated the possibility of automating the whole process, from BIM-GIS integration to different analyses, supporting fast and accurate analyses on a large scale.

Conclusions

This study investigated solutions for performance enhancement of different components of Spatial Decision Support Systems (SDSS) for environmental problems. This included different aspects of a SDSS, such as [geospatial] data integration from different domains, interactivity, model development and model integration. The fundamental method for this performance enhancement was efficient Data-Model-Technology integration, which was applied based on a geodesign framework. The chapters of this thesis addressed one or more of the geodesign models, which together form the modules of environmental SDSSs.

Improvements in the scope of *representation models* were performed through efficient integration of massive 2D and 3D open geospatial data from different domains, which were accessible and interoperable through the implementation of web services and open standard protocols. In addition, this study contributed to the development of a boosted interactive 3D visualization platform, through game engine-GIS integration, where massive geospatial data on a large extent and from different domains can be served on-the-fly to the game engine with optimized scene rendering properties.

Enhancements in the context of *process models* were carried out through the development and implementation of these models on a large extent and, at the same time, with a high level of

detail. This was fulfilled through the efficient employment of geospatial open data and technology as well as algorithms and routines for the automated extraction of detailed information on spatial elements on a large extent.

For *change models*, this study contributed in the development of a 3D interactive multidisciplinary design platform wherein different stakeholders from different domains can work collaboratively on configuring alteration scenarios. The responsiveness of this platform is boosted through the employment of game engine functionalities and the information content and extent is enhanced through embedding GIS techniques. These enhancements enabled seamless scenario configuration and analysis in any location of the country.

Improvements in the scope of *impact models* were performed through enhancement of their performance speed, efficient accessibility to input data and independence from third party software. These improvements were achieved through the efficient incorporation of impact models in the game engine-GIS integrated design platform wherein different game engine and GIS functionalities for the boosted performance of these models were applied. This has resulted in a fortified system where stakeholders can seamlessly configure different alteration scenarios in any location of the country and receive real-time feedbacks on different aspects of their design with no dependencies on third-party software.

In conclusion, it can be mentioned that efficient integration of Data-Model-Technology can significantly support the enhancement of environmental decision support systems. In this study, energy and liveability have been chosen as the case studies. However, the developed routines are scalable to other domains. This is, on the one hand, due to the cloud-based architecture of the developed modules and the technology applied for the accessibility to and interoperability of different datasets from different disciplines, and on the other hand, due to the development and application of loosely-coupled geospatial and/or game engine functionalities for the boosted performance of the different components of SDSS.

Samenvatting

Het nemen van passende beslissingen voor het verminderen van milieuproblemen en hun impact op ons leven is een uitdagende taak vanwege hun multi-criteria karakter, de betrokkenheid van belanghebbenden uit verschillende domeinen en de onzekerheid en complexiteit van milieuproblemen. Betrouwbare en bijgewerkte informatie over de huidige situatie is de eerste stap, waarop de juiste wijzigingsscenario's kunnen worden geconfigureerd. Vanwege de nauwe relatie tussen omgevingsverschijnselen en hun locaties, speelt georuimtelijke informatie een cruciale rol bij de analyse van milieuproblemen, evenals bij de configuratie van mitigatieoplossingen.

Ruimtelijke informatie kan worden verkregen uit Ruimtelijke gegevens via verschillende technieken. Dit proces vereist de definitie van een goed raamwerk voor efficiënte toegang, onderhoud, verwerking en presentatie van ruimtelijke datasets. In de afgelopen decennia, hebben verschillende milieustudies zich gericht op de definitie en / of implementatie van georuimtelijke kaders. In lijn met deze studies, is in deze studie een raamwerk onderzocht ter ondersteuning van milieubesluitvorming. Geodesign werd gekozen als het raamwerk voor multidisciplinaire besluitvormingsprocessen, vanwege de ontwerp-feedbacklus die iteratief moet worden herzien door de betrokken belanghebbenden uit verschillende domeinen.

Geodesign bevat verschillende onderling verbonden componenten waarvan de behendige prestaties een aanzienlijke impact hebben op de verbeterde prestaties van het gehele beslissingsondersteunende systeem. Deze componenten omvatten onder meer visualisatie, data-integratie, procesmodellen, ontwerpplatform en impactmodellen. De geoptimaliseerde prestaties van deze componenten zijn afhankelijk van verschillende factoren, waaronder de beschikbaarheid van gegevens, toegankelijkheid en interoperabiliteit, de prestatiecapaciteit van het systeem en de toegankelijkheid en integratie van proces- / impactmodellen. Gezien de huidige beperkingen van de prestaties van deze elementen, is deze studie gericht op het verbeteren van de [op geodesign gebaseerde] besluitondersteunende systeemcomponenten door efficiënte data-, model- en technologie-integratie. Het onderzoek dat in het kader van dit proefschrift wordt uitgevoerd, presenteert de verbetering van deze componenten ter ondersteuning van milieubesluitvorming.

Lokale impact van boomvolume op nachtelijk stedelijk hitte-eiland: een casestudy in Amsterdam

De verstedelijkingsgroei en de daaruit voortvloeiende ontwikkeling van de gebouwde omgeving in stedelijke gebieden heeft geleid tot een toename van het Urban Heat Island (UHI). Een van de factoren die van invloed is op UHI is de begroeiing. Hoewel verschillende studies de impact van vegetatie-oppervlak (2D) op het stedelijke hitte-eiland hebben onderzocht, zijn studies naar de impact van boomvolume op UHI op stadsschaal schaars. Dit komt door informatieschaarste van het boomvolume van een hele stad. Hoofdstuk 2 van dit proefschrift richt zich op een kwantificering van de impact van boomvolumes op het nachtelijke stadswarmte-eiland Amsterdam, met behulp van 3D-boommodellen van de hele stad. Sky View

Factor (SVF) en verstedelijkingsgraad als respectievelijk de lokale en regionale stedelijke compactheidsparameters zijn gebruikt in een multi-lineaire regressieanalyse, samen met stedelijk boomvolume, om de bijdrage van boomvolumes aan UHI te schatten. Schaaleffect werd onderzocht door het geaggregeerde boomvolume op verschillende radii te onderzoeken om de hoogste impact van boomvolume op UHI te onderzoeken. De resultaten van deze studie gaven aan dat in deze casestudy de grootste impact van boomvolume op UHI binnen 40 m ligt, waar in deze buffer een toename van het bladerdakvolume van 60.000 m3 leidt tot een UHI-reductie van één graad. Bovendien toonde deze studie aan hoe ruimtelijke technologie kan worden toegepast voor geautomatiseerde informatie-extractie, in detail en in grote omvang, voor een efficiënte analyse van de relatie tussen UHI en stedelijke elementen.

Ontwikkeling van een platform voor de planning van windturbines: integratie van een triplet "geluidsverspreidingsmodel-GIS-game engine"

Milieuproblemen als gevolg van het gebruik van fossiele brandstoffen hebben ons ertoe aangezet om energieproductie met hernieuwbare energiebronnen te overwegen. Windenergie is een veel voorkomende duurzame energiebron die veel wordt gebruikt in veel landen, waaronder Nederland. Ondanks de voordelen van windenergie, worden windturbineontwikkelingsprojecten echter geconfronteerd met tegenstand van burgers als gevolg van windturbine externaliteiten, zoals geluid. Een goed ontworpen informatiesysteem waarmee burgers, in samenwerking met andere belanghebbenden, hun ideeën kunnen uiten en informatie kunnen ontvangen over de huidige en ontworpen situatie, kan burgers helpen betrekken, wat het begrip bij de situering van windturbinetoewijzingsprojecten kan vergroten en het wind turbine planningsproces efficiënter kan maken. In Hoofdstuk 3 is een interactief informatiesysteem ontwikkeld voor het aanbrengen van windturbines, rekening houdend met de visuele en geluidseffecten ervan. Dit systeem is een integratie van geluidsverspreidingsmodellen, GIS en game-engine ingebed in een verenigd platform. Deze integratie ondersteunde de geoptimaliseerde prestaties van het systeem en de realtime berekening van het geluid van windturbines op elke locatie van het hele land. Game engine-GIS-integratie biedt een virtuele 3D-omgeving van het hele land, met bestaande georuimtelijke elementen, waardoor gebruikers kunnen navigeren, windturbines kunnen (her) plaatsen en hun visuele impact op het milieu kunnen verkennen. De integratie van modellen voor geluidsvoortplanting in de game-engine-GIS geïntegreerde omgeving maakte de real-time berekening mogelijk van het geluid van windturbines op de omliggende gebouwen op elke locatie van het land. De game-engine-component ondersteunt de geoptimaliseerde prestaties voor het renderen van scènes en het berekenen van geluidsmodellen. De GIS-component maakt het mogelijk om massale (on-the-fly) geogerefereerde gegevens te leveren door middel van tile technieken, evenals toegankelijkheid en interoperabiliteit van gegevens via cloudgebaseerde architectuur en open ruimtelijke standaardprotocollen, die zowel kunnen worden gebruikt voor visualisatie als voor invoer van de geluidsverspreidingsmodellen.

Interactieve 3D-tool voor geodesign voor multidisciplinaire planning van windturbines

De planning van windturbines is een multidisciplinaire taak waarbij belanghebbenden uit verschillende domeinen en met verschillende belangen en prioriteiten worden betrokken. Een informatiesysteem dat kennis over de verschillende aspecten van een windturbine kan integreren, kan van groot belang zijn om alle betrokken belanghebbenden een gemeenschappelijk beeld te geven. In Hoofdstuk 4 van dit proefschrift is een multidisciplinair interactief 3D informatiesysteem ontwikkeld voor het plannen van windturbinelocaties in heel Nederland. De architectuur die is ontwikkeld voor de planning van windturbines via de integratie van de game-engine-GIS-geluidsmodel van het vorige hoofdstuk, werd toegepast als de basisarchitectuur van dit systeem en wordt in dit hoofdstuk verder ontwikkeld om andere aspecten in de planning van windturbines op te nemen. De integratie van GIS, game-engine en de analytische modellen heeft geleid tot de ontwikkeling van een interactief platform met realtime feedback op de verschillende windturbine-aspecten voor verschillende omgevingsinstellingen. Dit systeem ondersteunt iteratieve ontwerplussen en is ontworpen op basis van een geodesign raamwerk. Elk van de geodesign-modellen is geïmplementeerd in dit systeem, dat samen een interactief multidisciplinair locatieplanningsplatform voor windturbines vormt voor naadloze configuratie van windturbines en realtime feedback in elke locatie van het land. Dit biedt ruimte voor een verweven discussieproces. De criteria die in dit systeem worden gehanteerd zijn: windturbinegeluid, schaduw, zichtbaarheid van gebouwen, energieopbrengst, wake-effecten en regelgeving. Verschillende analytische en geometrische modellen zijn ingebed in dit geïntegreerde game-engine-GIS-systeem om deze proces- / impactmodellen in realtime te berekenen bij het (her) plaatsen van windturbines in de scene. Het meervoudig aspect van dit systeem verbreedt zijn toepassingen en kan leiden tot de betrokkenheid van belanghebbenden met verschillende achtergronden.

Analyse van de impact van ruimtelijke context op het warmteverbruik van individuele huishoudens

De verwarming van woongebouwen in gematigde en koudere klimaten maakt een aanzienlijk deel uit van het totale energieverbruik van een land. Dit, in combinatie met het gebruik van fossiele brandstof voor huisverwarming, leidt tot een toename van de opwarming van de aarde en milieuproblemen. Het verminderen van het verbruik van huisverwarming leidt daarom tot een aanzienlijke vermindering van het totale energieverbruik. De eerste stap hier is om de factoren te onderzoeken die de warmtevraag van huishoudens beïnvloeden. De meeste van deze factoren zijn afhankelijk van individuele keuzes (bijv. gedrag van bewoners, interieurontwerp, efficiëntie van verwarmingssystemen) en zijn moeilijk te beïnvloeden door stadsplanning. Parameters die de warmtevraag van huishoudens met betrekking tot de ruimtelijke context beïnvloeden, kunnen echter worden beïnvloed door stedenbouwkundigen. Toch is de impact van de ruimtelijke context op de warmtevraag van huishoudens op stadsschaal niet voldoende bestudeerd. Dit komt voornamelijk door de schaarste aan georuimtelijke gegevens en de enorme computerverwerking die nodig is om de ruimtelijke configuratie-elementen van elk individueel huishouden voor de hele stad vast te leggen. Hoofdstuk 5 richt zich op het verkennen van de gecombineerde impact van gebouwvorm en omgeving op het huishoudelijk warmteverbruik van Amsterdam, zowel op individueel huishoudelijk niveau als op postcodeniveau, door middel

van regressieanalyse. De ruimtelijke context van individuele wooneenheden werd beschreven door middel van ruimtelijke gegevensverwerkingsroutines en algoritmen en met behulp van gedetailleerde 2D- en 3D-ruimtelijke gegevens. GIS-technieken werden gebruikt voor de efficiënte verwerking van enorme 3D-gruimtelijke gegevens voor alle gebouwen in de stad. De resultaten op het niveau van de lokale wooneenheden laten zien dat compacte buurten met minder open ruimte en gebouwen met een groter aantal wooneenheden en minder blootgestelde omtrekken een lagere warmtevraag hebben. Bomen bleken te leiden tot een vermindering van de warmtevraag wanneer ze zich aan de noordwestkant van gebouwen bevinden. De resultaten op postcodeniveau wezen op het belang van demografische samenstelling. (Grotere) huishoudens met kinderen hebben het hoogste warmteverbruik. Op zowel individuele als postcodeschalen hebben grootte en leeftijd van wooneenheden belangrijke gevolgen voor het warmteverbruik. Oudere huizen verbruiken meer energie, maar er werd een *rebound-effect* gevonden voor de nieuwste woningen.

Van BIM tot geo-analyse: zichtdekking en schaduwanalyse door BIM / GIS-integratie

Milieuanalyse in stedelijke gebieden, met betrekking tot zowel lopende processen als veranderingsscenario's, heeft een grote impact op de verschillende besluitvormingsprocessen. Hierbij speelt de integratie van data uit verschillende domeinen en disciplines een belangrijke rol. Deze integratie biedt de mogelijkheid voor meer uitgebreide en gedetailleerde analyses met betrekking tot de lopende processen. Het verschil tussen de disciplines, detailniveau en informatiemodel zorgen voor uitdagingen voor deze integratie. De integratie van het Building Information Model (BIM) en ruimtelijke data is zo'n voorbeeld. BIM bevat gedetailleerde geometrische en semantische informatie van een constructie. GIS daarentegen bestaat uit de fysieke en functionele representatie van de omgeving. Deze twee informatiebronnen zijn vaak niet geïntegreerd, wat vooral te wijten is aan het verschil in detailniveau, veroorzaakt door verschillende schalen. De integratie van BIM en GIS biedt de mogelijkheid om de wederzijdse effecten van een constructie en zijn omgeving te begrijpen en ondersteunt het uitvoeren van verschillende geautomatiseerde gedetailleerde analyses in grote mate. Hoofdstuk 6 introduceert een werkwijze voor de geautomatiseerde integratie van IFC BIM in een 3D GIS-omgeving. De BIM-GIS-integratie werd toegepast in twee onderzoeken: zichtdekking en schaduwanalyse. In deze studies werd de gedetailleerde informatie over ramen en daken uit het BIM-model gehaald en vervolgens samen met 3D-georuimtelijke elementen (bouw- en boommodellen) en procesmodellen gebruikt voor het schatten van de zichtdekkingskwaliteit en schaduwdekking op dak-segmenten. Deze analyses lieten de meerwaarde zien van het integreren van BIM en ruimtelijke data voor bijvoorbeeld ruimtelijke ordening. Daarnaast heeft het de mogelijkheid aangetoond om het hele proces te automatiseren, van BIM-GIS-integratie tot verschillende analyses, waardoor snelle en nauwkeurige analyses op grote schaal worden ondersteund.

Conclusies

Deze studie onderzocht oplossingen voor prestatieverbetering van verschillende componenten van ruimtelijke beslissingsondersteunende systeem (SDSS)[38] voor milieuproblemen. Dit omvatte verschillende aspecten van een SDSS, zoals [georuimtelijke] data-integratie vanuit verschillende domeinen, interactiviteit, modelontwikkeling en modelintegratie. De fundamentele methode voor deze prestatieverbetering was efficiënte Data-Model-Technology integratie, die werd toegepast op basis van een geodesign-raamwerk. De hoofdstukken van dit proefschrift behandelden een of meer van de geodesign-modellen, die samen de modules van SDSS's voor het milieu vormen.

Verbeteringen in de reikwijdte van *representatiemodellen* werden uitgevoerd door efficiënte integratie van grote hoeveelheid 2D en 3D open georuimtelijke gegevens uit verschillende domeinen, die toegankelijk en interoperabel waren door de implementatie van webservices en open standaardprotocollen. Bovendien heeft deze studie bijgedragen tot de ontwikkeling van een verbeterd interactief 3D-visualisatieplatform, door middel van game engine-GIS integratie, waar enorme georuimtelijke gegevens op grote schaal en uit verschillende domeinen on-the-fly aan de game engine, met geoptimaliseerde eigenschappen voor het renderen van scènes, kunnen worden aangeboden.

Verbeteringen in de context van *procesmodellen* zijn gerealiseerd door de ontwikkeling en implementatie van deze modellen op grote schaal en tegelijkertijd met een hoog detailniveau. Dit werd bereikt door de efficiënte inzet van georuimtelijke open data en technologie, evenals algoritmen en routines voor de geautomatiseerde extractie van gedetailleerde informatie over ruimtelijke elementen in grote mate.

Voor *verandermodellen* heeft deze studie bijgedragen aan de ontwikkeling van een 3D interactief multidisciplinair ontwerpplatform waarin verschillende belanghebbenden uit verschillende domeinen kunnen samenwerken aan het configureren van wijzigingsscenario's. De responsiviteit van dit platform wordt versterkt door de inzet van game engine functionaliteiten en de informatie-inhoud en omvang wordt verbeterd door het inbedden van GIS technieken. Deze verbeteringen maakten een naadloze configuratie en analyse van scenario's mogelijk op elke locatie in het land.

Verbeteringen in de reikwijdte van *impactmodellen* werden uitgevoerd door verbetering van hun prestatiesnelheid, efficiënte toegang tot invoergegevens en onafhankelijkheid van software van derden. Deze verbeteringen werden bereikt door de efficiënte integratie van impactmodellen in het game-engine-GIS geïntegreerde ontwerpplatform waarin verschillende game engine en GIS functionaliteiten voor de verbeterde prestaties van deze modellen werden toegepast. Dit heeft geresulteerd in een versterkt systeem waarin belanghebbenden naadloos verschillende wijzigingsscenario's kunnen configureren op elke locatie in het land en realtime feedback kunnen ontvangen over verschillende aspecten van hun ontwerp zonder afhankelijkheid van software van derden.

Concluderend kan worden gesteld dat efficiënte integratie van Data-Model-Technology de verbetering van milieubeslissingsondersteunende systemen aanzienlijk kan ondersteunen. In

[38] Spatial Decision Support System

deze studie is gekozen voor energie en leefbaarheid als case studies. De ontwikkelde routines zijn echter schaalbaar naar andere domeinen. Dit komt enerzijds door de cloudgebaseerde architectuur van de ontwikkelde modules en de toegepaste technologie voor de toegankelijkheid en interoperabiliteit van verschillende datasets uit verschillende disciplines, en anderzijds door de ontwikkeling en toepassing van losjes-gekoppelde georuimtelijke en / of game engine functies voor verbeterde prestaties van de verschillende componenten van SDSS.

References

Abtew, W., Melesse, A. (2013). Evaporation and Evapotranspiration Measurement. In: Evaporation and Evapotranspiration. Springer Netherlands, pp. 29-42.

Agency IE. The IEA World Energy Outlook 2011. 2011.

Agterbosch, S., Meertens, R. M., Vermeulen, W. J. (2009). The relative importance of social and institutional conditions in the planning of wind power projects. *Renewable and Sustainable Energy Reviews*, 13(2), 393-405.

Aitken, M. (2010). Wind power and community benefits: Challenges and opportunities. *Energy policy*, 38(10), 6066-6075.

Akbari, H. (2005). Energy Saving Potentials and Air Quality Benefits of Urban Heat Island Mitigation. No. LBNL--58285. Ernest Orlando Lawrence Berkeley National Laboratory, Berkeley, CA (US).

Akpinar, E. K., Akpinar, S. (2005). An assessment on seasonal analysis of wind energy characteristics and wind turbine characteristics. *Energy Conversion and Management*, 46(11), 1848-1867.

Albert, C., Vargas-Moreno. C. (2012). Testing GeoDesign in Landscape Planning–First Results. In *Digital Landscape Architecture conference* (Vol. 31).

Al-Kodmany, K. (1999). Using visualization techniques for enhancing public participation in planning and design: process, implementation, and evaluation. Landscape and Urban Planning, 45(1), 37-45.

Al-Kodmany, K. (2002). Visualization tools and methods in community planning: from freehand sketches to virtual reality. *Journal of planning Literature*, 17(2), 189-211.

Andrienko, G., Andrienko, N., Jankowski, P. (2003). Building spatial decision support tools for individuals and groups. *Journal of Decision Systems*, 12(2), 193-208.

ANZLIC. (1996). Spatial Data Infrastructure for Australia and New Zealand. *Canberra, ACT, Australia and New Zealand Land Information Council*.

Arampatzis, G., Kiranoudis, C. T., Scaloubacas, P., Assimacopoulos, D. (2004). A GIS-based decision support system for planning urban transportation policies. *European Journal of Operational Research*, 152(2), 465-475.

Arezes, P. M., Bernardo, C. A., Ribeiro, E., and Dias, H. (2014). Implications of wind power generation: exposure to wind turbine noise. Procedia-Social and Behavioral Sciences,109, 390-395.

Armson, D., Stringer, P., Ennos, A R. (2012). The effect of tree shade and grass on surface and globe temperatures in an urban area. Urban Forestry & Urban Greening 11, 245-255.

Attenborough, K. (1992). Ground parameter information for propagation modeling. The Journal of the Acoustical Society of America, 92 (1), 418–427.

Attenborough, K., Taherzadeh, S., Bass, H. E., Di, X., Raspet, R., Becker, G. R., Güdesen, A., Chrestman, A., Daigle, G. A., L'Espérance, A., Gabillet, Y., Gilbert, K. E., Li, Y. L., White, M. J., Naz, P., Noble, J. M., and Van Hoof, H. A. J. M. (1995). Benchmark cases for outdoor sound propagation models. The Journal of the Acoustical Society of America, 97(1), 173-191.

Attenborough, K., Li, K. M., and Horoshenkov, K. (2007). Predicting outdoor sound. New York, CRC Press.

Aydin, N. Y., Kentel, E., Duzgun, S. (2010). GIS-based environmental assessment of wind energy systems for spatial planning: A case study from Western Turkey. Renewable and Sustainable Energy Reviews, 14(1), 364-373.

Aydin, G. (2014). Modeling of energy consumption based on economic and demographic factors: The case of Turkey with projections. Renewable and Sustainable Energy Reviews, 35, 382-389.

Aydin, G. (2014). Production modeling in the oil and natural gas industry: An application of trend analysis. Petroleum science and technology, 32(5), 555-564.

Aydin, G. (2014). The modeling of coal-related CO2 emissions and projections into future planning. Energy Sources, Part A: Recovery, Utilization, and Environmental Effects, 36(2), 191-201.

Aydin, G. (2015). The development and validation of regression models to predict energy-related CO2 emissions in Turkey. Energy Sources, Part B: Economics, Planning, and Policy, 10(2), 176-182.

Bakker, R. H., Pedersen, E., van den Berg, G. P., Stewart, R. E., Lok, W., and Bouma, J. (2012). Impact of wind turbine sound on annoyance, self-reported sleep disturbance and psychological distress. Science of the Total Environment, 425, 42-51.

Bass, H., Sutherland, L., and Zuckerwar, A. (1990). Atmospheric absorption of sound: Update. The Journal of the Acoustical Society of America, 88(4), 2019–2021.

Batty, M. (1998). Digital planning: Preparing for a fully wired world. In the proceedings of Computers in Urban Planning and Urban Management, P. K. Sikdar, S. L. Dhingra, and K.V. Krishna Rao, eds. New Delhi: Narosa: 13-30.

Berkhout, P. H., Muskens, J. C., Velthuijsen, J. W. (2000). Defining the rebound effect. Energy policy, 28(6-7), 425-432.

Biljecki, F., Tauscher, H. (2019). QUALITY OF BIM–GIS CONVERSION. ISPRS Annals of Photogrammetry, Remote Sensing and Spatial Information Sciences, 35-42.

Bishop, I. D. and Stock, C. (2010). Using collaborative virtual environments to plan wind energy installations. Renewable Energy, 35(10), 2348-2355.

Bishop, I. D. (2011). Landscape planning is not a game: Should it be? Landscape and Urban Planning, 100(4), 390-392.

Bourbia, F., Boucheriba, F. (2010). Impact of street design on urban microclimate for semi arid climate (Constantine). Renewable Energy 35, 343-347.

Buffat, R., Froemelt, A., Heeren, N., Raubal, M., Hellweg, S. (2017). Big data GIS analysis for novel approaches in building stock modelling. Applied Energy, 208, 277-290.

Butenuth, M., Gösseln, G. V., Tiedge, M., Heipke, C., Lipeck, U., Sester, M. (2007). Integration of heterogeneous geospatial data in a federated database. ISPRS Journal of Photogrammetry and Remote Sensing, 62(5), 328-346.

Campagna, M., Di Cesare, E. A. (2014). Geodesign From Theory to Practice: In the Search for Geodesign Principles in Italian Planning Regulations. Tema. Journal of Land Use, Mobility and Environment.

CBS (2008). Bestand bodemgebruik productbeschrijving. Voorburg/Heerlen: Centraal Bureau voor de Statistiek.

CBS. (2015) http://statline.cbs.nl/StatWeb/publication/?DM=SLNL&PA=70960NED&D1=0-1,6,9&D2=a&D3=22-23&VW=T.

Celik, A. N. (2004). A statistical analysis of wind power density based on the Weibull and Rayleigh models at the southern region of Turkey. Renewable energy, 29(4), 593-604.

Chalal, M. L., Benachir, M., White, M., Shrahily, R. (2016). Energy planning and forecasting approaches for supporting physical improvement strategies in the building sector: A review. Renewable and Sustainable Energy Reviews, 64, 761-776.

Chang, N. B., Wei, Y. L., Tseng, C. C., Kao, C. Y. (1997). The design of a GIS-based decision support system for chemical emergency preparedness and response in an urban environment. Computers, Environment and Urban Systems, 21(1), 67-94.

Chang, C.R., Li, M.H. (2014). Effects of urban parks on the local urban thermal environment. Urban Forestry & Urban Greening 13, 672-681.

Chen, X.L., Zhao, H.M., Li, P.X., Yin, Z.Y. (2006). Remote sensing image-based analysis of the relationship between urban heat island and land use/cover changes. Remote sensing of environment 104, 133-146.

Chen, L., Ng, E., An, X., Ren, C., Lee, M., Wang, U., He, Z. (2012). Sky view factor analysis of street canyons and its implications for daytime intra-urban air temperature differentials in high-rise, high-density urban areas of Hong Kong: a GIS-based simulation approach. International Journal of Climatology, 32(1), 121-136.

Chessell, C. (1977). Propagation of noise along a finite impedance boundary. The Journal of the Acoustical Society of America, 62(4), 825–834.

Crocker, M. J. (2007). Handbook of noise and vibration control. John Wiley & Sons.

Daigle, G., Piercy, J., and Embleton, F. (1978). Effects of atmospheric turbulence on the interference of sound waves near a hard boundary. The Journal of the Acoustical Society of America, 64, 622–630.

Daigle, G. (1979). Effects of atmospheric turbulence on the interference of sound waves above a finite impedance boundary. The Journal of the Acoustical Society of America, 65, 45–49.

Davidson JE, Heinberg, J., Williamson, B. (2010). Guide to Energy Efficient Homes in Louisiana. Louisiana Department of Natural Resources: Baton Rouge, LA, USA.

Day R, Hitchings R. (2009). Older people and their winter warmth behaviours: understanding the contextual dynamics.

db net Solutions. (2007).
http://www.dbnetsolutions.co.uk/Articles/BenefitsOfWebBasedApplications.aspx

Deal, W. F. (2010). Wind power: an emerging energy resource. Technology and Engineering Teacher, 70, 9–15.

De Boeck, L., Verbeke, S., Audenaert, A., De Mesmaeker, L. (2015). Improving the energy performance of residential buildings: A literature review. Renewable and Sustainable Energy Reviews, 52, 960-975.

de La Beaujardière, J. (2002). Web Map Service Implementation Specification, OpenGIS® Implementation Specification, 1.1.1, OGC 01-068r3. Open Geospatial Consortium, Inc., https://portal.opengeospatial.org/files/?artifact_id=1081&version=1&format=pdf

De Laat, R., Van Berlo, L. (2011). Integration of BIM and GIS: The development of the CityGML GeoBIM extension. In Advances in 3D geo-information sciences (pp. 211-225). Springer, Berlin, Heidelberg.

Delany, M. and Bazley, E. (1970). Acoustical properties of fibrous absorbent materials. Applied Acoustics, 3(2), 105–116.

Dellwik, E., Bingöl, F., Mann, J. (2014). Flow distortion at a dense forest edge. Quarterly Journal of the Royal Meteorological Society, 140(679), 676-686.

Devine-Wright, P. (2005). Beyond NIMBYism: towards an integrated framework for understanding public perceptions of wind energy. Wind energy, 8(2), 125-139.

Dias, E., Linde, M., Rafiee, A., Koomen, E., Scholten, H. (2013). Beauty and brains: Integrating easy spatial design and advanced urban sustainability models. In Planning support systems for sustainable urban development (pp. 469-484). Springer Berlin Heidelberg.

Dias, E., Van de Velde, R., Nobre, E., Estêvão, S., Scholten, H. (2003). Virtual Landscape Bridging the Gap between Spatial Perception and Spatial Information. In Proceedings of the 21st International Cartographic Conference (ICC). Durban, South Africa, 10-16.

Dimoudi, A., Nikolopoulou, M. (2003). Vegetation in the urban environment: microclimatic analysis and benefits. Energy and buildings 35, 69-76.

Ding, R., Kang, S., Li, F., Zhang, Y., Tong, L. (2013). Evapotranspiration measurement and estimation using modified Priestley–Taylor model in an irrigated maize field with mulching. Agricultural and Forest Meteorology 168, 140-148.

Donalek, C., Djorgovski, S. G., Davidoff, S., Cioc, A., Wang, A., Longo, G., Norris J. S., Zhang J., Lawler E., Yeh S., Mahabal, A., Graham M., Drake A. (2014). Immersive and collaborative data visualization using virtual reality platforms. arXiv preprint arXiv:1410.7670.

Donkers, S., Ledoux, H., Zhao, J., Stoter, J. (2016). Automatic conversion of IFC datasets to geometrically and semantically correct CityGML LOD3 buildings. Transactions in GIS, 20(4), 547-569.

Donovan, J. J., Fischer, W. P. (1976). Factors affecting residential heating energy consumption.

Dreiseitl, S., Ohno-Machado, L. (2002). Logistic regression and artificial neural network classification models: a methodology review. Journal of biomedical informatics, 35(5-6), 352-359.

Dvorak, M. J., Archer, C. L., Jacobson, M. Z. (2010). California offshore wind energy potential. Renewable Energy, 35(6), 1244-1254.

Eikelboom, T., Janssen, R. (2017). Collaborative use of geodesign tools to support decision-making on adaptation to climate change. Mitigation and Adaptation Strategies for Global Change, 22(2), 247-266.

Embleton, T., Piercy, J., and Daigle, G. A. (1983). Effective flow resistivity of ground surfaces determined by acoustical measurements. The Journal of the Acoustical Society of America, 74 (4), 1239–1244.

Emerson (2019). Emerson Digital Twin: A Key Technology for Digital Transformation, https://www.emerson.com/documents/automation/emerson-digital-twin-a-key-technology-for-digital-transformation-en-5262472.pdf

Energy Data Facts: U.S. Department of Energy; [Available from: https://rpsc.energy.gov/energy-data-facts.

Energy consumption in households: Eurostat; 2018 [Available from: https://ec.europa.eu/eurostat/statistics-explained/index.php/Energy_consumption_in_households.

EU Directive (2009). Directive 2009/28/EC of the European Parliament and of the Council of 23 April 2009 on the promotion of the use of energy from renewable sources and amending and subsequently repealing Directives 2001/77/EC and 2003/30. Off. J. of the EU, European Commission, 5, 16-62.

European Commission. (2007). Directive 2007/2/EC of the European Parliament and of the Council of 14 March 2007 Establishing an Infrastructure for Spatial Information in the European Community (INSPIRE).

European Commission (2020). The European Digital Strategy, https://ec.europa.eu/digital-single-market/en/content/european-digital-strategy.

EWEA (2015). European Wind Energy Association: Wind in power: 2014 European statistics. (Retrieved 2014-11-05).

Evans, A., Vladimir, S. and Evans, T. J. (2009). Assessment of sustainability indicators for renewable energy technologies. Renewable and Sustainable Energy Reviews, 13(5), 1082-1088.

Faasen, C.J., P.A.L. Franck, and A.M.H.W. Taris. (2013). Handboek Risicozonering Windturbines. Rijksdienst voor Ondernemend Nederland.

Fabbri, K.(2002). A Framework for Structuring Strategic Decision Situations in Integrated Coastal Zone Management, Vrije Universiteit, Amsterdam.

Federal Geographic Data Committee. (1995). Development of a national digital geospatial data framework. Federal Geographic Data Committee.

Feng, Y. Y., Zhang, L. X. (2012). Scenario analysis of urban energy saving and carbon abatement policies: a case study of Beijing city, China. Procedia Environmental Sciences, 13, 632-644.

Filios, A. E., Tachos, N. S., Fragias, A. P. and Margaris, D. P. (2007). Broadband noise radiation analysis for an HAWT rotor. Renewable Energy, 32(9), 1497–1510.

Firestone, J., Kempton, W. (2007). Public opinion about large offshore wind power: underlying factors. Energy policy, 35(3), 1584-1598.

Fischler, M. A., Bolles, R. C. (1981). Random sample consensus: a paradigm for model fitting with applications to image analysis and automated cartography. Communications of the ACM, 24(6), 381-395.

Flaxman, M. (2010). Fundamentals of geodesign. Proceedings of Digital Landscape Architecture, Anhalt University of Applied Science, 2, 69-72.

Flaxman, M. (2010). Geodesign: Fundamental principles and routes forward. Talk at GeoDesign Summit.

Forrest, T. G. (1994). From sender to receiver: propagation and environmental effects on acoustic signals. American Zoologist, 34(6), 644-654.

Frayssinet, L., Merlier, L., Kuznik, F., Hubert, J. L., Milliez, M., Roux, J. J. (2018). Modeling the heating and cooling energy demand of urban buildings at city scale. Renewable and Sustainable Energy Reviews, 81, 2318-2327.

Freudenberg, B., Masuch, M., Strothotte, T. (2001). Walk-Through Illustrations: Frame-Coherent Pen-and-Ink Style in a Game Engine. In Computer Graphics Forum (Vol. 20, No. 3, pp. 184-192). Blackwell Publishers Ltd.

Fumo N, Biswas MR. (2015). Regression analysis for prediction of residential energy consumption. Renewable and sustainable energy reviews. 47:332-343.

Geertman, S. and Stillwell, J. (Eds.). (2012). Planning support systems in practice. Springer Science & Business Media.

Gemeente Rotterdam (2020). Marktconsultatie: De beste leverancier voor het platform Digitale Stad voor Rotterdam, https://platform.negometrix.com/DocumentViewer/DocumentViewer.aspx?documentGuid=1c5c3bdc-a4cc-4d08-b40b-d22d3d7c8a10 (in Dutch)

George, R. V. (1997). Hyper Space Communicating Ideas about the Quality of Urban Spaces. Journal of Planning Education and Research, 17(1), 63-70.

Giridharan, R., Lau, S.S. Y., Ganesan, S. (2005). Nocturnal heat island effect in urban residential developments of Hong Kong. Energy and Buildings 37, 964-971.

Giridharan, R., Lau, S.S.Y., Ganesan, S., Givoni, B. (2008). Lowering the outdoor temperature in high-rise high-density residential developments of coastal Hong Kong: The vegetation influence. Building and Environment 43, 1583-1595.

Goodall, J. L., Robinson, B. F., and Castronova, A. M. (2011). Modeling water resource systems using a service-oriented computing paradigm. Environmental Modelling & Software, 26(5), 573-582.

Gorsevski, P. V., Cathcart, S. C., Mirzaei, G., Jamali, M. M., Ye, X., Gomezdelcampo, E. (2013). A group-based spatial decision support system for wind farm site selection in Northwest Ohio. Energy Policy, 55, 374-385.

Gram-Hanssen, K. (2010). Residential heat comfort practices: understanding users. Building Research & Information, 38(2), 175-186.

Gregory, J. (2009). Game engine architecture, 2nd edn. CRC Press, pp. 28-38.

Grosveld, F. W., Shepherd, K. P., and Hubbard, H. H. (1995). Measurement and prediction of broadband noise from large horizontal axis wind turbine generators. Wind Turbine Technology, 1, 211–220.

Grassi, S., Chokani, N., Abhari, R. S. (2012). Large scale technical and economical assessment of wind energy potential with a GIS tool: Case study Iowa. Energy Policy, 45, 73-85.

Grimmond, C. S. B., Oke, T. R. (1999). Aerodynamic properties of urban areas derived from analysis of surface form. Journal of applied meteorology, 38(9), 1262-1292.

Groth, T. M. and Vogt, C. (2014). Residents' perceptions of wind turbines: An analysis of two townships in Michigan. Energy Policy, 65, 251-260.

Grynszpan, D. (2003). Lessons from the French heatwave. The Lancet 362, 1169-1170.

Guerra-Santin, O., Itard, L. (2010). Occupants' behaviour: determinants and effects on residential heating consumption. Building Research & Information, 38(3), 318-338.

Hagedorn, B., Döllner, J. (2007, November). High-level web service for 3D building information visualization and analysis. In Proceedings of the 15th annual ACM international symposium on Advances in geographic information systems (pp. 1-8).

Hall, N., Ashworth, P., and Devine-Wright, P. (2013). Societal acceptance of wind farms: Analysis of four common themes across Australian case studies. Energy Policy, 58, 200-208.

Hamada, S., Ohta, T. (2010). Seasonal variations in the cooling effect of urban green areas on surrounding urban areas. Urban Forestry & Urban Greening 9, 15-24.

Harding, G., Harding, P., Wilkins, A. (2008). Wind turbines, flicker, and photosensitive epilepsy: Characterizing the flashing that may precipitate seizures and optimizing guidelines to prevent them. Epilepsia, 49(6), 1095-1098.

Harris, C. M. (1966). Absorption of sound in air versus humidity and temperature. The Journal of the Acoustical Society of America 40(1), 148-159.

Herwig, A. and Paar, P. (2002). Game engines: tools for landscape visualization and planning. Trends in GIS and Virtualization in Environmental Planning and Design, 161, 172.

Heusinkveld, B.G., Van Hove, L.W.A., Jacobs, C.M.J., Steeneveld, G J., Elbers, J.A., Moors, E J., Holtslag, A.A.M. (2010). Use of a mobile platform for assessing urban heat stress in Rotterdam. In: Matzarakis, A., Mayer, H., Chmielewski F.M. (Eds), Proceedings of the 7th Conference on Biometeorology Vol. 12, Self-publishing company of the Meteorological Institute, Albert-Ludwigs-University of Freiburg, Germany, pp. 433-438.

Heusinkveld, B.G., Steeneveld, G.J., Hove, L.W. A., Jacobs, C.M.J., Holtslag, A.A.M. (2014). Spatial variability of the Rotterdam urban heat island as influenced by urban land use. Journal of Geophysical Research: Atmospheres 119677-692.

Hijazi, I., Ehlers, M., Zlatanova, S., Becker, T., van Berlo, L. (2011). Initial investigations for modeling interior Utilities within 3D Geo Context: Transforming IFC-interior utility to CityGML/UtilityNetworkADE. In Advances in 3D Geo-information sciences (pp. 95-113). Springer, Berlin, Heidelberg.

Hijazi, I., Ehlers, M., Zlatanova, S., Isikdag, U. (2009). IFC to CityGML transformation framework for geo-analysis: a water utility network case. In 4th International Workshop on 3D Geo-Information, 4-5 November 2009, Ghent, Belgium.

Hong, S. H., Oreszczyn, T., Ridley, I., Warm Front Study Group. (2006). The impact of energy efficient refurbishment on the space heating fuel consumption in English dwellings. Energy and buildings, 38(10), 1171-1181.

Ihara, T., Kusaka, H., Hara, M., Matsuhashi, R., Yoshida, Y. (2011). Estimation of mild health disorder caused by urban air temperature increase with midpoint-type impact assessment methodology. Journal of Environmental Engineering (Transaction of AIJ) 76, 459-467.

Irizarry, J., Karan, E. P. (2012). Optimizing location of tower cranes on construction sites through GIS and BIM integration. Journal of information technology in construction (ITcon), 17(23), 351-366.

Irizarry, J., Karan, E. P., Jalaei, F. (2013). Integrating BIM and GIS to improve the visual monitoring of construction supply chain management. Automation in construction, 31, 241-254.

Isikdag, U., Underwood, J., Aouad, G. (2008). An investigation into the applicability of building information models in geospatial environment in support of site selection and fire response management processes. Advanced engineering informatics, 22(4), 504-519.

Isikdag, U., & Zlatanova, S. (2009). Towards defining a framework for automatic generation of buildings in CityGML using building Information Models. In 3D Geo-Information Sciences (pp. 79-96). Springer, Berlin, Heidelberg.

Jallouli, J., and Moreau, G. (2009). An immersive path-based study of wind turbines' landscape: A French case in Plouguin. Renewable Energy, 34(3), 597-607.

Janke, J. R. (2010). Multicriteria GIS modeling of wind and solar farms in Colorado. Renewable Energy, 35(10), 2228-2234.

Jauregui, E. (1991). Influence of a large urban park on temperature and convective precipitation in a tropical city. Energy and Buildings 15, 457–463.

Jenks, G.F. (1967). The data model concept in statistical mapping. In: Frenzel, K. (Ed). International yearbook of cartography, Vol. 7, George Philip, pp. 186–190.

Jobert, A., Laborgne, P., and Mimler, S. (2007). Local acceptance of wind energy: Factors of success identified in French and German case studies. Energy Policy, 35(5), 2751-2760.

Johnson, G.T., Watson, I.D. (1984). The determination of view-factors in urban canyons. Journal of Climate and Applied Meteorology 23, 329-335.

Johnson, M., Raspet, R., and Bobak, M. (1987). A turbulence model for sound propagation from an elevated source above level ground. The Journal of the Acoustical Society of America, 81(3), 638–646.

Jones, C. R., Eiser, J. R. (2010). Understanding ‘local’opposition to wind development in the UK: How big is a backyard?. Energy Policy, 38(6), 3106-3117.

Jude, S. (2008). Investigating the potential role of visualization techniques in participatory coastal management. Coastal Management, 36(4), 331-349.

Justus, C. G., Hargraves, W. R., Yalcin, A. (1976). Nationwide assessment of potential output from wind-powered generators. Journal of applied meteorology, 15(7), 673-678.

Justus, C. G., Hargraves, W. R., Mikhail, A., Graber, D. (1978). Methods for estimating wind speed frequency distributions. Journal of applied meteorology, 17(3), 350-353.

Kastner-Klein, P., Rotach, M. W. (2004). Mean flow and turbulence characteristics in an urban roughness sublayer. Boundary-Layer Meteorology, 111(1), 55-84.

Khazzoom J. D. (1987). Energy saving resulting from the adoption of more efficient appliances. The Energy Journal, 8(4), 85-89.

Khan, J. (2003). Wind power planning in three Swedish municipalities. Journal of Environmental Planning and Management, 46(4), 563-581.

Köne, A. Ç., Büke, T. (2010). Forecasting of CO2 emissions from fuel combustion using trend analysis. Renewable and Sustainable Energy Reviews, 14(9), 2906-2915.

Kooij F, de Boer, A., Jessen, L. (2018). Catalogus Basisregistratie Adressen en Gebouwen. Ministerie van Infrastructuur en Milieu.

Koomen, E., Rietveld, P., Bacao, F. (2009). The third dimension in urban geography: the urban-volume approach. Environment and Planning B: Planning and Design, 36(6), 1008-1025.

Koomen, E., Diogo, V. (2015) .Assessing potential future urban heat island patterns following climate scenarios, socio-economic developments and spatial planning strategies. Mitigation and Adaptation Strategies for Global Change, 1-20.

Koop, H. (1989). Forest Dynamics. SILVI-STAR: A comprehensive monitoring system. Springer-Verlag, pp. 40-58.

Kurze, U. and Anderson, G. (1971). Sound attenuation by barriers. Applied Acoustics, 4(1), 35–53.

Kurze, U. (1971). Noise and vibration control. Noise and vibration control. Ed. by Beranek, L.L. McGraw-Hill.

Lamancusa, J. S., Daroux, P. A. (1993). Ray tracing in a moving medium with two-dimensional sound-speed variation and application to sound propagation over terrain discontinuities. The Journal of the Acoustical Society of America, 93(4), 1716-1726.

Laukkanen, S., Kangas, A., Kangas, J. (2002). Applying voting theory in natural resource management: a case of multiple-criteria group decision support. Journal of Environmental Management, 64(2), 127-137.

Lee, D. J., Dias, E., Scholten, H. J. (2014). Introduction to geodesign developments in Europe. In Geodesign by Integrating Design and Geospatial Sciences (pp. 3-9). Springer, Cham.

Lejeune, P., Feltz, C. (2008). Development of a decision support system for setting up a wind energy policy across the Walloon Region (southern Belgium). Renewable Energy, 33(11), 2416-2422.

Li, W., Milburn, L. A. (2016). The evolution of geodesign as a design and planning tool. Landscape and Urban Planning.

Limpo, J. R. (2011). Assessment of offshore wind energy in Portuguese shallow waters site selection, technical aspects and financial evaluation. A Master's Thesis Instituto Superior Técnico, Universidade Técnica de Lisboa. Lisbon, Portugal.

Lissaman, P. B., Gyatt, G. W., Zalay, A. D. (1982). Numeric-modeling sensitivity analysis of the performance of wind turbine arrays (No. PNL-4183). Pacific Northwest Lab., Richland, WA (USA); AeroVironment, Inc., Pasadena, CA (USA).

Liu, X., Song, Y., Wu, K., Wang, J., Li, D., Long, Y. (2015). Understanding urban China with open data. Cities, 47, 53-61.

Longley, P. A., Goodchild, M. F., Maguire, D. J., Rhind, D. W. (2001). Geographic information systems and science. John Wiley & Sons Ltd.

Lu, L., Yang, H., Burnett, J. (2002). Investigation on wind power potential on Hong Kong islands—an analysis of wind power and wind turbine characteristics. Renewable Energy, 27(1), 1-12.

Ledoux, H. (2018). val3dity: validation of 3D GIS primitives according to the international standards. Open Geospatial Data, Software and Standards, 3(1), 1.

Macdonald, R. W., Griffiths, R. F., Hall, D. J. (1998). An improved method for the estimation of surface roughness of obstacle arrays. Atmospheric environment, 32(11), 1857-1864.

Maekawa, Z. (1968). Sound attenuation by screens. Applied Acoustics, 3(1), 157-173.

Maillebouis, C. (2003). Nimby ou la colère des lieux. Le cas des parcs éoliens. Natures sciences sociétés, 11(2), 190-194.

Malczewski, J. (1996). A GIS-based approach to multiple criteria group decision-making. International Journal of Geographical Information Systems, 10(8), 955-971.

Malczewski, J. (2006). GIS-based multicriteria decision analysis: a survey of the literature. International Journal of Geographical Information Science, 20(7), 703-726.

Malczewski, J., Rinner, C. (2015). Multicriteria decision analysis in geographic information science. New York, NY, USA: Springer.

Manning, W. (1913) The Billerica town plan. Landscape Architecture, 3(5), 108–118.

Manwell, J., McGowan, J., and Rogers, A. (2002). Wind energy explained: Theory, design and application. West Sussex, UK, John Wiley.

Manwell, J. F., McGowan, J. G., Rogers, A. L. (2010). Wind energy explained: theory, design and application. John Wiley & Sons.

Mari, R., Bottai, L., Busillo, C., Calastrini, F., Gozzini, B., Gualtieri, G. (2011). A GIS-based interactive web decision support system for planning wind farms in Tuscany (Italy). Renewable Energy, 36(2), 754-763.

Martin, S., Foulonneau, M., Turki, S., Ihadjadene, M. (2013, June). Open data: Barriers, risks and opportunities. In Proceedings of the 13th European Conference on eGovernment: ECEG (pp. 301-309).

Masó, J., Pomakis, K., and Julià, N. (2010). Web Map Tile Service Implementation Standard, OpenGIS® Implementation Standard, 1.0.0 : OGC 07-057r7. Open Geospatial Consortium, Inc., http://portal.opengeospatial.org/files/?artifact_id=35326.

Mastrucci, A., Baume, O., Stazi, F., Leopold, U. (2014). Estimating energy savings for the residential building stock of an entire city: A GIS-based statistical downscaling approach applied to Rotterdam. Energy and Buildings, 75, 358-367.

McMichael, A.J. (2000). The urban environment and health in a world of increasing globalization: issues for developing countries. Bulletin of the World Health Organization 78, 1117-1126.

McPherson, E.G., Rowntree, R.A., Wagar, J.A. (1995). Energy-efficient landscapes. In: Bradley, G. A. (Ed), Urban Forest Landscapes. University of Washington Press, Seattle, pp. 150-160.

Mekonnen, A. D., Gorsevski, P. V. (2015). A web-based participatory GIS (PGIS) for offshore wind farm suitability within Lake Erie, Ohio. Renewable and Sustainable Energy Reviews, 41, 162-177.

Mignard, C., Nicolle, C. (2014). Merging BIM and GIS using ontologies application to urban facility management in ACTIVe3D. Computers in Industry, 65(9), 1276-1290.

Minelli, A., Marchesini, I., Taylor, F. E., De Rosa, P., Casagrande, L., Cenci, M. (2014). An open source GIS tool to quantify the visual impact of wind turbines and photovoltaic panels. Environmental Impact Assessment Review, 49, 70-78.

Misseyer, M. (1999). Time, Area, Substance and Human Activity Referenced Emission Inventory, Vrije Universiteit, Amsterdam.

Moriarty, P., Guidati, G., and Migliore, P. (2005). Prediction of turbulent inflow and trailing-edge noise for wind turbines. Proceedings of the 11th AIAA/CEAS Aeroacoustics Conference (Monterey, Canada). AIAA Paper 2881.

Mulvaney, K. K., Woodson, P., Prokopy, L. S. (2013). A tale of three counties: Understanding wind development in the rural Midwestern United States. Energy Policy, 56, 322-330.

Nakamura, Y., Oke, T.R. (1988). Wind, temperature and stability conditions in an east-west oriented urban canyon. Atmospheric Environment (1967) 22, 2691-2700.

Nedkov, S., Dias, E., Linde, M. (2014). People Centered Geodesign: Results of an Exploration. In Geodesign by Integrating Design and Geospatial Sciences (pp. 299-314). Springer International Publishing.

Nicolas J., Berry, J., and Daigle, G. (1985). Propagation of sound above a finite layer of snow. The Journal of the Acoustical Society of America, 77(1), 67–73.

Nobre, A., Pacheco, M., Jorge, R., Lopes, M. F. P., Gato, L. M. C. (2009). Geo-spatial multi-criteria analysis for wave energy conversion system deployment. Renewable energy, 34(1), 97-111.

Nouvel, R., Mastrucci, A., Leopold, U., Baume, O., Coors, V., Eicker, U. (2015). Combining GIS-based statistical and engineering urban heat consumption models: Towards a new framework for multi-scale policy support. Energy and Buildings, 107, 204-212.

O'Coill, C. and Doughty, M. (2004). Computer game technology as a tool for participatory design. In: eCAADe2004: Architecture in the Network Society, Copenhagen, Denmark.

Oerlemans, S., Sijtsma, P., and Méndez López, B. (2007). Location and quantification of noise sources on a wind turbine. Journal of Sound and Vibration, 299(4), 869-883.

Oerlemans, S. and Schepers, J. (2009). Prediction of wind turbine noise and validation against experiment. Acoustics, 8, 555–584.

Oerlemans, S., Schepers, J. G. (2010). Prediction of wind turbine noise and validation against experiment. noise notes, 9(2), 3-28.

Ohori, K. A., Biljecki, F., Diakité, A., Krijnen, T., Ledoux, H., Stoter, J. (2017, October). Towards an integration of GIS and BIM data: what are the geometric and topological issues?. In ISPRS Annals of Photogrammetry, Remote Sensing & Spatial Information Sciences, Proceedings of ISPRS 12th Geoinfo Conference, Melbourne, Australia (pp. 26-27).

Oke, T. R. (1981). Canyon geometry and the nocturnal urban heat island: comparison of scale model and field observations. Journal of climatology, 1(3), 237-254.

Oke, T.R. (1982). The energetic basis of the urban heat island. Quarterly Journal of the Royal Meteorological Society 108, 1-24.

Oke, T.R. (1988). Street design and urban canopy layer climate. Energy and buildings 11, 103-113.

Oke, T. R. (1995). The heat island of the urban boundary layer: characteristics, causes and effects. In: Cermak, J. E., Davenport, A. G., Plate, E. J., Viegas D. X. (Eds), Wind climate in cities. NATO ASI Series, Vol. 277, Springer Netherlands, pp. 81-107.

Oláh, A.B. (2012). The possibilities of decreasing the urban heat island. Applied Ecology and Environmental Research 10, 173-183.

Ontwerp-structuurvisie Windenergie op land. (2013). https://www.rijksoverheid.nl/binaries/rijksoverheid/documenten/rapporten/2013/03/28/ontwerp-structuurvisie-windenergie-op-land/ontwerp-structuurvisie-windenergie-op-land-tcm318-341048.pdf

Open data van de Overheid (2019). https://data.overheid.nl/

OS OpenData (2019). https://www.ordnancesurvey.co.uk/opendatadownload/products.html.

Ouammi, A., Ghigliotti, V., Robba, M., Mimet, A., Sacile, R. (2012). A decision support system for the optimal exploitation of wind energy on regional scale. Renewable Energy, 37(1), 299-309.

Pacheco, R., Ordóñez, J., Martínez, G. (2012). Energy efficient design of building: A review. Renewable and Sustainable Energy Reviews, 16(6), 3559-3573.

Pasqualetti, M. J., Energy, G. (2002). Living with wind power in a hostile landscape. Wind power in view: Energy landscapes in a crowded world, 153-72

Pedersen, E. (2011). Health aspects associated with wind turbine noise—Results from three field studies. Noise Control Engineering Journal 59(1), 47-53.

Perini, K., Magliocco, A. (2014). Effects of vegetation, urban density, building height, and atmospheric conditions on local temperatures and thermal comfort. Urban Forestry & Urban Greening 13, 495-506.

Piercy, J. E., Embleton, T. F. W., and Sutherland, L. C. (1977). Review of noise propagation in the atmosphere. The Journal of the Acoustical Society of America, 61(6), 1403-1418.

Pierpont, N. (2009). Wind turbine syndrome: A report on a natural experiment. Santa Fe, NM, USA: K-Selected Books.

Prospathopoulos, J. M. and Voutsinas, S. G. (2007). Application of a ray theory model to the prediction of noise emissions from isolated wind turbines and wind parks. Wind Energy, 10(2), 103–119.

Qiu, G.Y., Li, H.Y., Zhang, Q.T., Chen, W., Liang, X.J., Li, X.Z. (2013). Effects of evapotranspiration on mitigation of urban temperature by vegetation and urban agriculture. Journal of Integrative Agriculture 12, 1307-1315.

Rafiee, A., Dias, E., Koomen, E. (2016). Local impact of tree volume on nocturnal urban heat island: A case study in Amsterdam. Urban forestry & urban greening, 16, 50-61.

Rafiee, A., Van der Male, P., Dias, E., Scholten, H. (2017). Developing a wind turbine planning platform: Integration of “sound propagation model–GIS-game engine” triplet. Environmental Modelling & Software, 95, 326-343.

Ramírez-Rosado, I. J., García-Garrido, E., Fernández-Jiménez, L. A., Zorzano-Santamaría, P. J., Monteiro, C., Miranda, V. (2008). Promotion of new wind farms based on a decision support system. Renewable Energy, 33(4), 558-566.

Ratti, C., Baker, N., Steemers, K. (2005). Energy consumption and urban texture. Energy and buildings, 37(7), 762-776.

Reynolds, J. (2014). A Geodesign Inspired Multiple Criteria Decision Tool for Prioritizing Levee Setback Project Sites (Doctoral dissertation, University of Washington).

Righter, R. W. (1996). Wind energy in America: A history. University of Oklahoma Press.

Rode, P., Keim, C., Robazza, G., Viejo, P., Schofield, J. (2014). Cities and energy: urban morphology and residential heat-energy demand. Environment and Planning B: Planning and Design, 41(1), 138-162.

Rodman, L. C., Meentemeyer, R. K. (2006). A geographic analysis of wind turbine placement in Northern California. Energy Policy, 34(15), 2137-2149.

RVO, last visit 2016, http://www.rvo.nl/onderwerpen/duurzaam-ondernemen/duurzame-energie-opwekken/windenergie-op-land/spelers/grondeigenaren

Saidur, R., Rahim, N. A., Islam, M. R., and Solangi, K. H. (2011). Environmental impact of wind energy. Renewable and Sustainable Energy Reviews, 15(5), 2423-2430.

Sanaieian, H., Tenpierik, M., Van Den Linden, K., Seraj, F. M., Shemrani, S. M. M. (2014). Review of the impact of urban block form on thermal performance, solar access and ventilation. Renewable and Sustainable Energy Reviews, 38, 551-560.

Santhanam, R., Wiedenbeck, S. (1993). Neither novice nor expert: the discretionary user of software. International Journal of Man-Machine Studies, 38(2), 201-229.

Santin, O. G., Itard, L., Visscher, H. (2009). The effect of occupancy and building characteristics on energy use for space and water heating in Dutch residential stock. Energy and buildings, 41(11), 1223-1232.

Say, N. P., Yücel, M. (2006). Energy consumption and CO2 emissions in Turkey: Empirical analysis and future projection based on an economic growth. Energy policy, 34(18), 3870-3876.

Sebastian, R., Böhms, M., van den Helm, P. (2013, October). BIM and GIS for low-disturbance construction. In Proceedings of the 13th International Conference on Construction Applications of Virtual Reality (pp. 30-31).

SenterNovem (2005), Windkaart van Nederland op 100 m hoogte (2005). https://www.rvo.nl/sites/default/files/2014/01/windkaart_van_nederland.pdf

SER (2013). Energieakkoord voor duurzame groei, http://www.ser.nl/~/media/files/internet/publicaties/overige/2010_2019/2013/energieakkoord-duurzame-groei/energieakkoord-duurzame-groei.ashx

Shashua-Bar, L., Hoffman, M. E. (2003). Geometry and orientation aspects in passive cooling of canyon streets with trees. Energy and Buildings 35, 61-68.

Shiffer, M. J. (1992). Towards a collaborative planning system. Environment and Planning B: Planning and Design, 19(6), 709-722.

Scholten, H. J., Stillwell, J. C. (1990). Geographical information systems: the emerging requirements. In Geographical information systems for urban and regional planning (pp. 3-14). Springer, Dordrecht.

Simao, A., Densham, P. J., Haklay, M. (2009). Web-based GIS for collaborative planning and public participation: An application to the strategic planning of wind farm sites. Journal of environmental management, 90(6), 2027-2040.

Simonovic, S. P., Bender, M. J. (1996). Collaborative planning-support system: an approach for determining evaluation criteria. Journal of hydrology, 177(3-4), 237-251.

Simpson, J. R. (2002). Improved estimates of tree-shade effects on residential energy use. Energy and Buildings 34, 1067-1076.

Smeds, J., Wall, M. (2007). Enhanced energy conservation in houses through high performance design. Energy and Buildings, 39(3), 273-278.

Solecki, W.D., Rosenzweig, C., Parshall, L., Pope, G., Clark, M., Cox, J., Wiencke, M. (2005). Mitigation of the heat island effect in urban New Jersey. Global Environmental Change Part B: Environmental Hazards 6, 39-49.

Sonderegger RC. (1978). Movers and stayers: the resident's contribution to variation across houses in energy consumption for space heating. Energy and buildings. 1(3):313-24.

Steadman, P., Hamilton, I., Evans, S. (2014). Energy and urban built form: an empirical and statistical approach. Building Research & Information, 42(1), 17-31.

Steeneveld, G.J., Koopmans, S., Heusinkveld, B.G., Theeuwes, N.E. (2014). Refreshing the role of open water surfaces on mitigating the maximum urban heat island effect. Landscape and Urban Planning 121, 92-96.

Steinitz, C. (1990). A framework for theory applicable to the education of landscape architects (and other environmental design professionals). Landscape journal, 9(2), 136-143.

Steinitz, C. (2012). A framework for geodesign: Changing geography by design. esri.

Steinitz, C. (2014). Which Way of Designing?. In Geodesign by integrating design and geospatial sciences (pp. 11-40). Springer International Publishing.

Stock, C., Bishop, I. D., O'Connor, A. N., Chen, T., Pettit, C. J., and Aurambout, J. P. (2008). SIEVE: Collaborative decision-making in an immersive online environment. Cartography and Geographic Information Science, 35(2), 133-144.

Strachan, P. A., Lal, D. (2004). Wind energy policy, planning and management practice in the UK: hot air or a gathering storm?. Regional Studies, 38(5), 549-569.

Strobl, J. (2006). Visual interaction: Enhancing public participation. 7th International Conference on Information Technologies in Landscape Architecture: Trends in Knowledge-Based Landscape Modelling.

Swaid, H., Hoffman, M.E. (1990). Climatic impacts of urban design features for high-and mid-latitude cities. Energy and Buildings 14, 325-336.

Swofford, J., Slattery, M. (2010). Public attitudes of wind energy in Texas: Local communities in close proximity to wind farms and their effect on decision-making. Energy policy, 38(5), 2508-2519.

Tadamasa, A. and Zangeneh, M. (2011). Numerical prediction of wind turbine noise. Renewable Energy, 36(7), 1902–1912.

Tegou, L. I., Polatidis, H., Haralambopoulos, D. A. (2010). Environmental management framework for wind farm siting: Methodology and case study. Journal of environmental management, 91(11), 2134-2147.

Theeuwes, N.E., Solcerová, A., Steeneveld, G.J. (2013). Modeling the influence of open water surfaces on the summertime temperature and thermal comfort in the city. Journal of Geophysical Research: Atmospheres 118, 8881-8896.

Theodoridou, I., Papadopoulos, A. M., Hegger, M. (2011). Statistical analysis of the Greek residential building stock. Energy and Buildings, 43(9), 2422-2428.

Thomas, M. R. (2002). A GIS-based decision support system for brownfield redevelopment. Landscape and Urban Planning, 58(1), 7-23.

Tippett, J. (2005). The value of combining a systems view of sustainability with a participatory protocol for ecologically informed design in river basins. Environmental Modelling & Software, 20(2), 119-139.

Toke, D. (2002). Wind power in UK and Denmark: can rational choice help explain different outcomes?. Environmental politics, 11(4), 83-100.

Vallado, D. A. (2001). Fundamentals of astrodynamics and applications. Fundamentals of astrodynamics and applications/by David A. Vallado with technical contributions by Wayne D. McClain. 2nd ed. El Segundo, CA: Microcosm Press; Dordrecht: Kluwer Academic Publishers, 2001. Space technology library; v. 12, 1.

van Beurden A.U.C.J. Scholten H.J. (1990). The environmental geographical information system of the Netherlands and its organizational implications. In: Proceedings First European

Conference on Geographical Information Systems. Amsterdam 10-13 April. Utrecht, Vol. 1, 59-67.

Van der Hoeven, F., Wandl, A. (2015). Amsterwarm: Mapping the landuse, health and energy-efficiency implications of the Amsterdam urban heat island. Building Services Engineering Research and Technology 36, 67-88.

Van der Zon, N. (2011). Kwaliteitsdocument ahn-2. Rijkswaterstaat & Waterschappen, Technical Report (In Dutch), 1.

Van der Zon, N. (2013). Kwaliteitsdocument AHN2.

van Herwijnen, M.(1999). Spatial Decision Support for Environmental Management, Vrije Universiteit, Amsterdam.

Van Hove, L.W. A., Jacobs, C.M.J., Heusinkveld, B.G., Elbers, J.A., Van Driel, B.L., Holtslag, A.A.M. (2015). Temporal and spatial variability of urban heat island and thermal comfort within the Rotterdam agglomeration. Building and Environment 83, 91-103.

Van Leeuwen N. (2004). Bestand Bodemgebruik en Top10Vector geharmoniseerd. Geo-Info, 5, 218-22.

van Praag, E., Borrero, S. (2012). GeoSUR: estableciendo las bases de una IDE regional en América Latina y el Caribe. Revista Cartográfica, (88), 31.

Vitolo, C., Elkhatib, Y., Reusser, D., Macleod, C. J., and Buytaert, W. (2015). Web technologies for environmental Big Data. Environmental Modelling & Software, 63, 185-198.

von Goesseln, G. (2005). A matching approach for the integration, change detection and adaptation of heterogeneous vector data sets. In XXII International Cartography Conference. A Coruña, Spain: The International Cartographic Association.

Voogt, J. A., Oke, T. R. (2003). Thermal remote sensing of urban climates. Remote sensing of environment 86, 370-384.

Vonk, G., Geertman, S., Schot, P. (2005). Bottlenecks blocking widespread usage of planning support systems. Environment and planning A, 37(5), 909-924.

Vretanos, P. A. (2005). Web Feature Service Implementation Specification. OpenGIS® Implementation Specification, 1.1.0, OGC 04-094. Open Geospatial Consortium, Inc. (2005), https://portal.opengeospatial.org/files/?artifact_id=8339.

Wang, Z., Srinivasan, R. S. (2017). A review of artificial intelligence based building energy use prediction: Contrasting the capabilities of single and ensemble prediction models. Renewable and Sustainable Energy Reviews, 75, 796-808.

Warren, C. R., Lumsden, C., O'Dowd, S., Birnie, R. V. (2005). 'Green on green': public perceptions of wind power in Scotland and Ireland. Journal of environmental planning and management, 48(6), 853-875.

Warren-Kretzschmar, B., Haaren, C. V., Hachmann, R., Albert, C. (2012). The potential of GeoDesign for linking landscape planning and design. In DLA Conference.

Watson, I.D., Johnson, G.T. (1987). Graphical estimation of sky view-factors in urban environments. Journal of climatology 7, 193-197.

Wagner, S., Bareiss, R., and Guidati, G. (1996). Wind Turbine Noise. Berlin, Germany, Springer.

Whitman, S., Good, G., Donoghue, E.R., Benbow, N., Shou, W., Mou, S. (1997). Mortality in Chicago attributed to the July 1995 heat wave. American Journal of Public Health 87, 1515-1518.

Wolsink, M. (2007). Wind power implementation: the nature of public attitudes: equity and fairness instead of 'backyard motives'. Renewable and sustainable energy reviews, 11(6), 1188-1207.

Wong, N.H., Yu, C. (2005). Study of green areas and urban heat island in a tropical city. Habitat International 29, 547-558.

Wu, I. C., Hsieh, S. H. (2007). Transformation from IFC data model to GML data model: methodology and tool development. Journal of the Chinese Institute of Engineers, 30(6), 1085-1090.

Yamasaki, E., Tominaga, N. (1997). Evolution of an aging society and effect on residential energy demand. Energy policy, 25(11), 903-912.

Yamashita, S., Sekine, K., Shoda, M., Yamashita, M., K., Hara, Y. (1986). On relationships between heat island and sky view factor in the cities of Tama River basin, Japan. Atmospheric Environment (1967) 20, 681-686.

Yu, C., Hien, W.N. (2006). Thermal benefits of city parks. Energy and Buildings 38, 105-120.

Zeep-Architecten (2013). http://www.zeep-architecten.nl/.

Zhang X, Arayici Y, Wu S, Abbott C., Aouad G. Integrating BIM and GIS for large scale (building) asset management: a critical review. (2009). The Twelfth International Conference on Civil Structural and Environmental Engineering Computing.

Zhao, H. X., Magoulès, F. (2012). A review on the prediction of building energy consumption. Renewable and Sustainable Energy Reviews, 16(6), 3586-3592.

2020 climate energy package (2009). European Commission, Climate Action, package. http://ec.europa.eu/clima/policies/strategies/2020/index_en.htm (last accessed 11.02.16).

Formatted: Font color: Auto, English (United States)